GEOLOGY AND UAV-BASED LANDSLIDE RISK AREA MAPPING OF KAMPUNG PENDUK, JELI KELANTAN

by

NUR AINA SHAHIRA BINTI NORAZAMI

Report submitted in fulfilment of the requirement for the degree of Bachelor of Applied Science (Geoscience) with Honors

FACULTY OF EARTH SCIENCE

UNIVERSITI MALAYSIA KELANTAN

2019

DECLARATION

I declare that this thesis entitled "GEOLOGY AND UAV-BASED LANDSLIDE RISK AREA MAPPING OF KAMPUNG PENDUK, JELI KELANTAN" is the result of my own research except as cited in the references. The thesis has not been accepted for any degree and is not concurrently submitted in candidature of any other degree.

Signature: ____________________________

Name: ____________________________

Date: ____________________________

APPROVAL

"I/ We hereby declare that I/ we have read this thesis and in our opinion this thesis is sufficient in terms of scope and quality for the award of the degree of Bachelor of Applied Science (Geoscience) with Honors"

Signature : ……………………………........

Name of Supervisor :

Date : ………………………………………..

ACKNOWLEDGEMENT

First and foremost, I have to thank you my thesis supervisor, Dr. Wani Sofia binti Udin. Without her assistance and dedicated involvement in every step throughout the process, this paper would have never been accomplished. I would like to thank you very much for the support throughout the process of conducting this paper.

I would also like to dedicate my gratitude to the authority of University Malaysia Kelantan and Faculty of Earth Science for all the facilities and equipment provided throughout this paper.

Besides that, I would like to acknowledge my parents and siblings for their sincere moral supports. With their unfailing supports and continuous encouragements throughout my years of study, through the process of researching and writing this thesis, this accomplishment would not have been possible without them.

Finally, I must express my very profound gratitude to my friends. For many memorable evenings out and in, I must thank everyone above for listening to and, at times having to tolerate me over the past four years. I cannot begin to express my gratitude and appreciation for their friendship as they have been unwavering in their personal support during the time I spent at the University.

I also place on record, my sense of gratitude to one and all, who directly or indirectly, have lent their hands in this paper.

Thank you.

Nur Aina Shahira bin Norazami

2019

GEOLOGY AND UAV-BASED FOR LANDSLIDE RISK AREA MAPPING OF KAMPUNG PENDUK, JELI, KELANTAN

ABSTRACT

Malaysia as one of the tropical countries has frequently faced landslide hazard. One of the most frequent landslide areas of landslides occurrence in Malaysia is along Jeli-Gerik Highway. Therefore, it is important to understand the general geology surrounding the area and identify the landslide prone area to avoid or minimize the effect of landslide hazard. Kampung Penduk is a small village in Jeli district near the boundaries of Perak and Kelantan. Kampung Penduk is located alongside Jeli-Gerik Highway. The geological information specifically in the study area is insufficient because previous study around the study area only cover the lithology and structure around the study area. An updated geological map of the study area in scale 1:25,000 was produced from the geological mapping conducted. This research also present an integrated approach for mapping and analyzing spatial features of a landslide from remote sensing image and UAV technology. In order to assess the capabilities of UAV in landslide hazard mapping, digital photogrammetric products such as orthophotos, Digital Elevation Models and 3D Image based on landslide risk area along Jeli-Gerik Highway were produced. Landslide risk area map was also generated by using data such as elevation, slope angle and aspect of the landslide area which can be categorized into very low, low, moderate, high and very high. Hence, the identification of landslide-prone area is essential for carrying out quicker and safer mitigation programs. Both geological map and landslide risk area map are important for hazard management and future strategic planning to minimize the risk of landslide hazard in the study area.

GEOLOGI DAN UAV BERDASARKAN KAWASAN RISIKO LANDSLIDE MAPPING KAMPUNG PENDUK, JELI, KELANTAN

ABSTRAK

Malaysia sebagai salah satu negara tropika sering menghadapi bahaya tanah runtuh. Salah satu kejadian tanah runtuh yang paling kerap terjadi di Malaysia adalah sepanjang Lebuhraya Jeli-Gerik. Oleh itu, adalah penting untuk memahami geologi umum di sekeliling kawasan tersebut dan mengenal pasti kawasan berisiko tanah runtuh untuk mengelakkan atau meminimumkan kesan bahaya tanah runtuh. Kampung Penduk adalah sebuah kampung kecil di daerah Jeli berhampiran sempadan Perak dan Kelantan. Kampung Penduk terletak di sebelah Lebuhraya Jeli-Gerik. Maklumat geologi khusus di kawasan kajian tidak mencukupi kerana kajian sebelumnya di sekitar kawasan kajian hanya meliputi litologi dan struktur di sekitar kawasan kajian. Peta geologi terkini kawasan kajian dalam skala 1: 25,000 dihasilkan daripada pemetaan geologi yang dijalankan. Penyelidikan ini juga membentangkan pendekatan bersepadu untuk pemetaan dan menganalisis ciri-ciri spatial tanah runtuh dari imej penginderaan jauh dan teknologi UAV. Untuk menilai keupayaan UAV dalam pemetaan bahaya tanah runtuh, produk fotogrametri digital seperti orthophotos, Model Ketinggian Digital dan Imej 3D berdasarkan kawasan risiko tanah runtuh di sepanjang Lebuhraya Jeli-Gerik dihasilkan. Peta kawasan risiko tanah runtuh juga dijana dengan menggunakan data seperti ketinggian, sudut cerun dan aspek kawasan tanah runtuh yang boleh dikategorikan menjadi kawasan sangat rendah, rendah, sederhana, tinggi dan sangat tinggi. Oleh itu, pengenalpastian kawasan risiko tanah runtuh adalah penting untuk menjalankan program-program mitigasi yang lebih cepat dan selamat. Kedua-dua peta geologi dan peta kawasan risiko tanah runtuh adalah penting untuk pengurusan bahaya dan perancangan strategik masa depan untuk meminimumkan risiko bahaya tanah runtuh di kawasan kajian.

TABLE OF CONTENT

LIST OF TABLES

LIST OF FIGURES

CHAPTER 1

INTRODUCTION

1.1 General Background

Geology is the study of earth science cover from the formation of the universe, solar system and planet Earth to the components of rocks and minerals of geological landform. Geology also includes the study of geological processes and geohazards. The study of general geology is usually conducted through a geological surveying method. A geological survey is a practical method of research to study the geology of the study area with the purpose of producing a geological map. Geological surveying methods employ research techniques such as the common walk-over survey to studying outcrops and landforms.

Next, geophysical methods and remote sensing tools frequently use in geological surveying. Example of Remote Sensing (RS) method are seismic methods (active and passive), electrical methods, magnetic methods, gravity methods and radiometric method. Examples of remote sensing techniques use during geological mapping are aerial photography and satellite imagery. All the remote sensing imagery/data was integrated within a Geographic Information System (GIS) to produce a geological map. A geological map generally displays the boundaries of geological units on a topographic map. General geological map includes cross sections below the geological map to portray the three-dimensional interpretation.

Landslide is sudden downslope slip movement of a mass of rocks, debris and soils under the influence of gravity. The movement of slope occurs when the shear strength of the earth materials that compose the slope overpower the force that acting downslope such as gravitational and other types of shear stresses within a slope. Turner et al. (2015) state that landslide is a massive things that can cause huge negative impact on mental and physical on a person which a few time cause deaths. There is two fundamental aspect that can cause the occurrence landslide which is human and environmental factor. Human effect is controllable while environmental effects are uncontrollable. An environmental factor that can initiate landslide is on slopes that already on the verge of movement are heavy rainfall, earthquakes, shift in water and groundwater level, snowmelt, stream erosion, and volcanic activity. Landslides are one of the major disasters around the world. Landslide hazards cause huge damages and casualties to human and environment.

Landslide risk area mapping is conducted to produce a landslide risk area map. Basically, landslide risk area maps classify the area into high, moderate and low risk area for a landslide to occur. A good landslide risk area map shows the probability of landslide occurrence at a particular area. It also should be able to show how big the affected area and how far the landslide can possibly move.

Remote sensing is a software that has to be combined with other techniques to produce landslide risk area map (Mantovani et al., 1996). There are a few types of remote sensing platforms can be used to monitor landslide occurrences. For example manned aerial vehicles, remote sensing satellites, land vehicles that has equip with special machine/software and Unmanned Aerial Vehicles (UAV) as one of the newest technique (Rau et al., 2011). Monitoring landslides using UAV systems revolve around two process which are aerial mapping and ground surveying methods. Most of the measurement devices that require details information are collected during flight time. The measument that needed to be taken on the ground surface is measuring and determining the control points (Nagai et al., 2008).

1.2 Study Area

1.2.1 Location

The study area are located inside Batu Melintang, Jeli, Kelantan. Kelantan state is located in the north-eastern part of the Peninsula Malaysia where Kota Bharu is the capital city. It is located in-between 3 states which area Perak to the west, Pahang to the south, and Terengganu to the east. Kelantan has an area of 15,022 km2. Jeli is one of the districts in western Kelantan, bordered by Thailand to the north, Perak to the west, Kuala Krai district to the south-east and Tanah Merah district to the northeast. The coordinate of Jeli area is 5°42′N, 101°50′E and 5.700°N, 101.833°E. Batu Melintang is a neighbourhood in Jajahan Jeli, Kelantan. One of the main attraction in Batu Melintang is Gunung Reng. Kampung Gunung is the closest village to Gunung Reng, but the name Batu Melintang is more popular and commonly used by everyone. The neighbourhood around Batu Melintang is in scattered settlements.

To be more precise, the research study area is along Jeli-Gerik highway alongside with Kampung Pendok, Kelantan. The study area covered approximately 25.0 km^2 bounded between latitude $N\,5°\,41'\,10''$ to $N\,5°\,38'\,29''$ and longitude $E\,101°\,41'\,52''$ to $E\,101°\,44'\,36''$. Figure 1.1 is the base map of the study area.

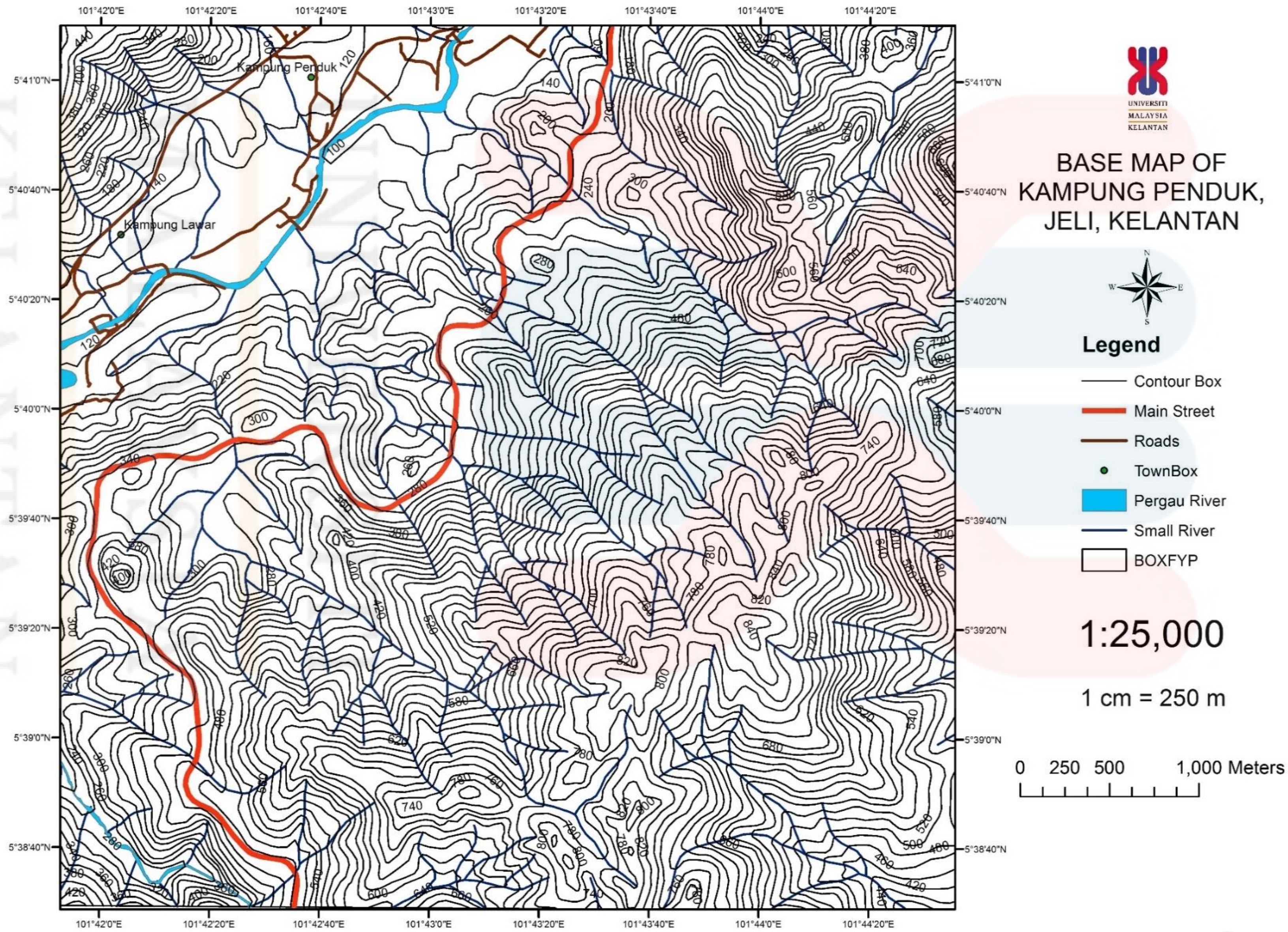

Figure 1.1: Base Map of the study area

1.2.2 Road

The study area can be accessed by using two pathways. The first pathway is through Jeli-Gerik highway which is a highway that crosses the border of Perak and Kelantan state. This path takes about 22 minutes by using car from UMK Campus Jeli. This road can be access by most vehicles except for train and flight. It takes about 4 hours 42 minutes by walking. The distance of this path from UMK Campus Jeli is 21.8 km. Figure 1.2 show the first pathway to enter the study area.

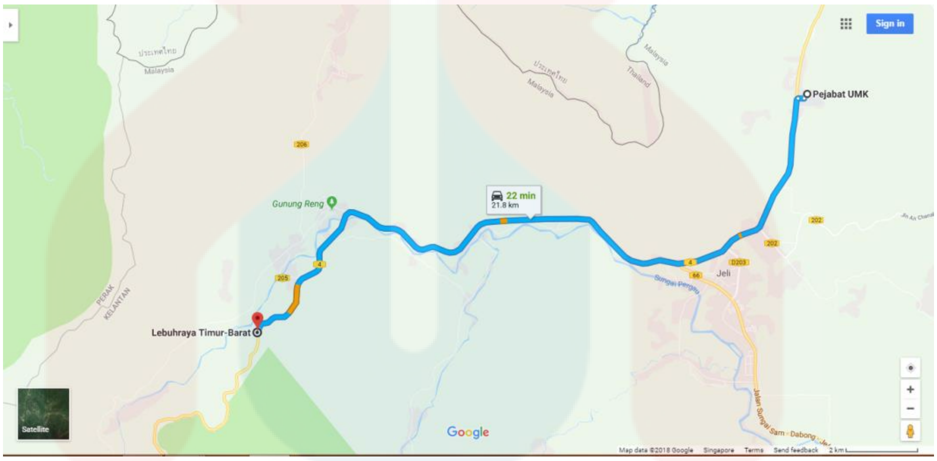

Figure 1.2: First pathway to enter study area (Google Earth, 2018)

The second pathway is through Batu Melintang. This path take about 26 minutes by car from UMK Campus Jeli and takes about 5 hour 2 minutes by walking. This path can also be access by most vehicles except for trains and flight. The distance of this pathway is 23.6 km. Figure 1.3 show the second pathway to enter the study area.

Figure 1.3: Second pathway to enter study area (Google Earth, 2018)

1.2.3 Demography

Based on Jabatan Perangkaan Penduduk Negara Negeri Kelantan, the total number of residents in Kelantan is 1,641,9001 (2010), 690,300 (2011), 1,772,800 (2012), 1,806,100 (2013), and 1,849,700 (2014). The number show an increasing rate in the number of residents in Kelantan from 2010 until 2014

In Jeli district, the number of residents in Jeli also increase every years from 2010 until 2014. In 2010, the number of residents are 48,000. The number increase to 53,200 in 2014. Jeli district has the lowest number of residents in all districts in Kelantan State. The highest number of residents belong to Kota Bharu with 560,100 residents. Table 1.1 show the projection of residents in Kelantan 2010-2014

Table 1.1: Projection of Residents in Kelantan 2010-2014

(Source: Jabatan Perangkaan Penduduk Negara Negeri Kelantan)

Districts	**Years**				
	2010	**2011**	**2012**	**2013**	**2014**
Bachok	142,100	146,000	149,900	153,800	157,700
Kota Bharu	509,600	522,000	534,500	547,200	560,100
Machang	101,300	103,900	106,400	109,000	111,700
Pasir Mas	212,000	217,300	222,800	228,300	233,800
Pasir Putih	134,200	137,700	141,100	144,600	148,200
Tanah Merah	133,400	136,700	140,000	143,300	146,700
Tumpat	137,200	177,700	182,200	186,800	191,400
Gua Musang	103,300	106,000	108,800	111,700	114,500
Kuala Krai	120,800	123,700	136,500	129,500	132,400
Jeli	**48,000**	**49,300**	**50,600**	**51,900**	**53,200**
Kelantan	**1,641,900**	**1,690,300**	**1,772,800**	**1,806,100**	**1,849,700**

1.2.4 Land Use

Area of the Jeli district is 131,916 hectares which total 7.83% of the total area in Kelantan. Jeli district is the fourth largest colony in the State where the largest district is Gua Musang followed by Kuala Krai and then Lojing. Table 1.2 show the capacity and percentage of each district in Kelantan

Table 1.2: Capacity and percentage of Kelantan

(Source: Department of Survey and Mapping Malaysia, Kelantan, 2015/2016)

District	Area (Hectare)	Percentage (%)
Kota Bharu	40,144	2.38
Pasir Mas	56,707	3.36
Tumpat	17,725	1.06
Pasir Putih	42,302	2.52
Bachok	27,825	1.65
Kuala Krai	227,670	13.52
Machang	52,791	3.14
Tanah Merah	87,948	5.22
Jeli	**131,916**	**7.83**
Gua Musang	817,595	48.54
Lojing	181,700	10.78
Total	**1,684,323**	**100%**

1.2.5 Social Economy

Jeli mainly compose of rubber tappers. The local owns rubber plantations attract outsider to come and work in Jeli rubber plantation business. Due to lineage, most local families own a small plantation of about 6 acres to 50 acres land. According to history, Jeli area began to develop when the government encouraged the Kelantanese and people around them to start venturing into agriculture work prospect in a large scale manner.

There are 7 primary school in Jeli which are Sekolah Kebangsaan Jeli 1, Sekolah Kebangsaan Jeli 2, Sekolah Kebangsaan Pendok, Sekolah Kebangsaan Batu Melintang, Sekolah Kebangsaan Sungai Long, Sekolah Kebangsaan Bukit Jering and Sekolah Kebangsaan Kalai (Kalai National School). Jeli has 2 famous boarding school which are MARA junior science college and Sekolah Mara Sains Jeli. Sekolah Mara Sains Jeli is a full boarding school and widely known as JeSS.

Politeknik Jeli and Universiti Malaysia Kelantan (UMK), Kampus Jeli are two higher learning institutions, located in Jeli. UMK Kampus Jeli is science oriented and has been operating since 2012.

1.3 Problem Statement

Kampung Penduk Village is a small village nearby Kelantan-Perak boundary. It located alongside Jeli-Gerik Highways there are a few research conducted nearby or around the study area. Unfortunately,the research does not cover general geology of the study area. Thus, there is less geological data and information about the study area that can be used as a reference to others. In order to tackle this issue, a geological survey was conducted to collect data and information about the geological features of the study area. From the data and information collected, a complete geological map can be produced by using GIS.

Malaysia as one of the tropical countries has frequently faced landslide hazard. A landslide triggered by natural sources such as rainstorm, flood and earthquake often results in major human casualties and property loss. It is one of the main constraints for development projects in the highlands of the country. Most of these landslides occur in steep hilly areas and highlands as shallow rainfall-induced landslides that usually trigger aftermath of a heavy rainfall. One of the most frequent areas of landslides occurrence in Malaysia is along Jeli-Gerik Highway. Thus, the aim of this research is to present an assimilated techniques for mapping and analysing spatial features of a landslide from remote sensing image and UAV technology.

Natural phenomena such as landslide are notoriously difficult to model and simulate. There are no laboratory exists out there that can predict natural hazardous events. Let say landslide, no company or laboratory currently able to preliminarily measure important variables, refine the techniques, and apply the results. Thus, the identification of landslide risk area is very important for future strategic planning of an area. It also important in helping carrying out faster, quicker and safer mitigation programs during emergency time.

1.4 Objectives

The objectives of this research are

1. To produce a geological map of the study area in scale 1; 25,000.
2. To assess capabilities of UAV in the production of digital photogrammetric products based on landslide risk area along Jeli-Gerik highway.
3. To produce landslide risk area map using UAV technology.

1.5 Scope of Study

This research covers the standard production of the geological map. The research is restricted in the study area only which is about $5 \times 5 \text{ km}^2$ around Kampung Pendok excluded the neighbouring district and state. This research uses the most basic geological tools such as GPS, compass, hammer and others. The samples that were collected during the fieldwork have undergone thin section if needed. This research covers the morphology, stratigraphy, regional geology and demography of the study area.

This research also focused on the technique in combining UAV technology, RS image acquisition, processing, and GIS-based assessment where the data collected are integrated in producing a landslide risk area map (Nagai et al., 2008). The process involves in this research are UAV flight planning, aerial image data collection and data processing by using Fix4D to produce orthomosiacs and Digital Elevation Model (DEM). By overlaying data in GIS and zoning process, a landslide risk area map is produced.

1.6 Significance of Study

Geological research is conducted to gather geological data and information of the study area with the final product of the geological research is a geological map. The research can be used by Jeli Land and District Office and Department of Public Work (JKR) Kelantan. Construction of buildings, damp, water distribution system and other requires planning because they have huge effect to their surroundings for a huge period of time in order to build and maintaining a sustainable society. Jeli Land and District Office are responsible for regional and municipal plans. The geological information contains in the geological map is important in solving many obstacle and planning problem. This information is to be used for assessing factors such as soil stability, geomorphological condition, geological formations with high natural values and natural resources. The research also can be referred to JKR Kelantan to build systematic and save roads in the study area. lastly, this research can be used by another researcher who wants to do research around the study area.

Geospatial technology can be used as an alternative to natural risk area research and environmental planning. The landslide risk area mapping research can be implemented under the guidance of experience expects that have a lot of experience in using the RS/GIS technology. This semi-automated image analysis technique can be comparably efficient. These expected results of a landslide risk area map is that it can show the location and detailed information of the landslide. It also can indicate the aerial extent of the possible damage range of the landslide.

CHAPTER 2

LITERATURE REVIEW

2.1 Introduction

This chapter composed of all literature review of the previous studies and researchers that related to this research. This chapter covers the literature review of both general geology of the study area and research specification. It included the regional geology and tectonic setting, structural geology, stratigraphy, sedimentology of Jeli. This chapter also covers the literature review of Remote Sensing, GIS and UAV technology in landslide risk area.

2.2 Regional Geology and Tectonic Setting

Kelantan is one of the states in the north-east of Peninsular Malaysia with Kota Bharu as the state capital. The state of Kelantan longitude aligned from E $101° \, 20'$ to E $102° \, 41'$. Whereas the latitude extend from N $4° \, 33'$ to N $6° \, 14'$. The state of Kelantan covers approximately $15,022 \, \text{Km}^2$ which then classify into four types of rock that cover the whole state of Kelantan. Those four types of rock are unconsolidated sediments, extrusive rocks, granitic rocks and sedimentary/metasedimentary rocks (Department of Mineral and Geoscience Malaysia, 2003). Table 2.1 displays the percentage of the distribution of the rock types in the Kelantan. Figure 2.1 shows the general geology map of Kelantan. Figure 2.2 show thematic stratigraphic column of Batu Melintang - Sungai Kolok Transect area in Malaysia

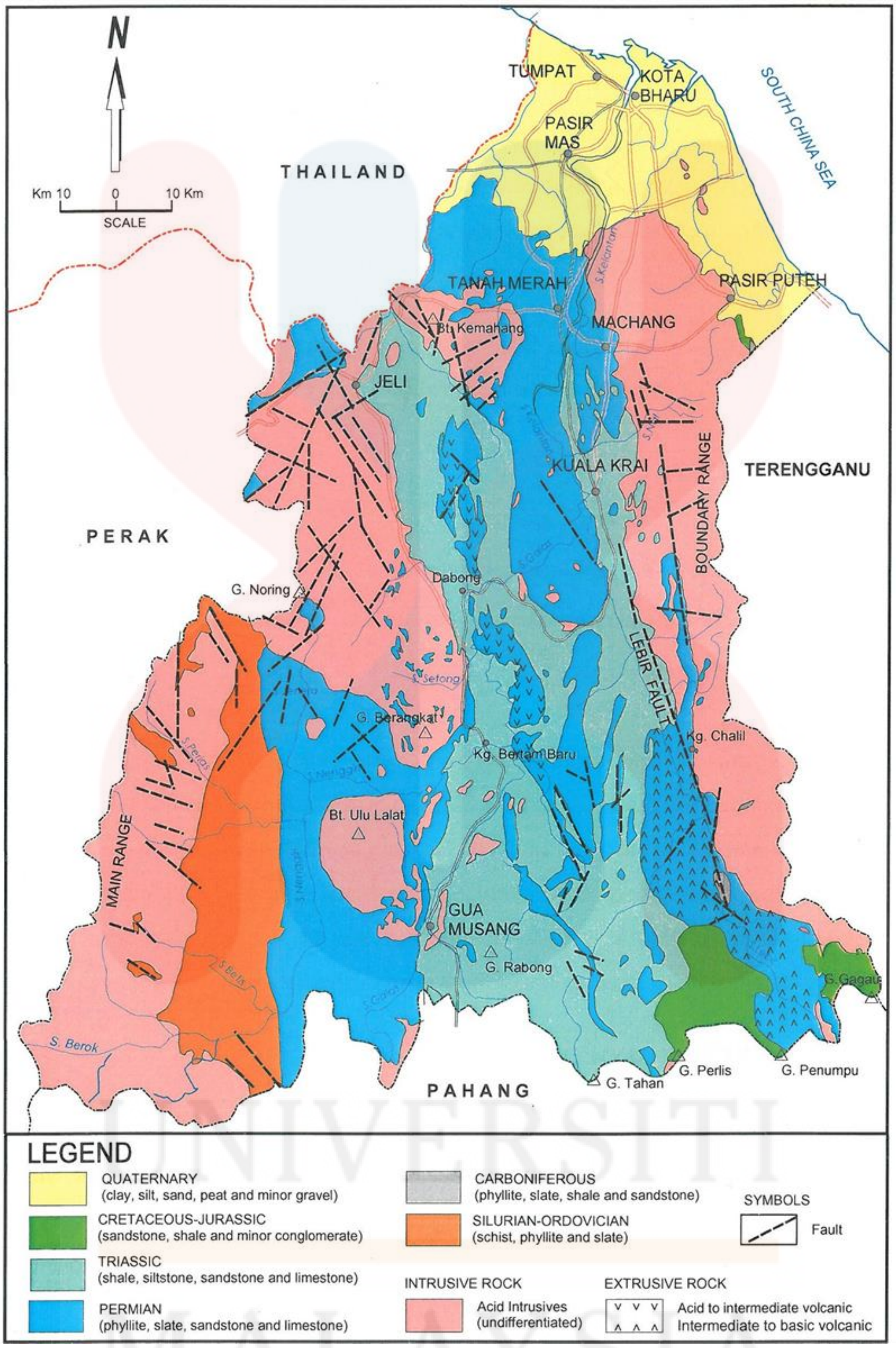

Figure 2.1: General geology map of Kelantan

(Modified from Department of Minerals and 812 Geoscience Malaysia, 2003)

Table 2.1: Distribution of rock types in the States of Kelantan

(Source: Department of Mineral and Geoscience Malaysia, 2003)

Types of Rock	Area
Unconsolidated sediments	6%
Extrusive rocks	10%
Sedimentary/Metasedimentary rocks	51%
Granitic rocks	33%

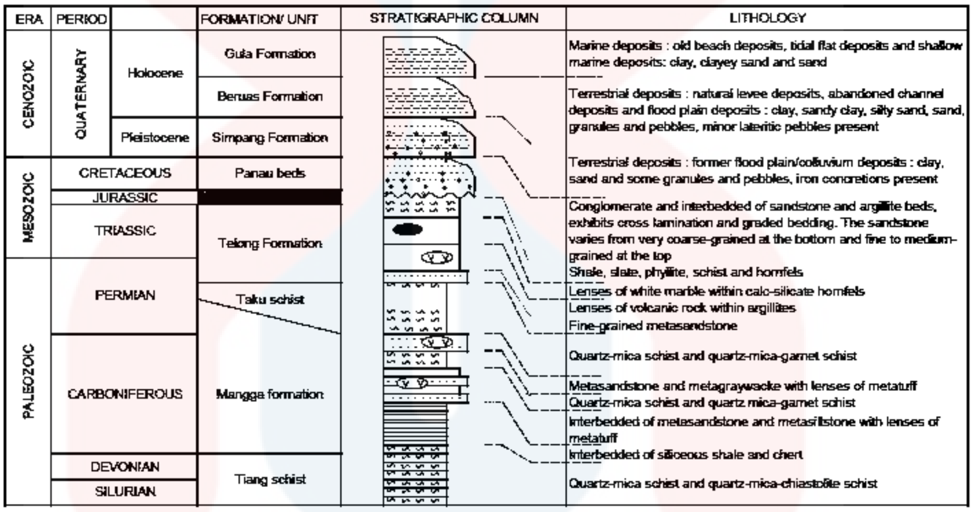

Figure 2.2: Schematic stratigraphic column of Batu Melintang - Sungai Kolok Transect area in Malaysia

The lithology of study area is dominated by metamorphic rocks such as of schist, interbedded phyllite, and quartzite. The slope of the weathered rock is characterised by high angle joints (74-80°) with dip directions between 20° and 330°. The rocks folded with northwest trending fold axes with dip direction and dip amount of the beddings are 250°/24°, 235°/25° and 246°/23°. The other bedding planes are 354°/24°, 351°/25°, 352°/24°. The joint orientations are approximately perpendicular to the direction of the beddings. Some reverse faults also cut across the bedding planes.

2.3 Stratigraphy

Tiang Schist is the oldest rock formation which occurs in the Paleozoic period while Gula Formation is the youngest rock formation which occurs in the Cenozoic period. The Silurian-Devonian Tiang Schist rock unit was then unconformably overlain by Mangga Formation which was probably around Carboniferous-Permian period. Taku Schist which probably Carboniferous was unconformably overlain by Telong Formation which was age Permo-Triassic. Rock unit of Jurassic age cannot be found then the Telong formation was overlain by the Panau beds of Cretaceous. The Panau beds underlaid the Simpang Formation of age Pleistocene and then Simpang Formation underlay the Beruas Formation then Gula Formation as the youngest formation.

The formation which was speculated to be found in the study area was the Tiang Schist Formation. The Tiang Schist Formation in Malaysia consists of quartz schist and quartz-mica schist. The quartz-mica schist is strongly schistose, well foliated, consisting essentially of quartz and mica (commonly muscovite) with chlorite, calcite and pyrite as accessory mineral. Although muscovite is predominant, biotite is fairly common. Lenses of amphibolite schist comprising quartz-actinolite-tremolite schist and quartz-hornblende schist occur at several localities along Sungai Tiang. Rohayu (1994) reported that sillimanite gneiss has been found at higher terrain along the East-West Highway in the Belum area, 10 km southwest of the Transect area. The presence of quartz-mica-chiastolite schist indicates that it might be the result of both contact and regional metamorphisms. Although granite is not exposed in the surrounding area of quartz-mica-chiastolite schist, it is believed that granite is sub-cropping below the metamorphic rocks. The foliation has various trends and dip steeply both eastwards and westwards resulting from intensive folding and faulting. The rock unit is highly folded and faulted throughout the area and it is difficult to estimate its thickness.

2.4 Structural Geology

The regional structures of the area included local anticlines and synclines with the minor structure of small-scale tight folding and parallel folding. The Tiang Schist start showed moderate to steep dipping. Besides, Mangga Formation was fairly folded and moderate to steep dipping. The folding and faulting might have occurred during Triassic to Cretaceous might due to granite intrusion. Faulting was found to be present in all rock units which were mostly of normal fault with minor displacement. The major faults were shown to be trending in direction of the northwest to the northeast (Malaysia and Thai working group, 2006). The Pergau fault was found trending northeast-southwest along part of Sungai Pergau which flowed from the boundary between Noring and Mangga Formation (Malaysia and Thai working group, 2006). The north-south trending Bentong Raub Nature Zone was probably located in the western part which shows indicator olistostrome occurrence that was exposed at east-west highway (Tjia, 1989).

2.5 Historical Geology

Since the Cretaceous deformations, the structural development of the late Palaeozoic metamorphic rocks in the study area has become weak. This is because of the presence of discontinuity. Long exposure, the weathering process and climatic factors have caused these rocks experienced failure and movements.

The geology of the study area was initiated by the development of folding at the NNW axis due to NNE compression during the Late Palaeozoic to Early Mesozoic deformation. Another deformation occurred during the Cretaceous period (Tjia, 1998) in an E-W compression direction. The later orogeny cut across the rocks and the previous fold axis by a NNE-trending lateral fault. The structural interpretation of the metamorphic rocks in the study area has been subjected to polyphase deformations, meaning that at least two phases of folding, with one fold axis trending NW-SE and another fold trending N-S, have been identified. The bed strikes NNW and SSE, with a dip steeply toward the SSW and ENE. It is also reported that a reverse fault system developed after brittle deformation occurred. The N-S fault zone is the youngest known fault zone in the study area, cutting across the young granitic rock and subsequently cut by a lateral fault system (Tjia, 1998). The direction N44°E was considered the main regional compression direction for the peninsula, because it was also recorded at Pulau Kapas (Gasim, 1988) and Terengganu (Gasim et al., 2010).

2.6 Landslide

Landslide is sudden downslope slip movement of a mass of rocks, debris and soils under the influence of gravity. A landslide occurs when the shear strength of the materials that make up the slope overpower the force that acting downslope such as gravitational and other types of shear stresses. Landslide is a global phenomenon that creates dramatic physical and economic effects and sometimes leads to tragic deaths (Turner et al. (2015).

According to data from the US National Aeronautics Space Administration (NASA), Malaysia had 171 landslides between 2007 and March 2016, making the country ranked the 10th highest in frequency of landslides. Ranked first is the United States (2,992), followed by India (1,265) and China (426). Titled the Global Landslide Catalog (GLC), the one-of-its-kind dataset was compiled based on online and media reports, and scientific journals since 2007.

The Star analysed the dataset and found that the number of landslides have been increasing in Malaysia, almost with each year, reaching a peak of 33 occurrences in 2014. On average, in the past 10 years, Malaysia experienced 18.5 landslides annually. The high number of landslides means that Malaysia ranked 5th for landslides per square kilometre among countries that have a land area greater than 100,000sq km.

2.6.1 Landslide Trigger Factor

There a few common factors that trigger or initiate landslide movement. Natural factor that caused landslide is commonly prolong heavy rainfall and earthquake. Excessive cutting and deep excavation on slope for construction of roads, building and mining without proper management and disposal of debris are the main man-made factor that can caused landslide.

Stability of slopes directly influences the mass rock movement. Factors that control the stability of slopes are angle of slope, attitude, lithology, structure, hydrological condition and sensitivity in the area. Studies revealed that the major forces operating on slopes are the weight of the material building the slope such as rocks, soils, vegetation and man-made structure act downward and the shear strength of the material acting in the potential slip plane.

2.6.2 Landslide Hazard Zonation Parameters (GIS Environment)

There are many basic map require for identification of landslide prone areas and landslide hazard zonation which can be delineated under GIS environment using remote sensing data. Example of basic requirement maps are digital elevation model, contour map, geological map, drainage map, slope angle map, relative relief map, and land use/land cover map.

The Digital Elevation Model (DEM) is the spatial variation in elevation. DEM can be used to generate a lot of map such as slope and relative relief map. Slope one of the major parameter in evaluating stability of an area. It is the first derivative of elevation with each pixel denoting the angle of slope at a particular location. Generally, the higher the angle of slope, the higher the shear stress in soil or other unconsolidated materials. The score rating have to be consider in an area with high vegetation because area with high vegetation tend to have higher slope stability. Relative relief is a calculated difference in maximum and minimum altitude within an area. The higher relief values, the higher the possibility of landslides occurrences.

2.7 Remote Sensing

Remote sensing is a multi-spatial technology. It can be used in many ways especially in the study of landslide. GIS can store a large volume of imaginary data in digital form. The imaginary data that was store can be store, acquired, and analysed in a matter of minutes. Numerous environmental issues was solved by using remotely sensed data. The difficulties of natural hazard research and environmental planning can be assist by remote sensing technology efficiently. Remote sensing technology able to provide terrain information, such as geology, land cover, drainage, and geomorphology. Other than that, quantification of human interference on the Earth's surface can be updated in the existing thematic information.

2.7.1 Geographical Information System (GIS)

GIS is a computer-based system for data input, output, capture, transformation, manipulation, visualization, query, combination, modelling, and analysis. It has superior spatial data processing capacity which is useful in natural disaster assessment. Some researchers have already have the thought of using GIS and remote sensing technologies together for landslide hazard zonation studies. In order to produce a landslide risk area map, the information was be collected from the aerial photograph were then added and overlaid with the information that already prepares to show the difference between features that occupy the same geographic. The zones of with the difference in the geological feature will undergo zonation process to produce landslide risk area map.

2.7.2 Unmanned Aerial Vehicles (UAV)

UAV or commonly known as a drone is an aircraft piloted by remote control or onboard computers. UAV has been widely used in defines and mapping systems around the world especially in developed countries. The discovery of this new technology especially in topographic areas led to the creation of many UAV models that were originally generated.

Unmanned aerial vehicle (UAV) has been widely used in military mission for a long time ago. As the time goes by, there are increased in UAV performance. The opportunities to photogrammetry field was open due to the development that has occurred in order to obtain digital images for large scale map production. The design, research and production of UAV platform is appropriate in aerial photogrammetry. There are two types of UAV units that can be used for mapping purpose; fixed-wing unit and rotor-wing units. Fixed-wing units need more time to stable before it can captured images on the ground. There are many kinds of fixed wing units have been produced according to its specific application or needs. Fixed-wing units take time to be stabilize when it start flying in the air while rotor-wing units are more stable which make it easier to capture image.

2.8 UAV for Landslide-Based Research

Landslide can occur anywhere in Malaysia without any warning. Most of landslide occurs at man-made slope and natural slopes due to their slope gradient. Landslide cost Malaysian government millions of Ringgit Malaysia (RM) in order to fix landslide affected area. Government take this tragedy serious and determine the best solution on early warning and real time monitoring of landslide.

Recently, Unmanned Aerial Vehicle (UAV) has been widely used for mapping purpose. UAV is able to take photo or aerial image at a certain flight height like 200 m above the ground surface. UAV need a professional controller to control UAV from the ground but the general concept is the same as using manned aerial vehicle. Aerial photograph produce by the UAV is the most reliable data for mapping. It will illustrate the images of the area and the image can easily be interpret.

Surface information can be potentially determined by using photogrammetry. The quality of remote sensing imaginary and DEMs determine the hazard assessment accuracy. UAV able to collect the post-landslide data of the landslide occurrence within a short interval. Usually, the DEM before the landslide is not in a reliable condition. Thus, the DEM before the landslide was produced from the topographical map at the scale of 1:50,000. In general, the hazard maps accuracy relies on the quality and resolution of the input data (Wei Hou et al., 2017). The image sensors integrated into the UAV was used to determine the location data. It was used to monitor the landslide rapid movement in forest areas. UAVs collect the landslide data was in a fast and sensitive way using UAVs (Yaprak, S., et al., 2018).

2.8.1 UAV Selection

The UAV type that was used in the research is a rotor-wing type UAV because it is more stable and able to capture image easily. The rotor-wing type UAV model used is DJI Phantom 4 Pro. The DJI Phantom 4 Pro Obsidian is a super sleek, eye-catching DJI drone, positively bursting with aesthetic appeal and practical functionality. The P4Pro drone line features great speed, range, and a solid camera. The mechanical shutter allows pilots to better capture swiftly moving objects, a marked improvement over the P4 electrical shutter. The result is a high quality image without distortion. Table 2.2 show the general information of DJI Phantom 4 Pro.

Figure 2.3: General information of DJI Phantom 4 Pro

Aircraft	
Weight (Battery & Propellers Included)	1388 g
Diagonal Size (Propellers Excluded)	350 mm
Max Ascent Speed	S-mode: 6 m/s; P-mode: 5 m/s
Max Descent Speed	S-mode: 4 m/s; P-mode: 3 m/s
Max Speed	45 mph (S-mode); 36 mph (P-mode)
Max Tilt Angle	42^o (S-mode); 25^o (P-mode)
Max Angular Speed	250^o/s (S-mode); 150^o/s (A-mode)
Max Service Ceiling Above Sea Level	19,685 ft (6,000 m)
Max Flight Time	Approx. 30 minutes
Operating Temperature	32^o to 104^o F (0^o to 40^o C)
Satellite Positioning Systems	GPS/GLONASS

2.9 Landslide Risk Area Map

According to Van Westen et al. (1999), Landslide Hazard can be separated into two categories which are direct hazard mapping and indirect hazard mapping. Direct hazard mapping determined the degree of hazard by mapping. The mapping is done by geologist according to his/her knowledge and experience about the landform situation. It the opposite of indirect hazard mapping procedure where landslide prone areas are predicted by using deterministic model and statistical models. This action can be done by referring on information obtained from the interrelation between the landslide distribution and landscape factors. A reliable hazard map was the outcome of an extensive comprehension of the combination between meticulous mapping and the geomorphological evolution of an area.

Remote sensing produce two type of information which area spatial and temporal thematic information. A few researchers have imagined the collaboration between remote sensing and GIS technologies for landslide hazard studies. By using various thematic layers, GIS is potential able to produce landslide hazard zonation.

The various causative factors in the form of thematic layers were integrated and analysed in a GIS environment to derive landslide hazard map. Various methods of data integration for landslide hard have been reviewed by Van Westen (1994). Two of significant methods in making landslide hazard map are landslide spatial distribution analysis which provide data and information on the situation of landslides and the ordinal scale approach using weighting-rating system of terrain parameters and the statistical method that finds suitability for small areas with detailed information. The quantitative approach can be adopted for landslide hazard in the Himalaya region due of limited amount of field data that can provided.

CHAPTER 3

MATERIALS AND METHODS

3.1 Introduction

All the materials and methods used in this research are discussed in this chapter. The methodology is the most important stages in conducting a research. It describes all the methods in detail. Remote Sensing, GIS and UAV technology are used to classify risk area of a landslide in the study area. The flowchart of overall research methodology is shown in Figure 3.1

3.2 Materials/Equipment

3.2.1 Geological Mapping Material

This is some equipment that was used during the geological mapping and laboratory analysis. Figure 3.2 shows the equipment used in the research.

a) Global Positioning System (GPS)

GPS is a space-based navigation system that displays accurate coordinate, altitude, bearing and time. GPS is used during geological fieldwork to facilitate finding one's position, mark important geological structures, measuring elevation and add notes of descriptions of formations when collecting the samples.

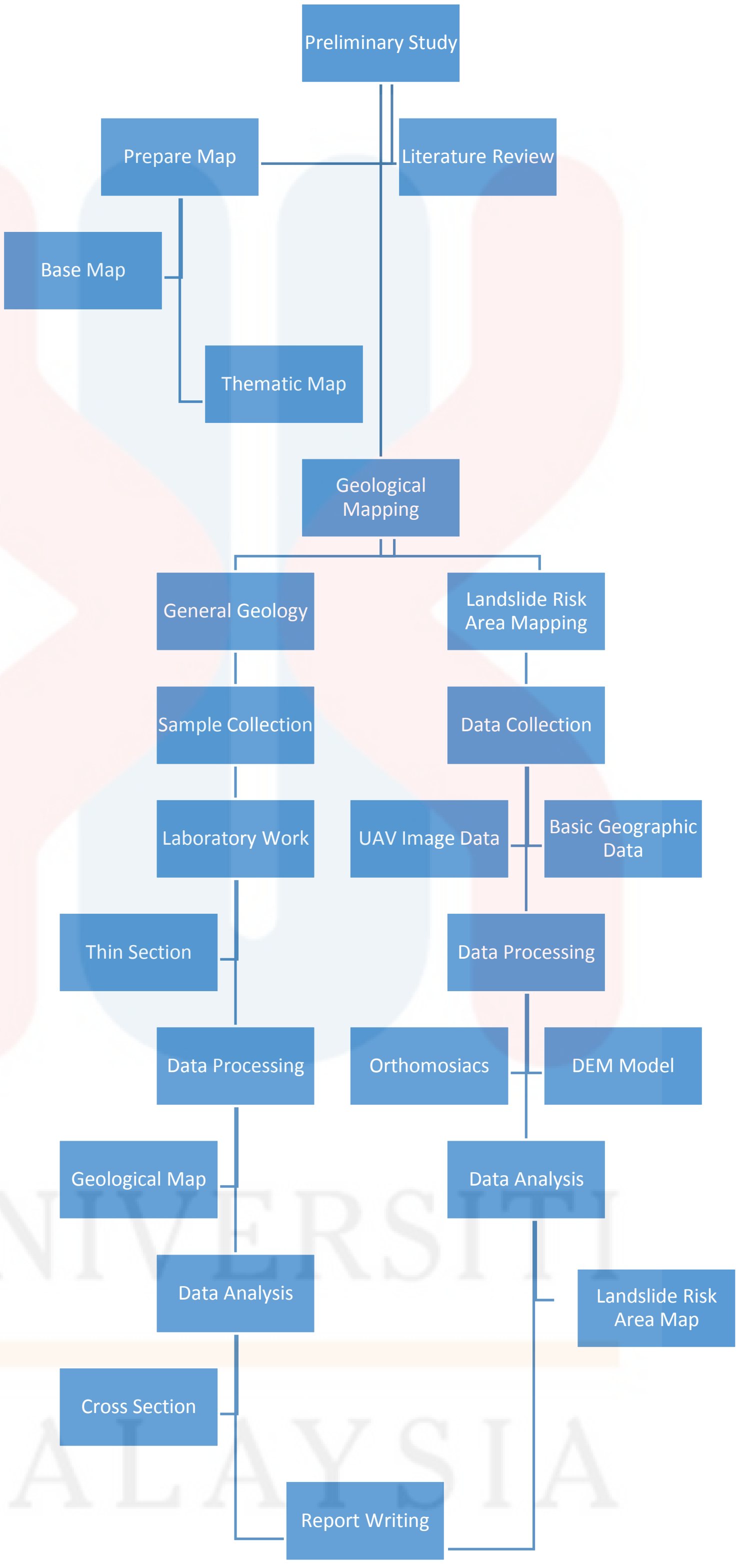

Figure 3.1: Flowchart of research methodology

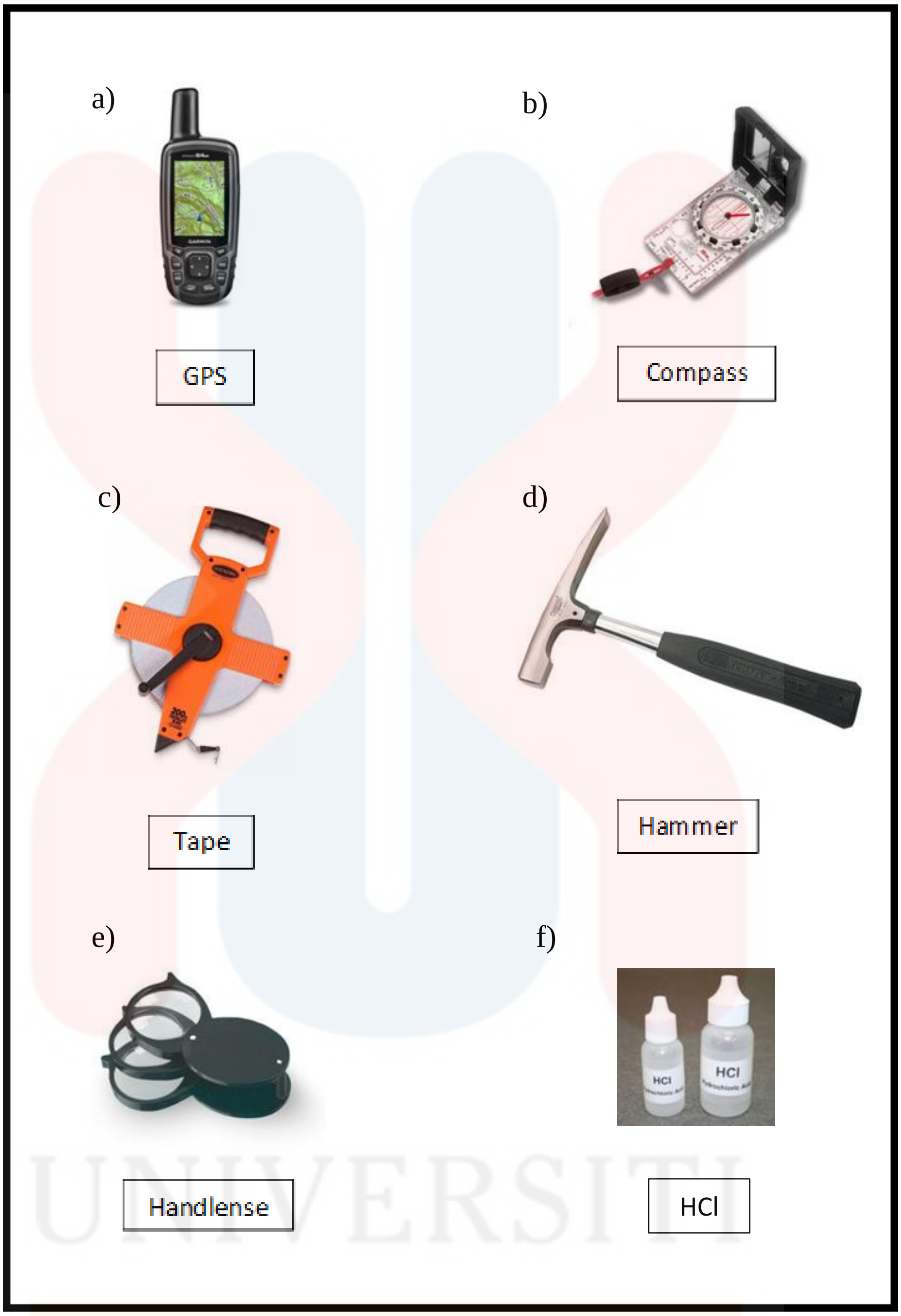

Figure 3.2: Equipment used during the geological research

b) Brunton Compass

Brunton compass is used to take the measurement of strike and dip of geological features such as the faults and sedimentary strata. The other uses included measuring vertical angles with a clinometer and magnetic declination setting and find the bearing.

c) Open Reel Fiberglass Tape Measure

Open Reel Fiberglass Tape Measure is used to take the measure of outcrop and geological features such as joint and the displacement of fault movement.

d) Geological hammer

Hammer is used for collecting samples.

e) Hand lens

A hand lens is used to take a closer look at the grain size and mineral in a sample collected during fieldwork. The detailed and descriptive about the rock type, colour, texture, identifiable mineralogy, alteration have been recorded in the field with the help of hand lens.

f) HCl

HCl is used to test the presence of carbonate in a rock sample during field work. This test can tell the difference between the most common carbonate rock such as limestone and dolomite from other type of rock.

3.2.2 UAV-Based for Landslide Risk Area Mapping Materials

Figure 3.3 show the example of materials that was used during landslide risk area mapping.

Figure 3.3: Equipment used during the specification research

a) ArcGIS 10.2 software

ArcGIS 10.2 is used to produce the base map and the geological map of the study area. The landslide zonation map also produces by using ArcGIS.

b) Satellite Imagery Google Earth

Satellite imageries are governments operated business that collect images of Earth surface by imaging satellites. This system are operated on global scale. Google Earth i used for planning location establishment of ground control point. Figure 3.4 shows the location of landslide area in the study area.

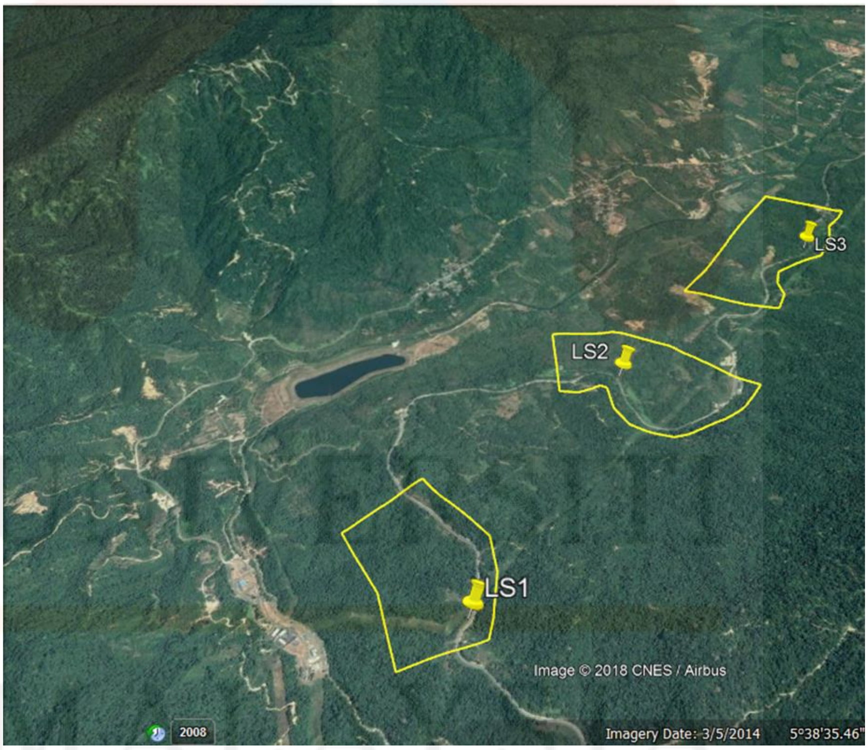

Figure 3.4: Location of landslide area

c) Galaxy G6 (GPS)

Ground Control Points (GCP) were measured by using the Real Time Kinematic (RTK) technique in along Jeli-Gerik highway study area. There were two devices installation involved in this field which are reference station and rover for GCP.

d) Unmanned Arial Vehicles(UAV) - DJI Phantom 4 Pro

UAV based remote sensing is used for mapping and surveying study area. UAV has been used as a platform for photogrammetric data acquisition. There two type of UAV which are fix-wing and rotor type UAV. DJI Phantom 4 Pro are a rotor type UAV. The DJI Phantom 4 Pro Obsidian is a super sleek, eye-catching DJI drone, positively bursting with aesthetic appeal and practical functionality. The P4Pro drone line features great speed, range, and a solid camera. The mechanical shutter allows pilots to better capture swiftly moving objects, a marked improvement over the P4 electrical shutter. The result is a high quality image without distortion.

e) Agisoft Photoscan Pro

Agisoft PhotoScan is a software system that carry out photogrammetric processing of digital images and produce 3D spatial data that can be used in documentation, GIS applications, visual effects production and cultural heritage. The result can be used for indirect measurements of objects of various scales.

3.3 Methodology

In methodology section, the steps to conduct the research are discussed. This section contains preliminary study, field studies, laboratory work, data processing, data analysis and interpretation and final report writing.

3.3.1 Preliminary Studies

Preliminary study is the first step to conduct this research in order to have a better understanding of the general condition of the study area and the basic concept of the research. The information from the published journals, articles and other publications served as the references for the unfamiliar study area. A base map of the study area was produced to display the basic geological feature and information about the study area. Variety thematic maps such as slide incidence map, equal landslide area map, slope map, drainage map was prepared. Merge of two or three themes to generate composite maps. Each of these composite maps was interpreted to arrive at a final hazard zonation. There is a fairly high degree of matching in the high risk zone area and stable zone. Lastly, pre-landslide data and image of the study area was collected from the Google Earth and online research method in order to estimate UAV flight area.

3.3.2 Field Studies

a) General Geology

The geological mapping is a method to collect sample, data and information of the study area. Geological mapping was conducted by using the usual geological survey method such field survey to study lithology and morphology of the study area.

b) Landslide Risk Area Mapping

The landslide risk area mapping was conducted by using the rotor-wing type UAV to collect aerial data. The UAV model used for the research is DJI Phantom 4 Pro. The design of the DJI Phantom 4 Pro consist of aircraft body, vision system and camera build in camera. The remote controller that controlled the UAV was programmed to shoot photos regularly for every two seconds to trigger the shutter of the camera at desire frequency intervals. The camera and the main flight controller card is connected using a special cable. All photos was taken in the JPEG, DNG (RAW), JPEG + RAW format during the flight session and store in the camera memory system.

Ground Control Points (GCPs) were measured by using the Real Time Kinematic (RTK) technique in along Jeli-Gerik highway study area. There were two devices installation involved in this field which are the reference station and rover for GCP The field data were computed and adjusted. Thus, the coordinate values for the GCPs were established. Total eight station were used as GCPs with full 3D (XYZ) coordinates points. Figure 3.5 shows the location of GCPs station in the study area while Table 3.1 shows X, Y, and Z coordinates.

Figure 3.5: Location of GCPs stations.

Table 3.1: The 3D location of GCPs

CODE	LATITUDE (N)	LONGITUDE (E)	H
GCP 1	5 39 48.9614	101 43 01.8412	236.478
GCP 2	5 39 50.7999	101 42 42.1229	255.291
GCP 3	5 39 53.7508	101 42 30.3708	267.870
GCP 4	5 39 51.1564	101 42 13.9529	282.646
GCP 5	5 39 44.7048	101 41 59.2662	308.871
GCP 6	5 39 26.9783	101 42 00.0269	335.756
GCP 7	5 39 12.6716	101 42 13.7947	372.845
GCP 8	5 38 54.9138	101 42 16.5273	414.889

The 3D GCPs was placed in an area that they can be easily detected in photos taken during flight time. The GCPs was place close by the landslide site but area will not be affected by future landslides. All GCPs was placed as concrete blocks which were topped with side wings with dimensions of 40×15 cm so they could be easily be detected in a computer environment. The 3D positional information of the GCPs was collected by the CORS-TR System (Mekik et al., 2011) using Topcon GR3 dual-frequency Global Navigation Satellite System (GNSS) receivers. Figure 3.6 show the Galaxy 6 GPS on a tripod.

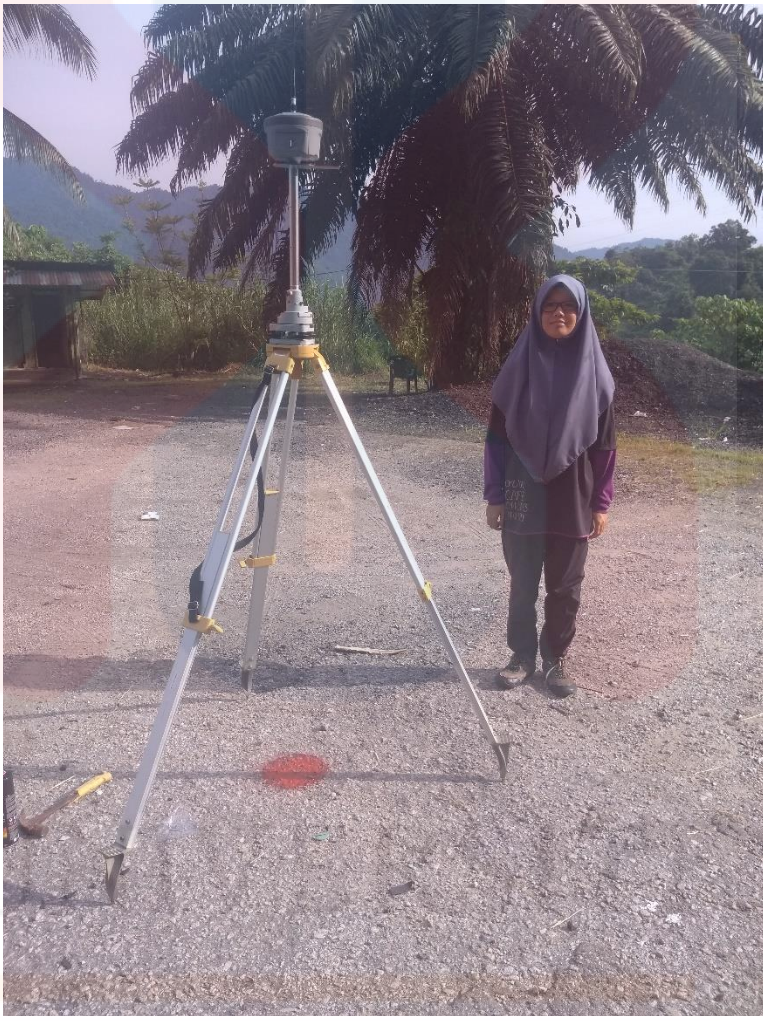

Figure 3.6: The Galaxy 6 GPS on a tripod

The flight plans was made following the GNSS measurements of the GCPs and obtaining their coordination via analysis. The flight plan for the study area was set within the Mission Planner software. A number of overlapping images was computed for each pixel of the orthomosaics. The map should include number of aerial photograph and flight strips. The overlap between photographs also should be more than 60% and 30% side lap. Figure 3.7, 3.8 and 3.9 show the overlap photograph for landslide 1, 2 and 3 respectively.

Figure 3.7: Overlap photograph of landslide 1

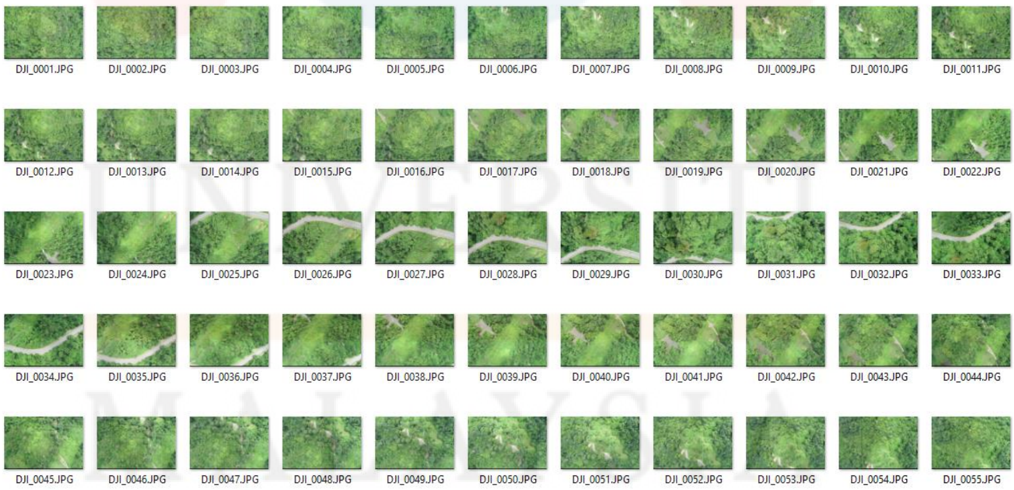

Figure 3.8: Overlap photograph of landslide 2

Figure 3.9: Overlap photograph of landslide 3

Flight planning system for DJI Phantom 4 Pro UAVs is essential for planning the number of sorties, take-off and landing. Meteorological factors was considered in shooting the aerial photos and the most suitable time periods will be chosen for the flights. Thus, weather conditions should be first verified in order to make sure it is suitable for flying. The planning software also examine specification (electronic parts) & test other function (GPS, rotor, electronic speed, etc.) during flight test. Next, it can be integrated with real-time weather and maps such as Google map. Aerial photographs of landslide area were captured at fixed speed and flying height of 200m. An inspection has been made after capturing strips of images of the study area in term of image quality and coverage completeness of the photographs. The end product of the steps is UAV Image data and basic geographic data. Figure 3.10, 3.11 and 3.12 show the UAV flight pathway in landslide 1, 2 and 3 respectively.

Figure 3.10: UAV flight pathway for landslide 1

Figure 3.11: UAV flight pathway for landslide 2

Figure 3.12: UAV flight pathway for landslide 3

3.3.3 Laboratory Work

The sample collected undergoes petrographic thin sections process for further analysis of the mineral composition under a microscope. Generally, the steps of the petrographic thin sections process start with cut the rock samples into glass slide size. Next, frost the glass slide. Then, cement the samples to slide. Lastly, grind the section on thin section machine and hand grind the section.

3.3.4 Data Processing

a) General Geology

All the geological data that obtained from the field observation was processed by using the GeoRose, Stereonet and ArcGIS software. For the joint, fold and fault analysis, GeoRose and Stereonet software was used by plotting the geological data such as strike and dip to explain the direction of force acted on the study area.

ArcGIS software will was used to update geological data of study area and produce a geological map at the end of the process.

b) Landslide Risk Area Mapping

The photo that was obtained from the flight period was stored in a computer. The photo was analyzed by using the Agisoft Photoscan Pro software. In the first stage, quality checks will be conducted for the images, dataset, camera optimization and GCPs. All these data was calculated and the software produces the quality check report. Figure 3.13 shows workflow to build DEM while Figure 3.14 shows the workflow to build orthomosiacs in Agisoft Photoscan Pro software.

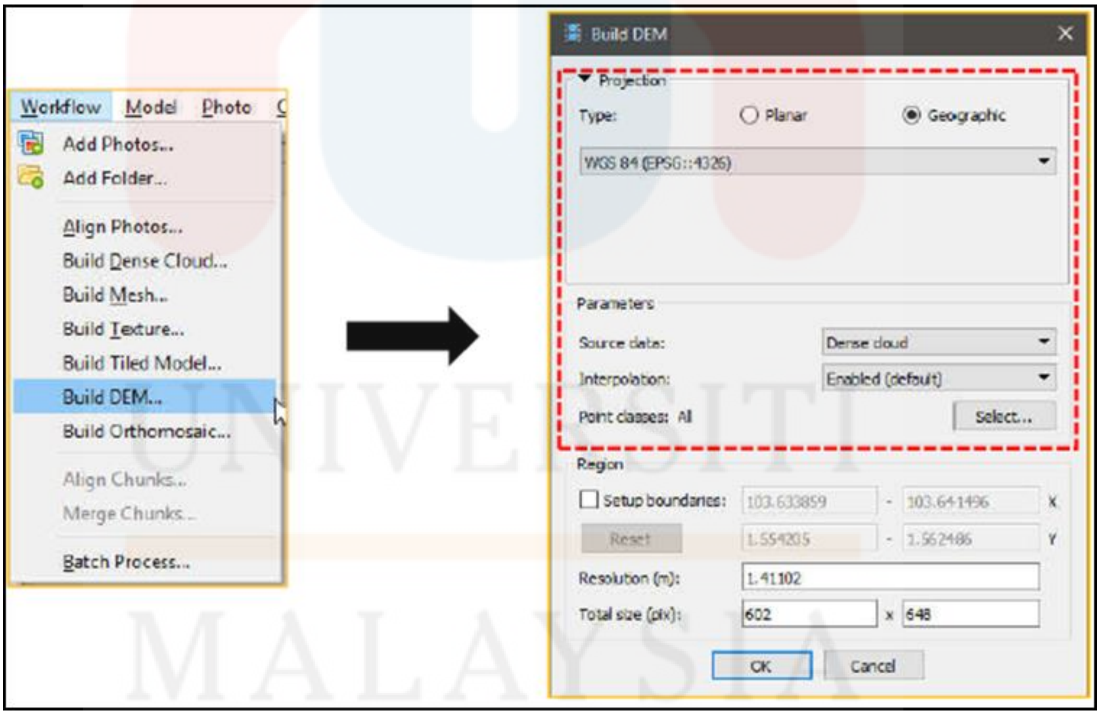

Figure 3.13: Workflow to build DEM

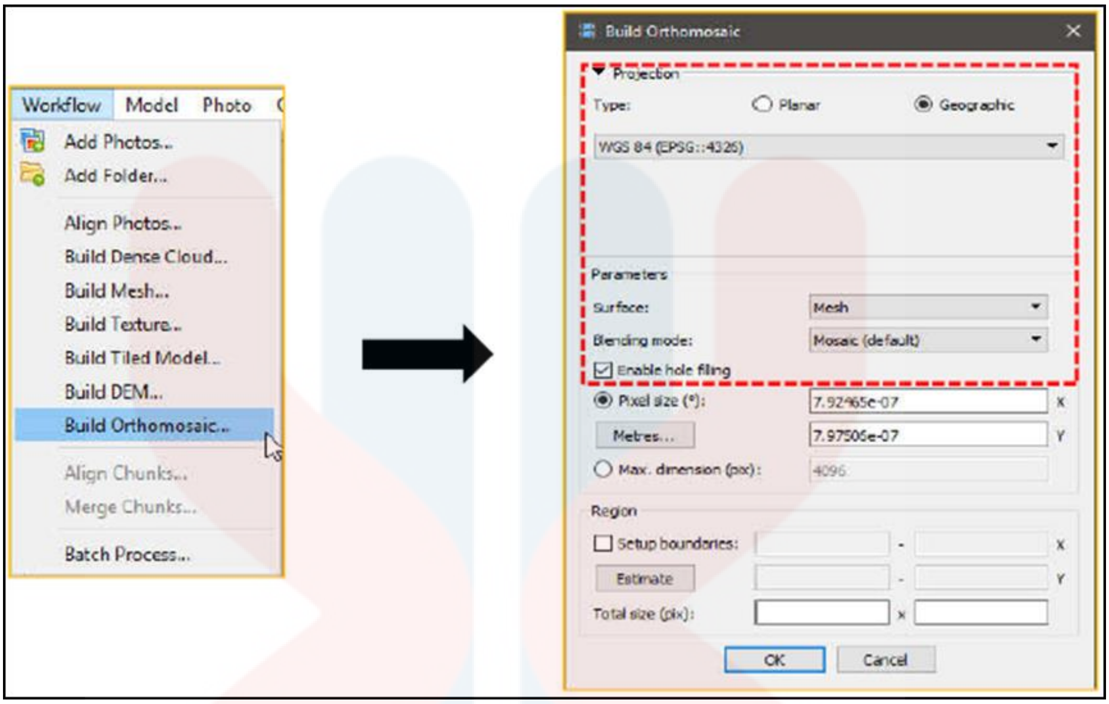

Figure 3.14: Workflow to build orthomosiacs

The Ground Sampling Distance (GSD) is the distance between two consecutive pixel centres measured on the ground. The bigger the value of the image GSD, the lower the spatial resolution of the image which resulting in less visible details. Minimum three GCPs are required to produce a point cloud, orthomosiacs and 3D model which come from the desired datum from the photographs taken. In this research, 8 GCPs was taken because optimum accuracy is obtained mostly with 5-10 GCPs. The GCPs station should be well distributed over the flight area. Helmert Transformation will be applied to orient and balance the point cloud and the 3D model (Niethammar et al., 2011; Watson, 2006; Crosilla and Alberto, 2002).

In the next stage, orthophoto, DEM and 3D image were produced. The terrain becomes generally flat and the elevation increased averagely 10 m within the zone of accumulation.

The area that will damage or affected directly or indirectly by landslides is an important information that can be used in planning emergency respond and mitigation program. The landslide hazard map can be created by overlying the extent of the landslide with settlements, traffic read and others thematic layers.

Photogrammetry had the potential to determine surface information. Photogrammetry processing will be apply in UAV images in order to remove error on the images. It is include interior and exterior orientation, tie point collection, aerial triangulation, mosaicking and generation of orthophoto. The accuracy of hazard evaluation relies on the resolution quality of orthophotos and DEMs. The post-landslide volumetric computations depend on the temporal and spatial resolution of DEMs. In many cases, the DEM before the landslide is not in a reliable condition. Commonly, the quality and resolution of the input data determine the accuracy of the produced hazard maps.

3.3.5 Data Analysis and Interpretation

a) General Geology

Rose diagram that was produced by GeoRose show the direction of forces acted to the study area. From the information collected in the study area such as strike and dip, lineament, faults and others, the deformation history of the study area also will be reconstructed and explained.

The detailed analysis of minerals by optical mineralogy in thin section helped in understanding the origin of rock. Generally, colour variation under the plane polarized light, fracture characteristics of the grains, refractive index and optical symmetry will be observed under a microscope. Malaysia as one of the tropical countries has frequently faced landslide hazard

b) Landslide Risk Area Mapping

The analysis was conducted in two stages which are quantitative analysis then follow by qualitative analysis. Quantitative analysis calculate the Root Mean Square Error (RMSE). RMSE is a computation for strip and block of digital aerial photographs. RMSE is the comparison between Ground Distance Values and distance values from Agisoft Photoscan software. RMSE determine the accuracy of satellite imagery data, thus, the role of remote sensing technique can also be identified in the study of landslide assessment. There are few types of accuracy standard that can be referred to the assessment of the outcome of satellite imagery including American Society for Photogrammetry and Remote Sensing (ASPRS) Accuracy for Large Scale Maps and U.S National Map Accuracy Standard (NMAS).

ASPRS has verified the accuracy of RMSE analysis. RMSE can be done by comparing the X, Y and Z coordinates from the ground control points during field mapping with the coordinates obtained from satellite imagery data. The ASPRS accuracy varies with the map scale and accuracy class while Table 3.2 shows the Class Accuracy for ASPRS

Table 3.2: Class Accuracy for ASPRS

ASPRS					
Map scale (m)	1:600	1:1200	1:2400	1:24000	1:25000
Accepted RMSE (m)	0.15	0.30	0.60	6.0	6.25

NMAS accuracy was defined when around 90% of the ground control points and the intervals between the contours were obtained to determine the map accuracy. Table 3.3 shows the accuracy of NMAS.

Table 3.3: Accuracy of NMAS

NMAS					
Map scale (m)	1:600	1:1200	1:2400	1:24000	1:25000
Accepted RMSE (m)	0.50	1.01	2.03	20.3	20.8

Landslide hazard zonation in the study area was carried out with the aid of geocoded IRS imageries and toposheet. The work resulted in separation of the landslide area into very low, low, medium, high and very high hazard zone. The critical part containing the high hazard zone was also identified where detailed information regarding geology, tectonics, engineering properties of slope material and land use pattern would be incorporated for evaluation of specific locations. Landslide hazard zonation has been attempted using GIS techniques by manipulation and interrelating geomorphic, geologic and meteorological variants of the study area.

3.3.6 Report Writing

The preliminary study, field observation and the data analysis and interpretation of the research are documented in the report. All the data that have been analysed and interpreted are compiled and written in the report. The report is divided into 6 chapters:

a) Chapter 1 Introduction

b) Chapter 2 Literature review

c) Chapter 3 Materials and methods

d) Chapter 4 General geology

e) Chapter 5 Landslide Risk Area Mapping

f) Chapter 6 Conclusion and suggestion

.

CHAPTER 4

GENERAL GEOLOGY

4.1 Introduction

4.1.1 Brief content of Chapter 4

This chapter discuss about the accessibility, settlement, forestry/vegetation, traverses and observation by using the traverses and observations map in the study area. Next, this chapter covered the geomorphology of the study area. The study of geomorphology include the geomorphology classification by using geomorphologic unit map, weathering processes, and drainage pattern. This chapter include the study of lithostratigraphy in the study area. The study of lithostratigraphy is conducted and then is shown in a geological map and cross section. The stratigraphic position are explain in units and all unit are further explain.

Furthermore, structural geology is also crammed in this chapter. All structural geology found in the study area are recorded in this chapter. Example of structural geology that was found are veins, joint, fracture and fold. The mechanism of the structure are also explain in this chapter. Last but not least, historical geology of the study area. Historical geology explain about the history of the formation of rock, structure and landform of the study area.

4.1.2 Accessibility

The study area as accessible by using two main roads. Firstly, Jeli-Gerik Highways. Jeli-Gerik Highways are build cross through the centre of the study area with length of 8.35 km road distance. The highways are fully paved road. The highways area accessible to most type of land vehicles such as bicycle, motorcycle, car, van and lorry. Figure 4.1 show the Jeli-Gerik Highways in the study area.

Figure 4.1: Jeli-Gerik Highways

Secondly, the study area can be access through the main road from Kampung Batu Melintang. This road connected with Timur-Barat Highway which exit at Gunung Reng. The road cross through at the upper right of the study area with 3.25 km road distance. The road are fully paved and can accessible to most road vehicle such as bicycle, car, van, and lorry. Figure 4.2 show the road from Kampung Batu Melintang.

Figure 4.2: Road from Kampung Batu Melintang

Both the highway and road are used to enter the study area by using a car. Inside the study area, the geological survey are conducted through walking method to easily access the more secluded area. The left side of the study area cannot be access by most method due to very thick forestry area.

4.1.3 Settlement

The type of settlements in the study area is rural settlements. Rural settlement commonly occupy a small land surface, here are sparsely populated and low population density.

In the study area, there are two small villages which area Penduk Village and Lawar Village. Penduk Village can be found at coordinate N 5° 41' 0.63'', E 101° 42' 38.17'' while Lawar Village can be found at coordinate N 5° 40' 31.81'', E 101° 42'

3.64" in the study area. Both villages is connected by one main road which is road that connect from Batu Melintang. Each villages has a few side smaller or side streets. There about 100-200 people in each villages. Basically, everyone who lives in the village know each other.

4.1.4 Forestry/Vegetation

In the study area, 2/3 of it is covered with forestry area while the other 1/3 is cover by plantation area, villages and others. Most of the plantation found in the study area are rubber plantation. According to information show in the official website of the Jeli Land and District Office, most of Jeli resident work as rubber tapper whether in their own plantation or work in other people/company bigger plantation. Figure 4.3 show the land cover map in the study area.

4.1.5 Traverse and Observation

Figure 4.4 show the traverse map of the study area. Figure 4.5 shows the observation and rock sampling point map. Table 4.1 shows the observation and rock sampling point coordinates.

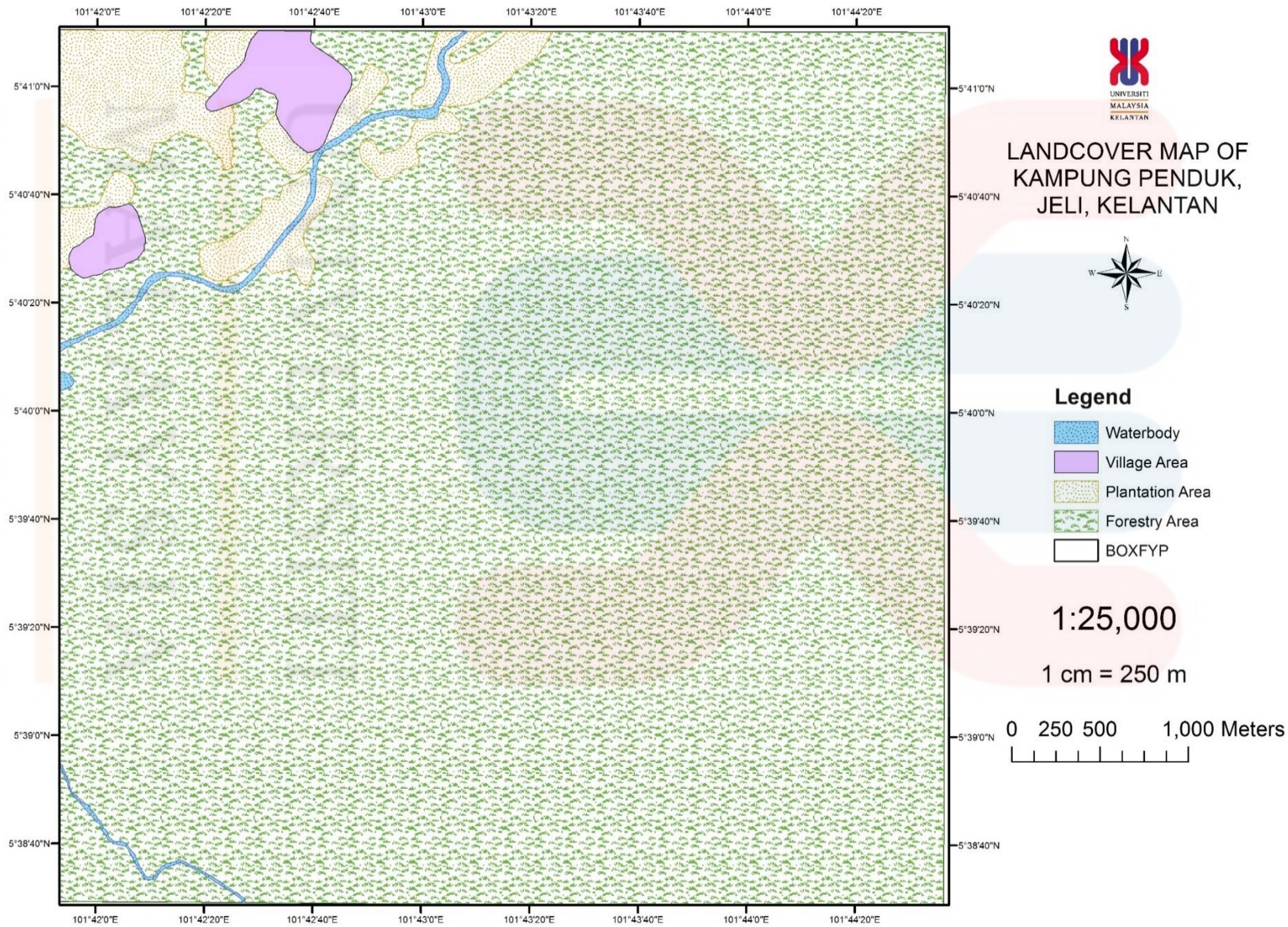

Figure 4.3: The land cover map of the study area

Table 4.1: The coordinate of observation and sampling point

STATION	COORDINATE
Observation Point	N 5º 40’ 35.17’’ E 101º 40’ 56.60’
	N 5º 41’ 0.21’’ E 101º 43’ 31.40’’
	N 5º 40’ 31.83’’ E 101º 43’ 32.66’’
	N 5º 40’ 14.05’’ E 101º 42’ 33.34’’
Rock Sampling Point	N 5º 40’ 40.24’’ E 101º 41’ 52.11’’
	N 5º 40’’ 36.38’’ E 101º 41’ 59.58’’
	N 5º 40’ 14.35’’ E 101º 42’ 33.05’’
	N 5º 41’ 0.74’’ E 101º 43’ 4.25’’
	N 5º 40’ 55.95’’ E 101º 43’ 0.39’’
	N 5º 41’ 7.68’’ E 101º 43’ 32.28’’
	N 5º 40’ 33.02’’ E 101º 43’ 32.66’’
	N 5º 39’ 47.22’’ E 101º 42’ 59.36’’
	N 5º 39’ 58.26’’ E 101º 42’ 52.18’’
	N 5º 39’ 57.30’’ E 101º 42’ 29.21’’
	N 5º 39’ 38.44’’ E 101º 42’ 14.04’’
	N 5º 39’ 28.84’’ E 101º 41. 58.55’’

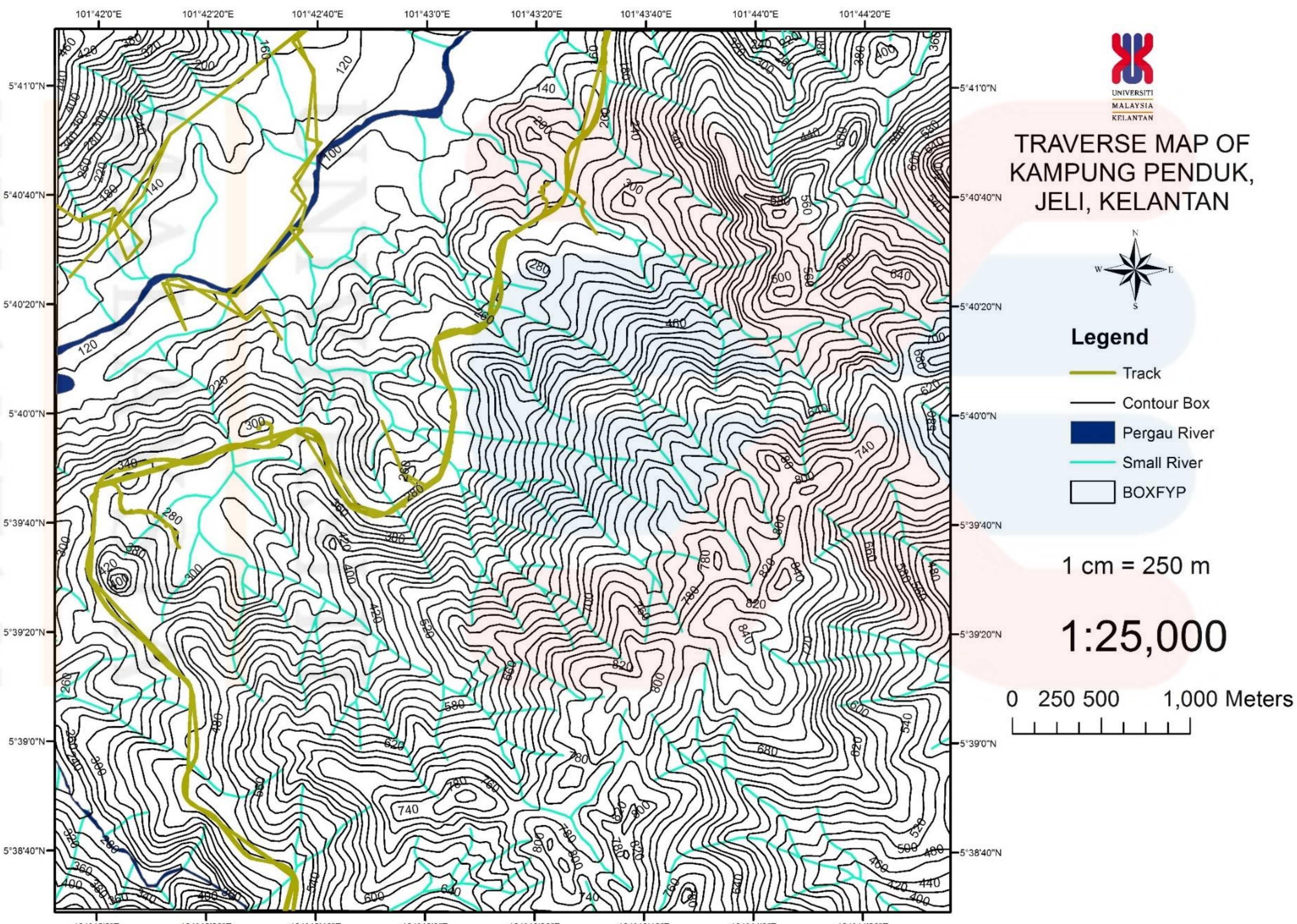

Figure 4.4: The traverse map of the study area

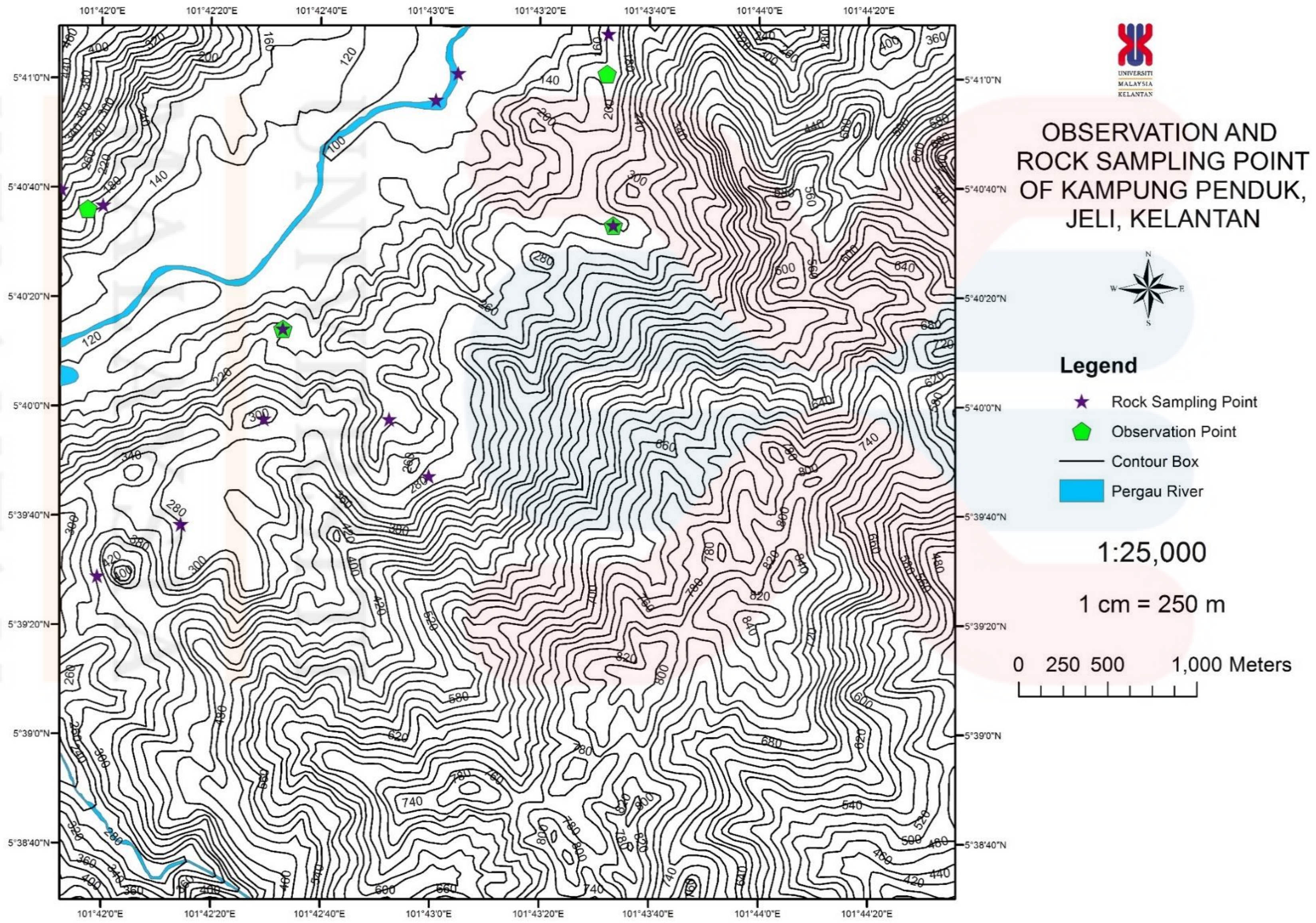

Figure 4.5: The observation and rock sampling point map

4.2 Geomorphology

Geomorphology is the study of landscapes/landforms. Study covered how the earth surface processes can mould landscape. Example of earth surface process are water, wind, and ice. Landforms are produced by erosion or deposition process. As rock surface worn out by these earth-surface processes, the sediment is then transported by natural transport agents such as water, wind and gravity and deposited to other area. Landform formation are directly affected by the climatic environments of the area. For example, sand dunes and ergs is deserts landforms are so different from the glacial and periglacial structure found in sub-polar and polar area.

Currently, landforms are shape by earth-surface processes. The process change the landscape in a huge amount of time in most cases. Most geomorphic processes engage at a slow rate. Sometimes a major scale event such as a landslide or flood occurs and cause rapid change to the environment. The rapid change in environment can be harmful to humans if occur near residential area.

4.2.1 Geomorphologic Classification

a) Landform

A landform is a natural feature on Earth surface of the Earth. A group of landforms form a landscape. The landforms arrangement in the landscape is known as topography. Typical ground landform include mountains, hills, canyons, valleys, and plateaus.

Other common type of landform is fluvial landform. Example of fluvial landform are peninsulas, bays, and seas. Fluvial landform also include submerged features such as volcanoes, ocean basin and mid-ocean ridges.

The landform in the study area are divided into two type of landform which are ground and hydrothermal landform. The ground landform that can be found in the study area are mountain and hill while hydrothermal landform that can be found is hot spring. Figure 4.6 shows mountainous landform while Figure 4.7 shows hot spring in the study area.

Figure 4.6: Mountainous landform in the study area

Figure 4.7: Hot spring in the study area

b) Topography

Topography is the physical feature study of an area such as hills, valleys, and rivers. Topography study also include the representation of the physical features on maps. According to Raj (2009), topographic unit could be classified into five units based on the mean elevation. Table 4.2 indicate the classification of the mean elevations.

The highest peat recorded is 850 m which is located at the left side of the study area. The range of the elevation of the study area is between 85 m – 850 m. About 60% of the study area are mountainous area while the other 40% are hilly area. Figure 4.8 shows the contour map in the study area. Figure 4.9 show the 3D landscape map of the study area. Figure 4.10 shows the topography map of the study area.

Table 4.2: Classification of the mean elevation

Class	Topographic Unit	Mean Elevation (above sea level, m)
1	Low lying	< 15
2	Rolling	16 – 31
3	Undulating	31 – 75
4	Hilly	76 – 300
5	Mountainous	> 301

4.2.2 Weathering

Weathering is the alteration rock mineral or the breakdown of rock masses or both when they are exposed to the atmosphere. Weathering processes is in-situ process with no or only slight movement of rock materials. Weathering processes changes fresh hard rocks state to a much weaker and softer state which make the rock more easily to be eroded.

There are 3 type of weathering. Firstly, physical weathering. Physical weathering also known as mechanical weathering is the disintegration processes of rock that breakdown the physical properties of the rock without any changes in their chemical properties. Physical weathering occur because of pressure, temperature, wind, frost and other. For example, fractures on rock surface are due to physical weathering. The increase of surface area exposed are subjected to chemical action as a result amplify the rate of disintegration.

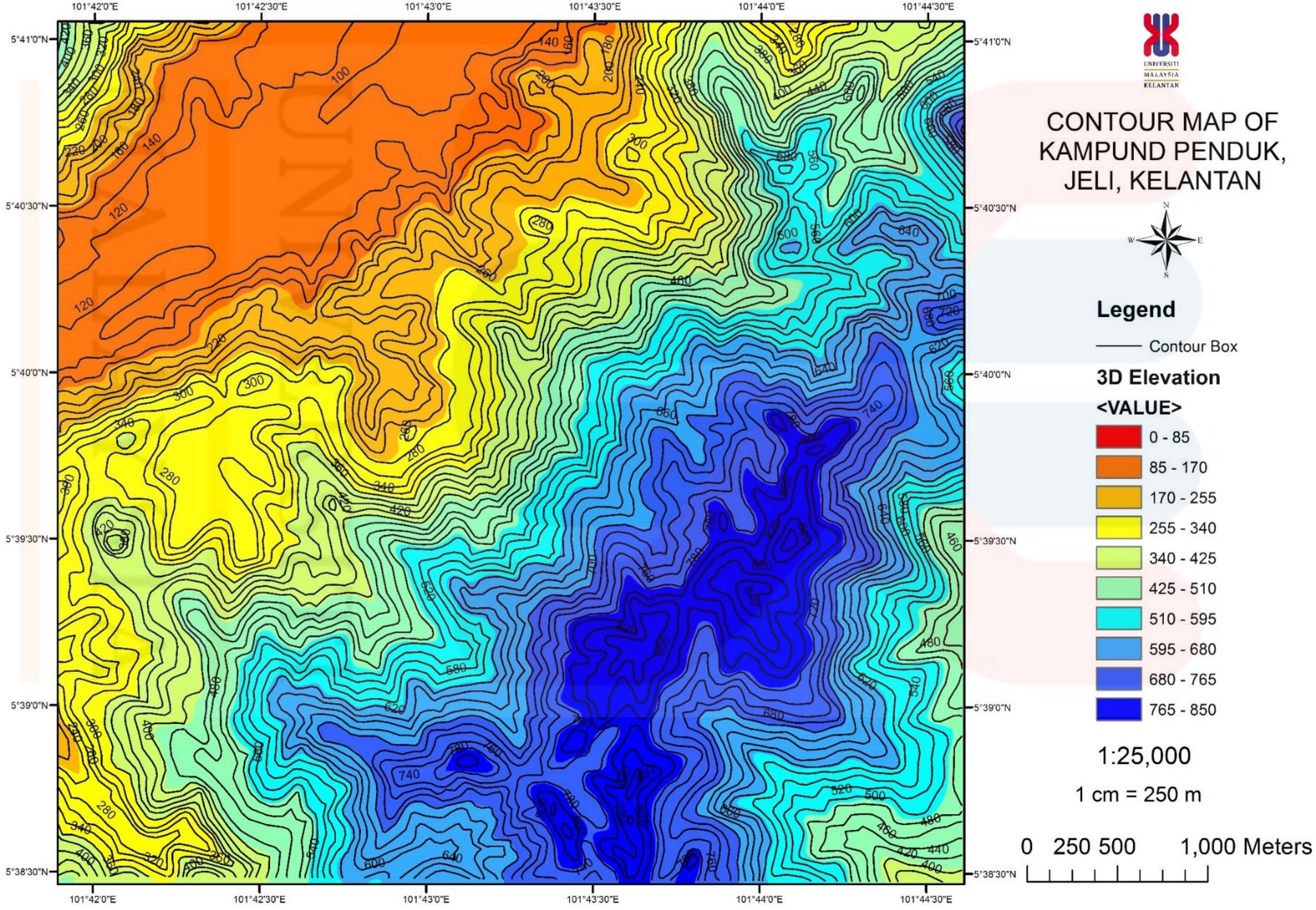

Figure 4.8: The contour map in the study area

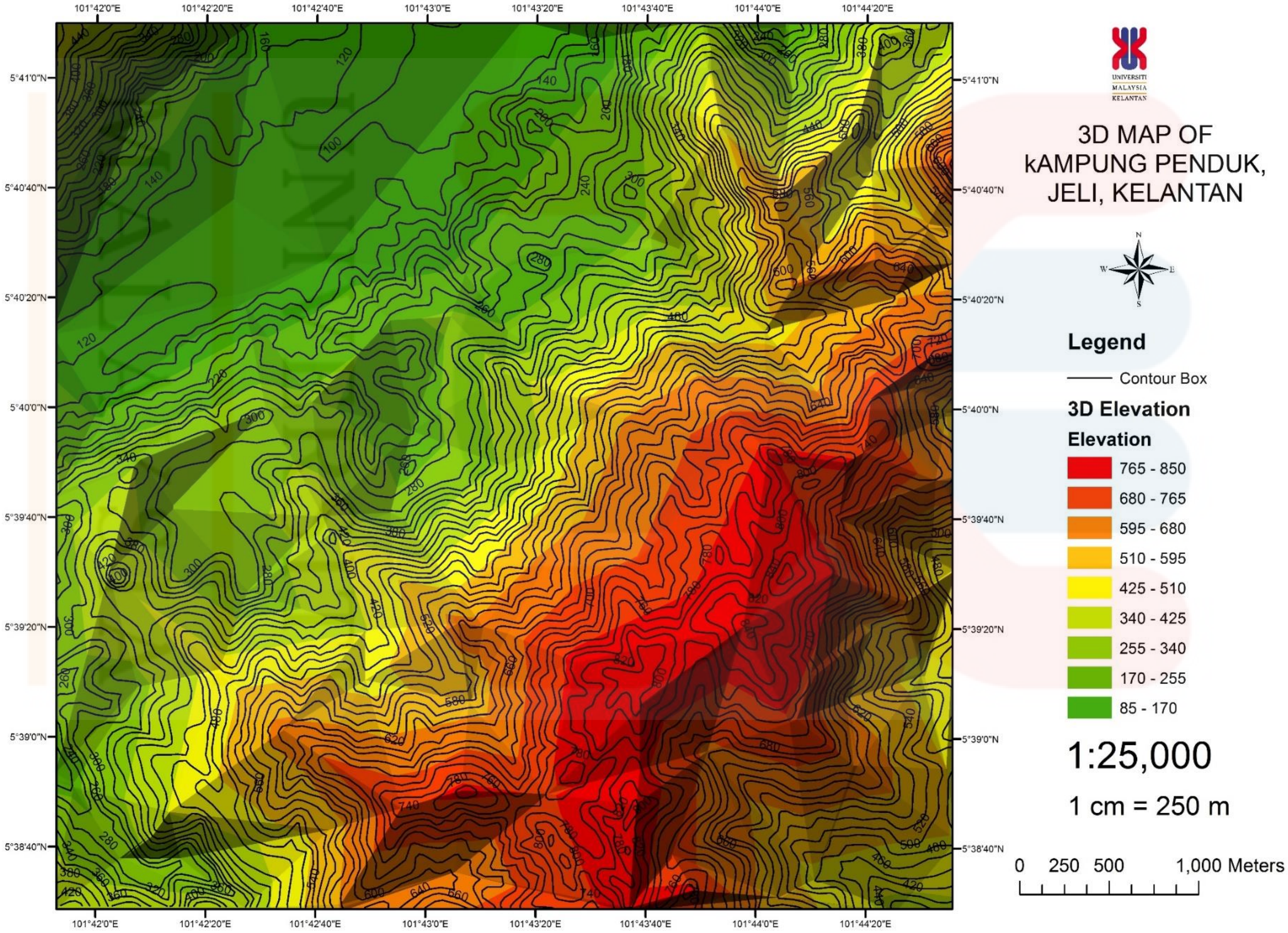

Figure 4.9: 3D landscape map of the study area

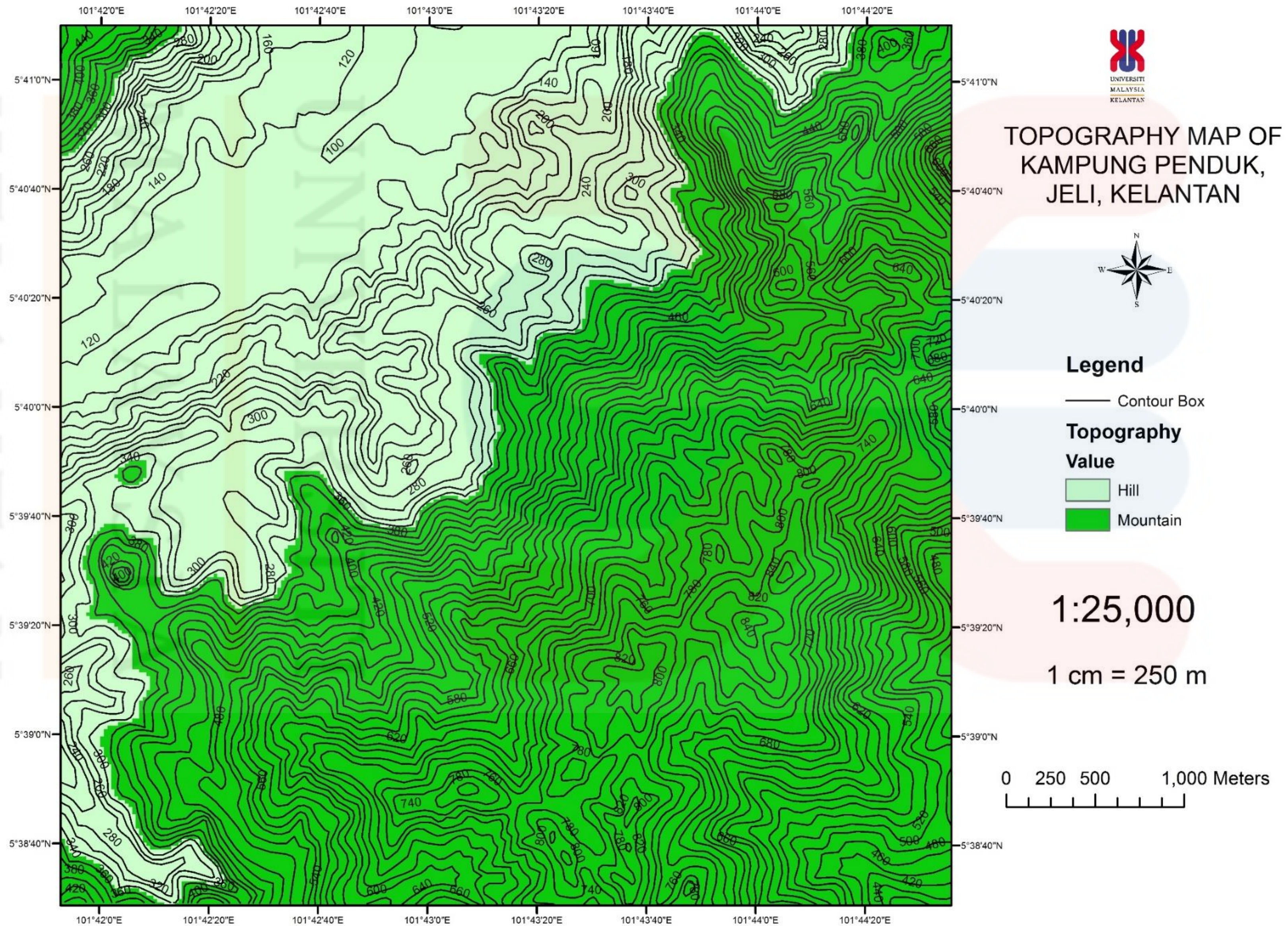

Figure 4.10: Topography map of the study area

Secondly, chemical weathering. Chemical weathering alter the chemical configuration of rocks. Chemical weathering usually occurs when mineral are exposed H^2O to generate numerous chemical reactions. Chemical weathering is a slow and continuous process as the mineral composition of the rock readjusted according to nearby area condition. As the result, the original mineral within the rock will transform into a new or secondary type mineral.

Lastly, biological weathering. Biological weathering are induce or boost by the presence of vegetation and animals. Vegetation cause root wedging and the production of organic acids while animal usually burrow in between rock crack or soil gap and expand the crack area.

Generally, the climate of the area dictate what type of weathering process occurred. Dry and cold climate monopolize by physical weathering. Humid and warm climate monopolized by chemical weathering and biological weathering because animal and vegetation favour this type of climate. All type of weathering occur in study area but physical and biological weathering is the most common due to the study area almost fully cover by forestry and vegetation. Chemical weathering can be found in the main river Sungai Pergau. Figure 4.11, 4.12 and 4.13 show physical, chemical and biological weathering that occur in the study area respectively.

Figure 4.11: Physical weathering in the study area

Figure 4.12: Chemical weathering in the study area

Figure 4.13: Biological weathering in the study area

4.2.3 Drainage Pattern

Drainage pattern is the design formed by the shape of rivers, streams, and lakes in a distinct catchment area. The topography of the area dictate the shape of the streams. The design of tributaries within a catchment area depends mostly on the type of rock and structures present in the area. Figure 4.14 show the types of drainage pattern.

A catchment area is the topographic location where a stream collect through-flow, groundwater flow and runoff. Watershed is a natural topographic fence that the catchment area from each other.

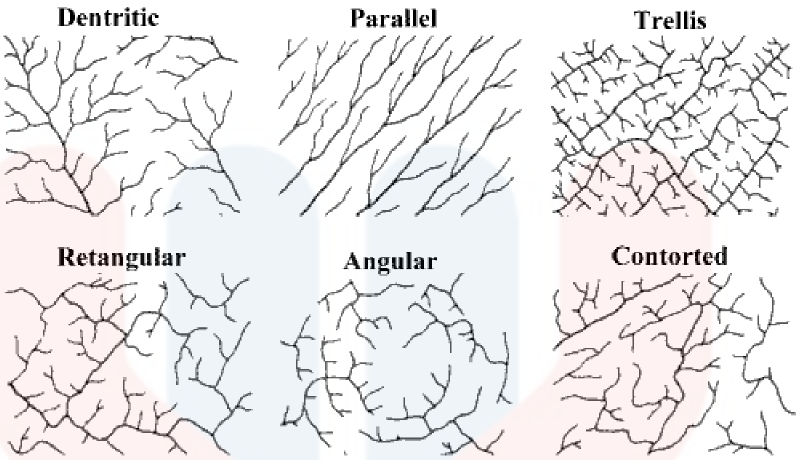

Figure 4.14: Types of drainage pattern

The study area consist of dendritic drainage pattern. Dendritic drainage system are not straight and are the most frequent pattern of drainage system. In a dendritic drainage system, there are various supplying stream that joined unite into the tributaries of the main river. The pattern of river channel is develop according to the slope of the terrain. Dendritic systems occurred in impervious and non-porous rock types. The study area are mostly cover by intrusion of granitic rock. Granite rock are hard and non-porous. Thus, is not possible the streams in the whole study area form a dendritic pattern due to the type of rock. Figure 4.15 shows the drainage pattern map of the study area. Figure 4.16 show the catchment area map in the study area.

4.3 Lithostratigraphy

The lithostratigraphy of the study area are portray in the geological map. The geological map consists of geological features including lithological unit distribution, geological structure, strike-dip of beds, foliation, fossils, dyke/sill, and other. Figure 4.17 shows the geological map of the study area.

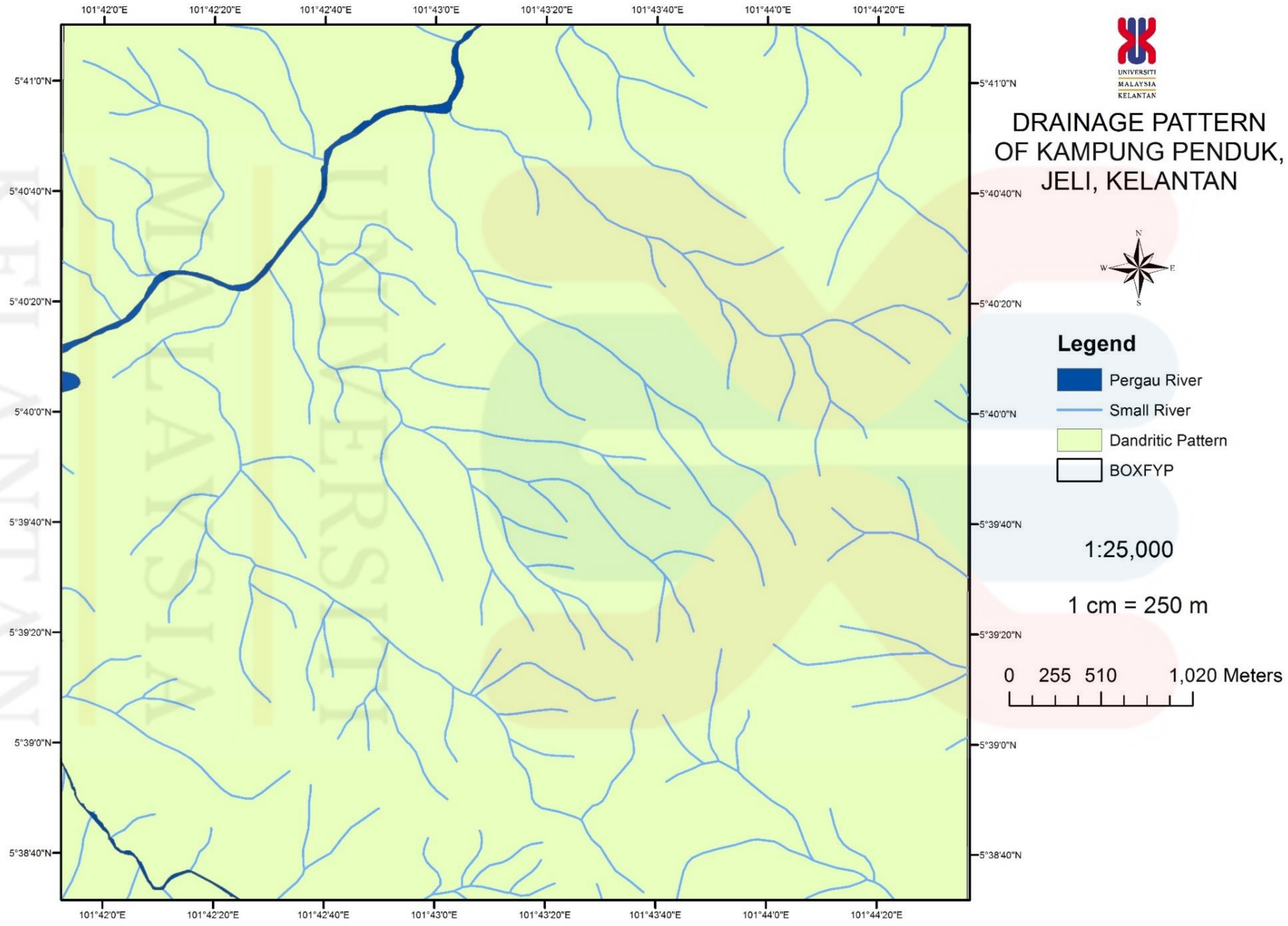

Figure 4.15: The drainage pattern map of the study area

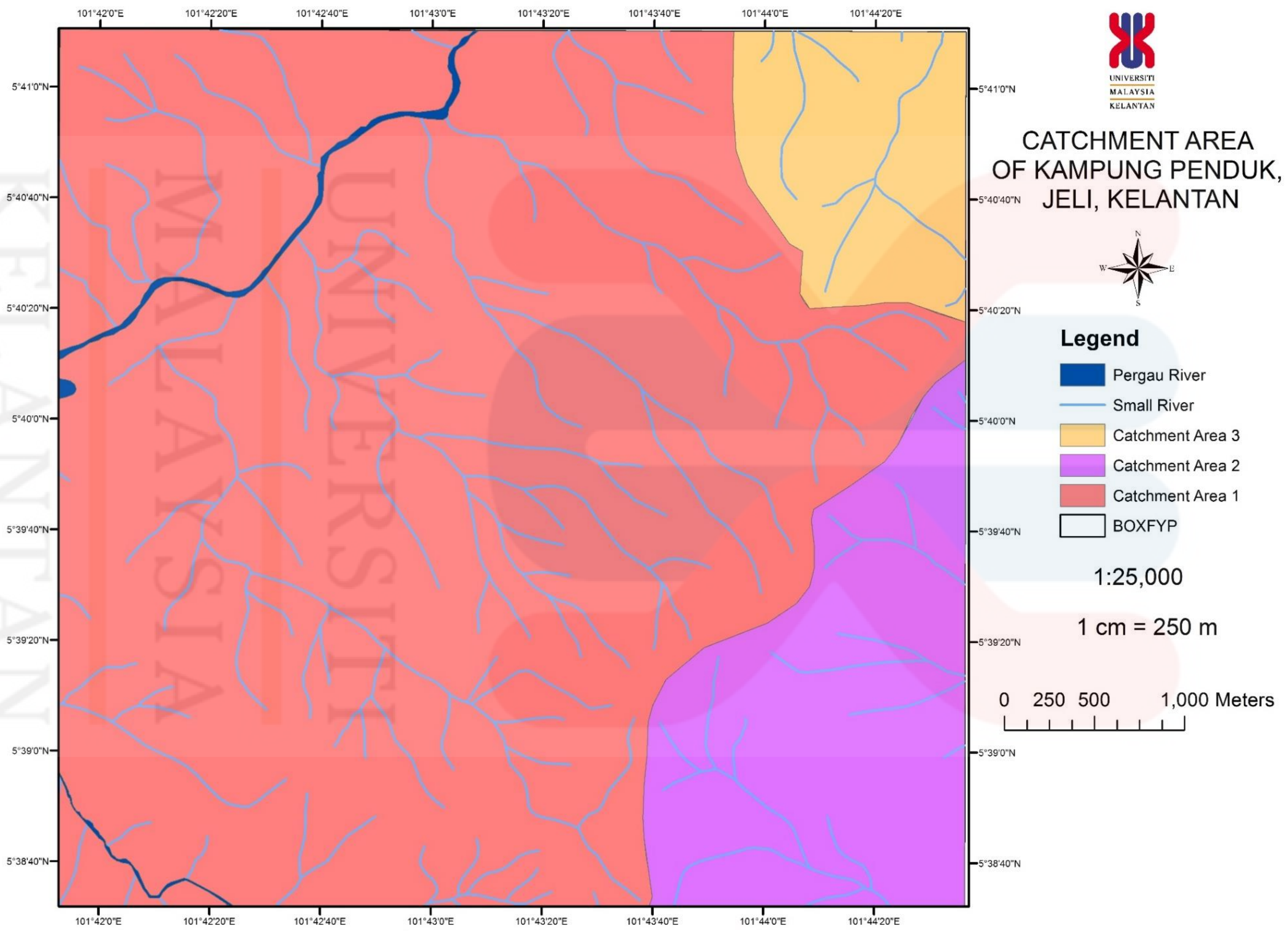

Figure 4.16: The catchment area map of the study area

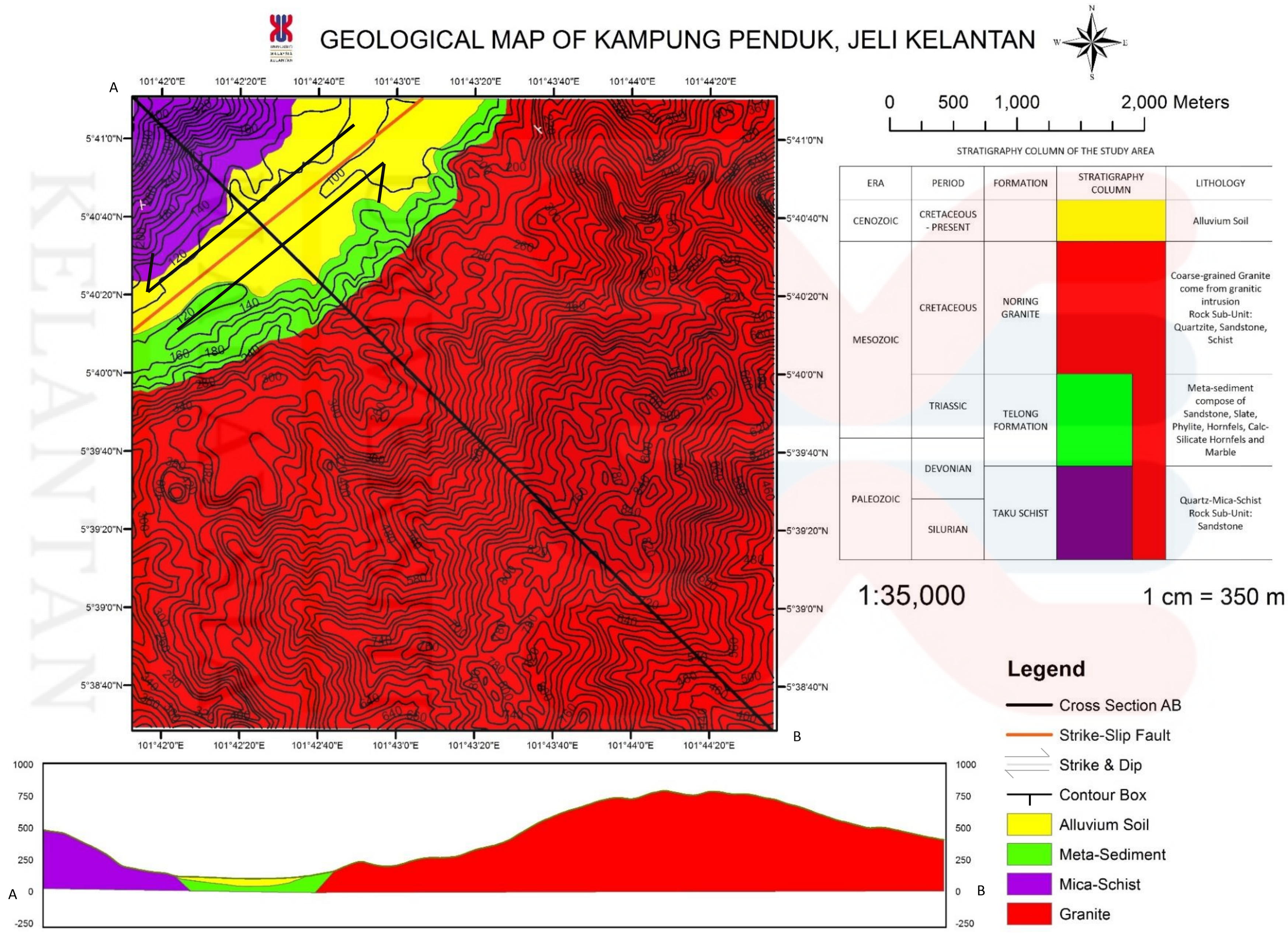

Figure 4.17: The geological map of the study area

4.3.1 Stratigraphy Position

A stratigraphic position comply with the law of superposition. Law of Superposition state that in any succession of strata, not disturbed or overturned since deposition, younger rocks lies above older rocks. The principle of lateral continuity states that a set of bed extends and can be traceable over a large area. Stratigraphic units are identify and characterize base on of observable rock characteristics. Facies are the descriptions of strata based on physical appearance. Stratigraphic units are characterized by lithic characteristics. The stratigraphic unit are not affected by age.

There are four stratigraphy rock layer in the study area. The youngest rock layer was placed at uppermost layer of the stratigraphy column. The youngest rock layer in the study area is alluvium soil. The alluvium soil was form during Cretaceous period until today. Next, the second layer belong to granitic rock layer. The granite in the study area come from intrusion during the Cretaceous period. The third layer belong metasedimentary rock layer. This layer of rock contain many type of rock such as sandstone, slate, hornfels and limestone. This layer was formed during the middle of Devonian period until Triassic period. At the bottommost layer which was the oldest rock layer belong to schist rock layer. The rock layer was formed during the Silurian period until the middle of Triassic period. Table 4.3 shows the stratigraphy column of the study area.

Table 4.3: Stratigraphy column of the study area

ERA	PERIOD	FORMATION	STRATIGRAPHY COLUMN	LITHOLOGY
CENOZOIC	CRETACEOUS – PRESENT			Alluvium Soil
MESOZOIC	CRETACEOUS	NORING GRANITE		Coarse-grained Granite come from granitic intrusion Rock Sub-Unit: Quartzite, Sandstone, Schist
	TRIASSIC	TELONG FORMATION		Meta-sediment compose of Sandstone, Slate, Hornfels, and limestone
PALEOZOIC	DEVONIAN			
	SILURIAN	TIANG SCHIST		Quartz-Mica-Schist Rock Sub-Unit: Sandstone

4.3.2 Unit Explanation

a) Schist Unit

The schist rock unit can be found at the top left corner of the study area. It cover about 15% of the study area. The schist rock layer is at the bottommost layer of the stratigraphy column because it was the oldest rock formation in the study area. Schist is a medium-grade metamorphic rock. It can be recognise at the field due to medium to large, flat, sheet-like grains in a preferred orientation. The schist sample found is light brown in colour, well foliated and very shiny under the light. This is due to high amount of mica and quartz mineral. Figure 4.18 shows the schist outcrop in the study area. Figure 4.19 shows the schist hand specimen. Table 4.4 shows the petrography analysis of schist.

No fossil assemblage was found in the study area and the thickness of the succession is indeterminable. However, owing to the fact that the Tiang schist and a well-documented Silurian-Devonian Kroh formation (about 20 km to the west of the Tiang schist in Malaysia) are only separated by the Main Range Granite, it is believed that both of them might be of the same age. Hence, the succession of the Tiang Schist Formation can be dated as probably Silurian-Devonian age.

Figure 4.18: Schist outcrop in the study area

Figure 4.19: Schist hand specimen

Table 4.4: Petrographic analysis of schist

Reference No. : **001** Location : N 5º 40’ 40.24’’, E 101º 41’ 52.11’’ Name of Rock : Schist	
Rock Type : Metamorphic Rock	
Description of Mineralogy	
Composition of Mineral	Description of Optical Mineralogy (Magnification 4X)
Biotite	Light brown to white colour interference under XPL
Muscovite	Colourless under PPL, colourless to pink colour interference under XPL
Quartz	Colourless under PPL, white to grey colour interference under XPL

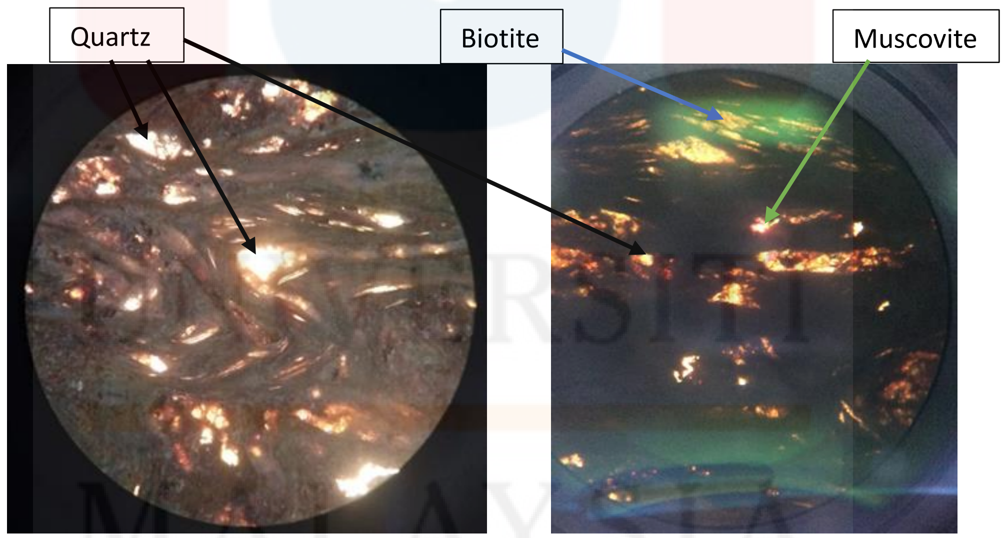

b) Metasedimentary Unit

Metasedimentary rock unit can be found in mainly at bottom of granite intrusion mountainous area. The rock unit can also be found in between granite intrusion at the middle of the granite mountainous area. Metasedimentary rock cover about 10% of the study area. Sandstone, slate, phyllite, hornfels, quartzite and limestone rocks can be scatter in the study area. Sandstone is a fine-grained sedimentary rock. It is recognizable as sandstone due to sand-size grains. The rock sample is brownish red in colour. Figure 4.20 show the sandstone outcrop in the study area.

Figure 4.20: Sandstone outcrop in the study area

Slate is a low-grade metamorphic rock that is created through the alteration of shale or mudstone. Slate outcrop found in the study area are fine-grained, foliated and dark grey in colour. Figure 4.21 shows the slate outcrop in the study area while Figure 4.22 shows the slate hand specimen. Table 4.5 shows the petrography analysis of slate.

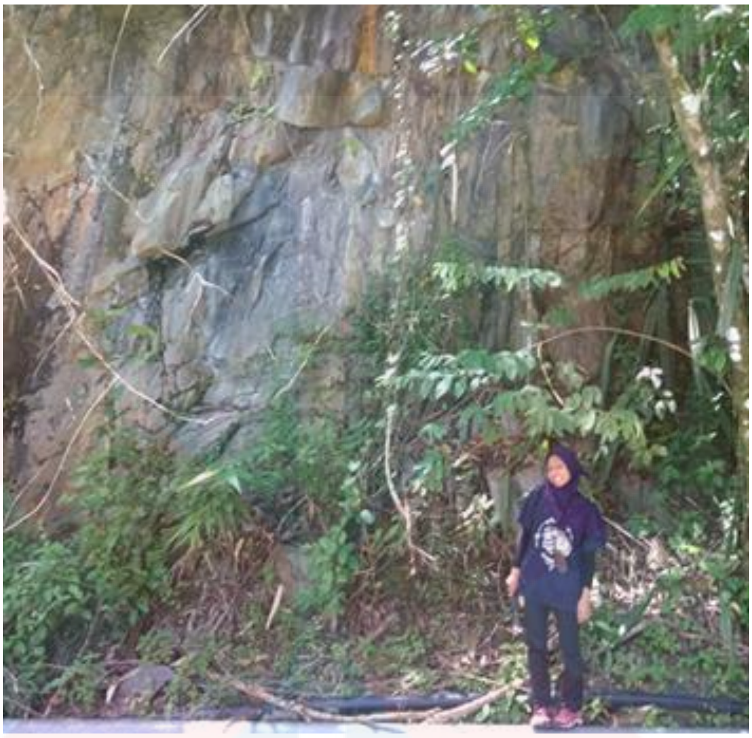

Figure 4.21: Slate outcrop in the study area

Figure 4.22: Slate hand-specimen

Table 4.5: Petrography analysis of slate

Reference No. : **002** Location : N 5º 41’ 7.68’’, E 101º 43’ 32.28’’ Name of Rock : Slate	
Rock Type : Metamorphic Rock	
Description of Mineralogy	
Composition of Mineral	Description of Optical Mineralogy (Magnification 4X)
Quartz	Colourless under PPL, white to grey colour interference under XPL
Muscovite	Colourless under PPL, white to pink interference under XPL
Chlorite	Colourless under PPL, emerald green under XPL

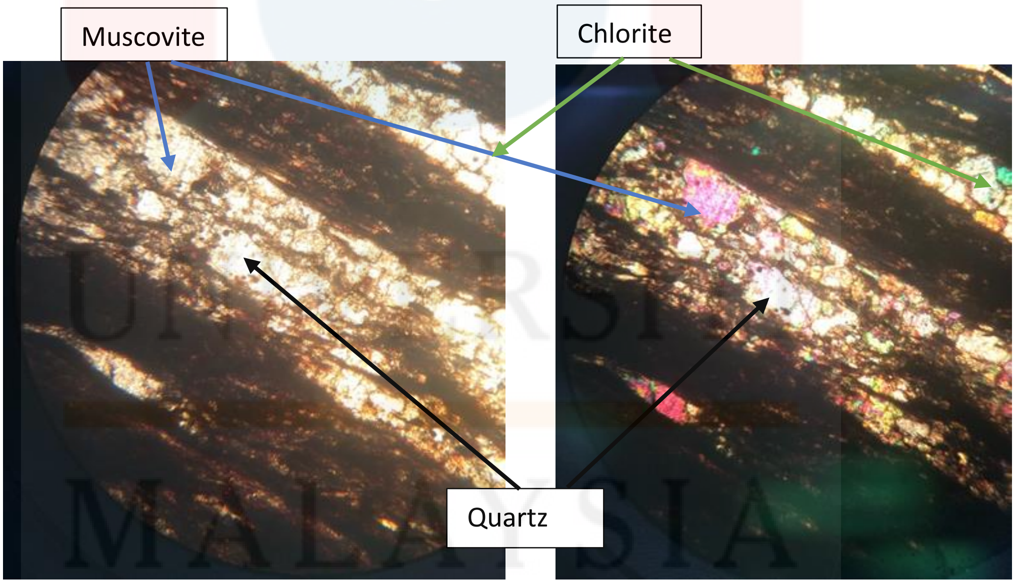

Hornfels is a fine-grained metamorphic rock that was subjected to the heat of contact metamorphism at a shallow depth. Hornfel outcrop found in the study area are fine-grained and dark grey in colour. Figure 4.23 shows the hornfels outcrop in the study area while Figure 4.24 shows the hornfels hand specimen. Table 4.6 show the petrography analysis of hornfels.

Figure 4.23: Hornfels outcrop in the study area

Figure 4.24: Hornfels hand specimen

Table 4.6: The petrography analysis of hornfels

Reference No. : **003** Location : N 5º 41’ 0.74’’, E 101º 43’ 4.25’’ Name of Rock : Hornfels	
Rock Type : Metamorphic Rock	
Description of Mineralogy	
Composition of Mineral	Description of Optical Mineralogy (Magnification 4X)
Biotite	Colourless under PPL, Light brown to white colour interference under XPL
Quartz	Colourless under PPL, white to grey colour interference under XPL

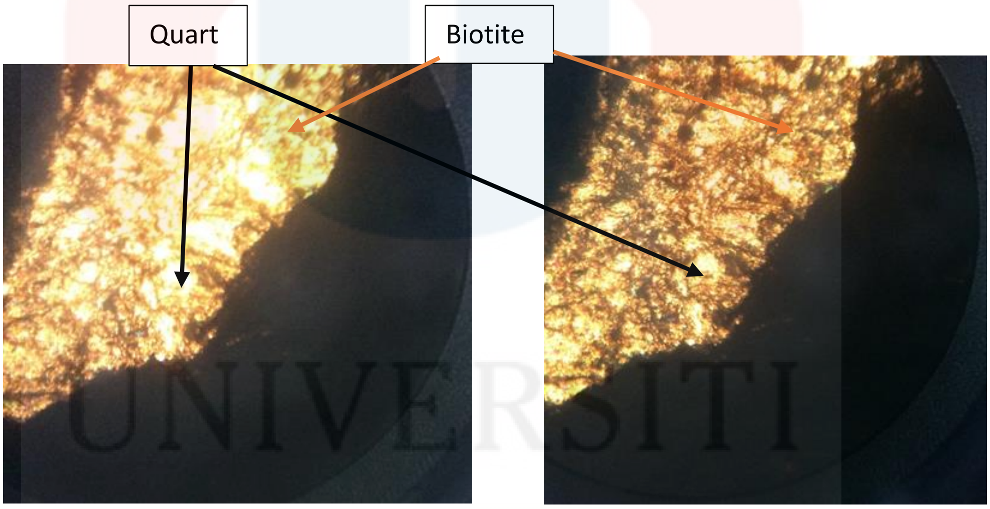

Limestone is a sedimentary rock composed primarily of calcium carbonate ($CaCO_3$) in the form of the mineral calcite. Limestone found in the study area are fine-grained and dark grey in colour. Figure 4.25 shows the limestone outcrop in the study area. Figure 4.26 shows the limestone hand specimen. Table 4.7 show the petrography analysis of limestone.

Figure 4.25: Limestone outcrop in the study area

Figure 4.26: Limestone hand specimen

Table 4.7: Petrography analysis of limestone

Reference No. : **004** Location : N 5º 41’ 7.68’’, E 101º 43’ 32.28’’ Name of Rock : Limestone	
Rock Type : Sedimentary Rock	
Description of Mineralogy	
Composition of Mineral	Description of Optical Mineralogy (Magnification 10X)
Quartz	Colourless under PPL, white to grey colour interference under XPL
Calcite	Colourless under PPL and XPL

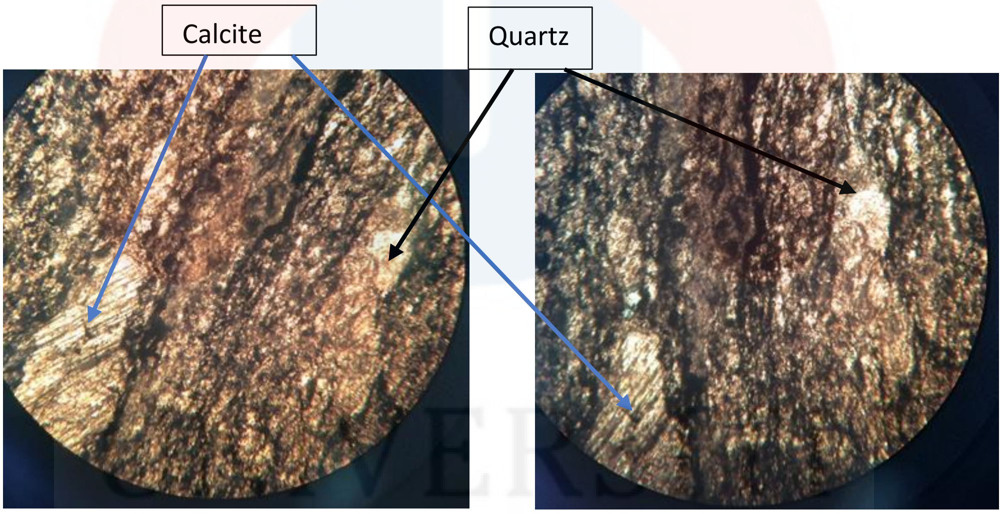

No fossil assemblage was found in the study area. The thickness of the rock layer is indeterminable. However, the age of the succession was assigned as Carboniferous-Permian by the Malaysian and Thai Working Groups, based on lithological and stratigraphic correlations.

c) Granite Unit

Granite rock unit can be found at the left side of the study area. The granite rock cover 65% of the study area. The granite rock come from intrusion. Thus, sometime granite outcrop was found alongside other older rock in the study area. Granite is an igneous rock. Granite can easily be identified due to light-coloured rock and large grains size that is large enough to be visible with the unaided eye. It forms from the slow crystallization of magma below Earth's surface. Granite outcrop found the study area is coarse-grained and light pink in colour. Figure 4.27 show the granite outcrop in the study area. Figure 4.28 show the granite hand specimen. Table 4.8 show the petrography analysis of granite.

Figure 4.27: Granite outcrop in the study area

Figure 4.28: Granite hand specimen

Table 4.8: Petrography analysis of granite

Reference No. : **005** Location : N 5º 39’ 38.44’’, E 101º 42’ 14.04’’ Name of Rock : Granite	
Rock Type : Igneous Rock	
Description of Mineralogy	
Composition of Mineral	Description of Optical Mineralogy (Magnification 4X)
Muscovite	Colourless under PPL, colourless to pink colour interference under XPL
Quartz	Colourless under PPL, white to grey colour interference under XPL
Calcite	Colourless under PPL and XPL

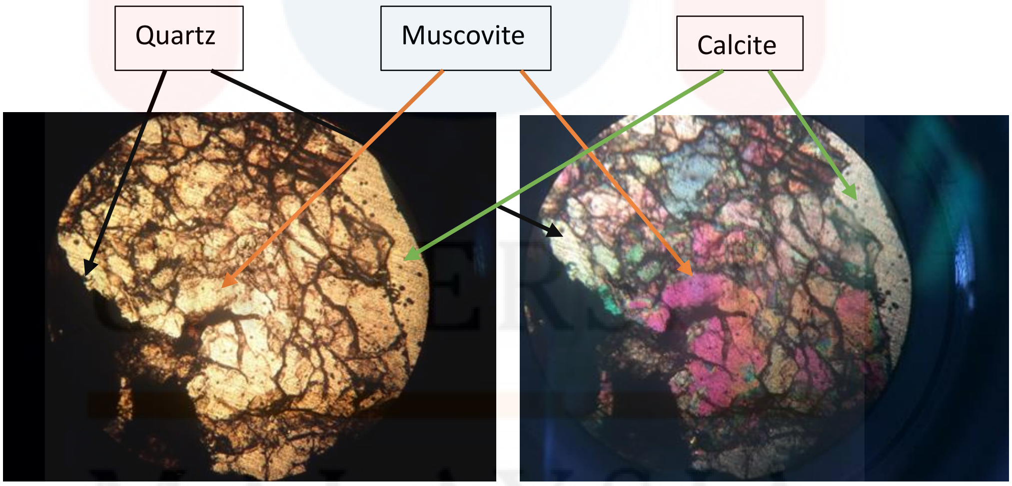

No fossil assemblage was found in the study area. The thickness of the rock layer is indeterminable. However, the age of the succession was assigned as Carboniferous-Permian by the Malaysian and Thai Working Groups, based on lithological and stratigraphic correlations. The Kenerong intrusions are often associated with magmatitic textures that appear to relate to the assimilation of metasedimentary country rocks (Hutchison, 1969, 2009; Searle et al., 2012).

d) Alluvium Soil Unit

Alluvium soil can be found in the river and village area in the study area. Alluvium soil is a loose soil on top of rock layer due to accumulation of weathered rock. Alluvium soil covered 10% of the study area. There are no fossil assemblage was found in the study area. The thickness of the rock layer is indeterminable. The age of the succession was unassigned. Based on the general knowledge of geomorphologic cycle, it was assume the age of alluvium soil unit start after intrusion of granite during Cretaceous period and still ongoing until today.

4.4 Structural Geology

Structural geology is the study of the three-dimensional distribution of rock units, their surface and the composition of the interior with respect to their past geological event and deformational histories. The main purpose of structural geology study is to unveil the historical information of deformation in the rocks by using measurements of present-day rock geometries and thus be able to understand the mechanism or process that resulted in the observed strain and geometries. The information about the dynamics of the stress field can be correlate to important events in the geologic past.

The geological structure that can be found in the study area are veins, joints, fracture, fold and intrusion. Some structure has its own structural analysis to extract data and information. For example, joint analysis was used to study joint and fold analysis was used to study fold structure.

4.4.1 Vein

Figure 4.29: Quartz vein in the study area

Figure 4.30: Quartzite vein in the study area

Vein is a crystallized minerals with a distinct sheet-like body within a rock. Veins form when mineral constituents within the rock mass carried by an aqueous solution are deposited through precipitation. The hydraulic flow involved is usually due to hydrothermal circulation. Figure 4.29 shows the quartz vein while Figure 4.30 shows the quartzite vein in the study area.

The formation of veins has two main mechanism. The first mechanism is open-space filling mechanism. Open space filling take placed at relatively low pressure epithermal vein systems where generally considered to be below 0.5 GPa. Open spaced filing veins exhibit an agate-like habit, colloform texture and appear to fill up the available open space. Example of open-space filling phenomena are cavities, geodes and vugs. The second mechanism is crack-seal growth. This mechanism occur under the condition the brittle-ductile rheological conditions predominate or the confining pressure is too great. It mean that, creak-seal frown mechanism occurs at higher pressures, with reopening of the vein fracture by progressive deposition of minerals on the growth surface. The veins that was found in the study area is quartz and quartzite veins. Both veins formed through open-spaced filling mechanism during magma intrusion.

4.4.2 Joint

Figure 4.31: Joints structure in the study area

A joint is a brittle-fracture surface in rocks along which little or no displacement has occurred. Joint usually occur as joint sets and systems. A joint set is a group of uniform-spaced parallel joints that can be recognized through analysis of the spacing, orientations and physical properties. Two or more intersecting joint set area called joint system. Joint structure can be found in Sungai which dominated by alluvial soil and metamorphic outcrop in the study area. Figure 4.31 shows the joint structure in the study area.

4.4.3 Fracture

Figure 4.32: Fracture structure in the study area

A fracture is any space gap in a geologic formation that split the rock into two or more pieces. Commonly, fractures are caused when stress overpowered the rock strength. This resulted in the rock to lose cohesion along its weakest plane. The outcrop with fracture can be found at the schist dominated area in the study area. Figure 4.32 shows the fracture structure in the study area.

4.4.4 Fold

Figure 4.33: Folding structure in the study area

Fold is bent or curved of one or a stack of originally flat level surfaces such as sedimentary strata due to the result of high temperature and pressure and high. The most common cause of folding is due to some aspect of plate tectonics. Original flat rock surface bent into folds when two forces act towards each other from opposite sides. The process by which folds are formed due to compression is known as folding. Folding takes place within the Earth's crust. Thus, it is an endogenetic processes. There are large-scale and small-scale folding structure. The one that was found in the study area is a small-scale folding structure. Figure 4.34 shows the folding structure in the study area.

4.4.5 Intrusion

Figure 4.34: Igneous intrusion in the study area

Intrusion is when magma from under the Earth's surface is slowly pushed up from deep within the earth into any cracks or spaces. This process can take millions of years. In the study area, the intrusion is igneous intrusion. Figure 4.34 shows the igneous intrusion into the older rock in the study area. Igneous intrusions form when hot molten magma cools down, recrystallize and solidifies before it reaches the earth surface.

4.4.6 Mechanism of Structure

a) Lineament Analysis

Lineament is the linear or curvature feature which is an expression of underlying geological structure. It usually influenced by the structures of regional area such as ridge, fault-aligned valley, a series of fault or fold-aligned hills, inconsistency and boundaries between stratigraphic formations.

Lineaments are strongly correlative with structures that have obvious surface expression. Perceived lineament represents the reflectance contrast that is related to variations in vegetation, soils, and topography. As these linear stream channels, lines of vegetation, soil and relief break and other surface alignments coincide with patterns in geologic substrate, these features are recognized as lineaments in photographs and maps. The long lineaments measured may be useful for indicating the continuity of faults and other structures. Figure 4.35 shows the lineament of the study area.

Figure 4.36 shows the local lineament rose diagram in study area. The bearing readings for lineament analysis are attached as Appendix I. From the orientation of lineaments shown in the rose diagram, it indicates the major stress, $\sigma 1$ acted on the study area is in N 75° E direction.

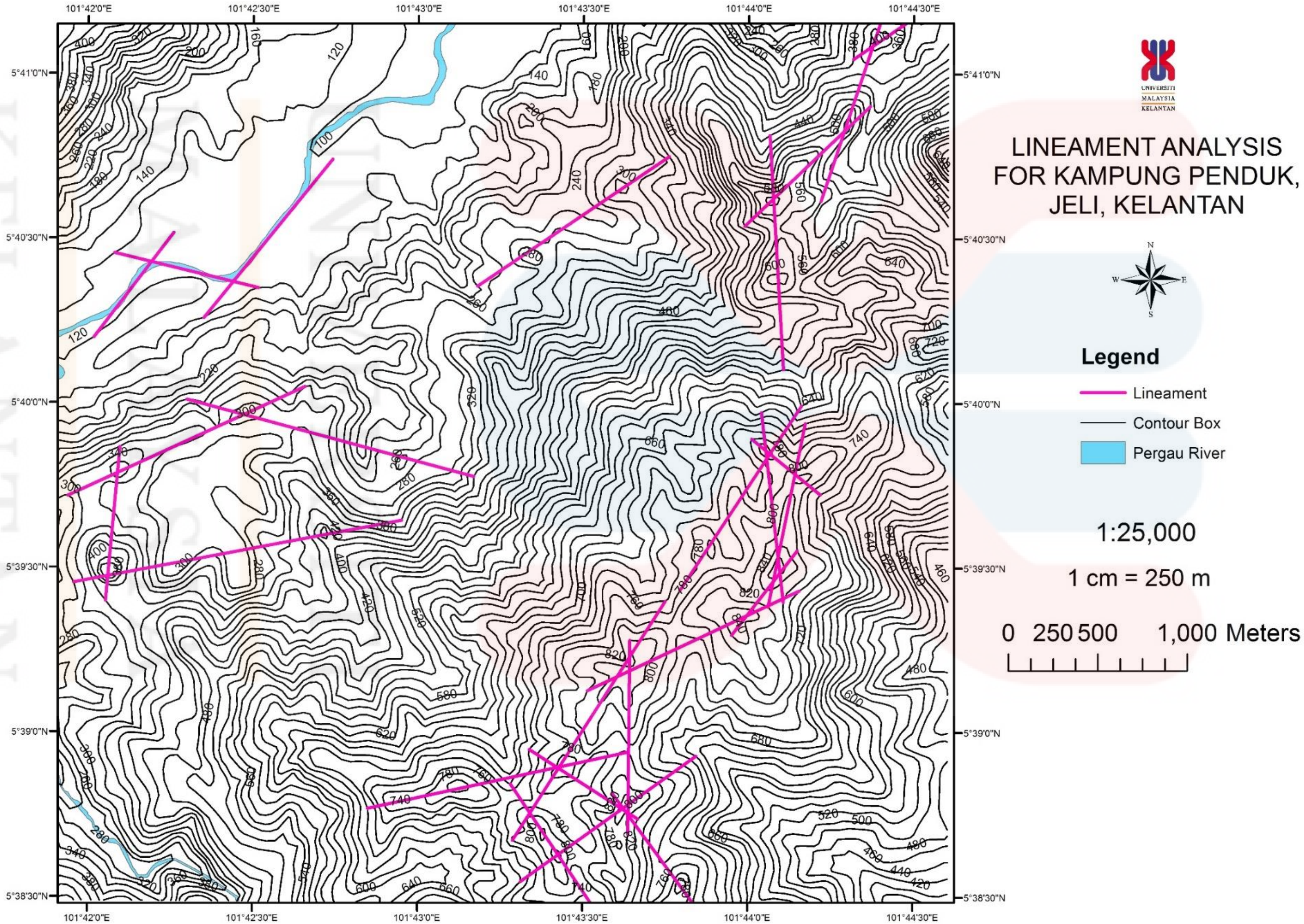

Figure 4.35: Lineaments map of the study area

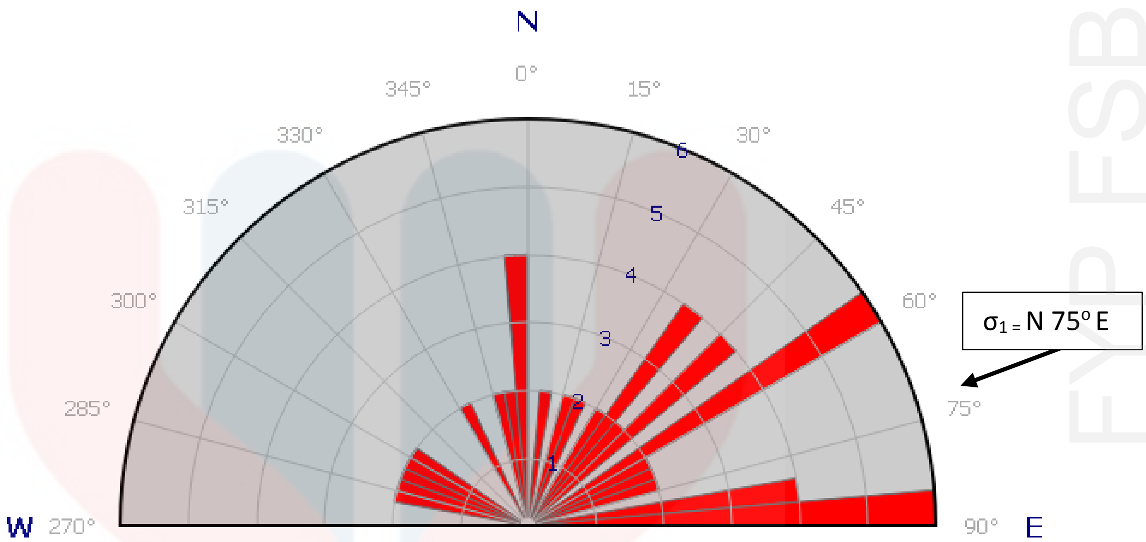

Figure 4.36: Rose diagram of lineament

b) Joint Analysis

Joint is a discrete, brittle fracture that naturally formed in continuity splitting rock into two parts. It presents nearly in all type of rock and extend in various directions based on the forces acted on the rock. The joints usually vary in appearance, dimensions and arrangement. It appears more obvious when the rock is undergoes weathering and erosion process. When there is water enter the joints, it will lead to the enlargement of the fractures and formed the caves and underground rivers. If it is filled by precipitated minerals, it is known as veins and if it is filled by solidified magma, it is called as dykes.

From the field observation, the flow structures and joints of rock are identified. Based on these joint analyses, the potential of these discontinuities lead to the rock failure can be known. One joint analyses are done at different area in the study area. The joints reading are taken at coordinate N 5° 41' 9.14", E 101° 43' 6.92". Figure 4.37 shows the joint outcrop in the study area. Figure 4.38

shows the rose diagram of joint. The orientation of joints is attached as Appendix II.

Figure 4.37: Joints outcrop in the study area

From the orientation of joint observed in the field, it enables to indicate on each occasion of most dominant fracture direction. From the rose diagram, it can be observed that the major compressional force, σ^1 is acted at N 65° E direction.

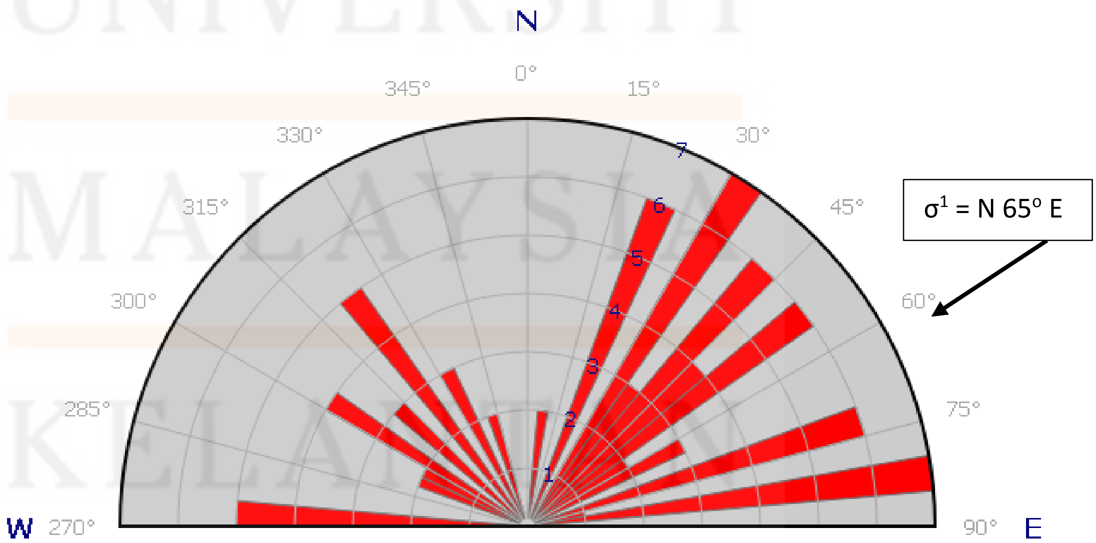

Figure 4.38: Rose diagram of joint

4.5 Historical Geology

The Silurian-Devonian Tiang schist is considered as the oldest rock unit. It is highly folded and faulted, forming north-south trending moutainous belt distributed in the western part of the Transect area. The rock predominantly comprises quartz-mica schist and quartz garnet schist. This rock unit is unconformably overlain by the Mangga formation, which consists of low-grade metamorphic sequence of arenaceous, argillaceous, pyroclastic, hornfelsic and calcareous rocks of probably Carboniferous-Permian age. The formation is found at the south-western part of the Transect area.

Four granitic bodies were identified namely Merah, Kemahang, Lawar and Kenerong Granites. The Triassic Merah granite is part of the Main Range Granite exposed as a north-south trending mountainous belt, west of the Transect area. It is moderate to strongly foliate in nature. The Triassic Kemahang Granite forms an N-S trending mountainous area near the Jeli town which is located in the central part of the Transect area. It is granodiorite, showing a strongly foliated with some gneissic textures occurred together with porphyritic granite. The minor intrusion of I-type, Jurassic to Cretaceous Lawar granite is distributed in the northern part of the Transect area near the border. It is sheared granite to granodiorite. The Cretaceous Kenerong granite is exposed in the south-eastern part in between the Kemahang and Noring Granite masses. It is light grey to grey, leucocratic, and equigranular texture.

CHAPTER 5

UAV-BASED FOR LANDSLIDE RISK AREA MAPPING

5.1 Introduction

This research is focus to assess the capabilities of UAV in the production of digital photogrammetric products based on landslide risk area. This research also focus in producing a landslide risk area map by using the UAV technology along Jeli-Gerik Highway in the study area.

5.2 Study Area

Jeli-Gerik Highway has a long history of landslide occurring since it is first build in 1970. According to Jabatan Kerja Raya (JKR), every year there is a maintenance program for Jeli-Gerik highway to fix or control the damage for landslide. In 2018 maintenance program, there are 14 cases involve with whopping RM 7 280 000.00 budget cost. The work that was done in the maintenance program are soil nail and grid beam, backfilling, road side drain, close turfing, construction of concrete rubble wall, micro pile, tie back wall and new guardrail.

5.2 Capabilities of UAV in the Production of Digital Photogrammetric Products Based On Landslide Risk Area

Technology in remote sensing has develop exponentially and has a wide range of application in landslide studies. Landslide – related studies can be arrange in three stages. The first stage is detection and identification. The second stage is monitoring. The third and last step is spatial analysis and hazard prediction. The use of remote sensing data such as airborne, satellite or ground- based data varies according to the three main stage in landslide-related studies. In this research, it is only to assess the capability of UAV in the production of digital photogrammetric products based on landslide risk area along Jeli-Gerik Highway in the study area. Figure 5.1 show the landslide area in the study area.

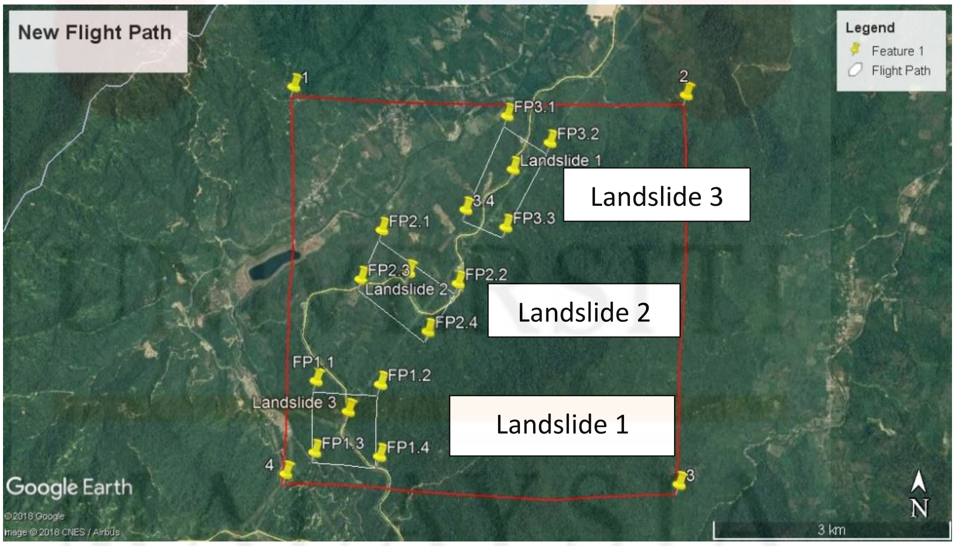

Figure 5.1: Landslide area in the study area

On 28 July 2018, a DJI Phantom 4 Pro flight campaign was carried out covering three selected landslide area along Jeli-Gerik Highway in the study area. In total, there are 2 532 optical photos and POS (position and orientation system) data was collected from the three flights where 534 photos from landslide 1, 999 photos from landslide 2 and another 999 photos for landslide 3. POS data contains the aerial photo number, space position X, Y, h coordinate, small aircraft attitude rolling, pitching, flip, and other information.

To serve the geological disaster analysis, two processing procedures were carried out which are generate an ortho-mosiac, and establish a DEM model using point cloud data. First, each image was rectified onto the centre point coordinates recorded in POS data, photo size, and ground control points and flip angle. Then, all rectified photographs were merged to a uniform ortho-mosaic with a spatial resolution of 0.1 m. All correction was carried out by using PhotoScan software, which is an advanced image-based 3D modeling solution also created by using PhotoScan. DEM was also created by PhotoScan software, which can extract the point cloud data from the coordinate information of POS data, and reconstruct the digital elevation model. The DEM after landslide was produced in a 2 m resolution and it was converted to vector format (TIN) for further analysis.

5.3.1 Landslide 1

a) Orthophoto Landslide 1

The orthophoto of Landslide 1 illustrated that 95% of the landslide 1 area are covered by forestry area minus the highway and 1 clear/bald area can be seen near the highway at the middle of orthophoto. Figure 5.2 show the orthophoto of Landslide 1.

Figure 5.2: Orthophoto Landslide 1 area

b) Digital Elevation Model (DEM)

The DEM of Landslide 1 illustrated the elevation of the landform in Landslide 1 area. The highest elevation is 500 m while the lowest elevation is 220 m. The DEM resolution is 21.6 cm/pix. The DEM point density is 21.4589 points per sq. m. Figure 5.3 show the DEM of Landslide 1 area.

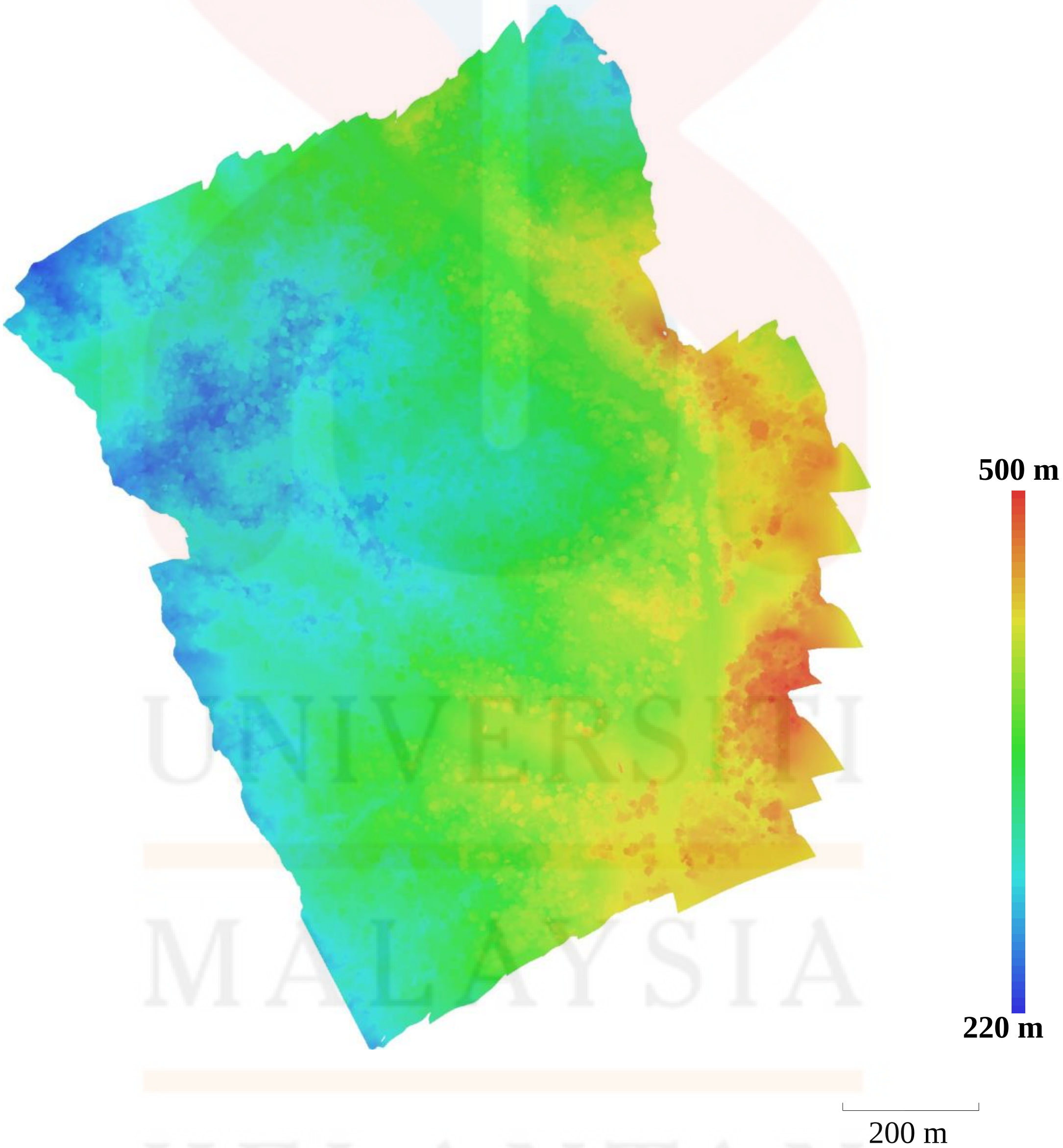

Figure 5.3: DEM of Landslide 1 area

5.3.2 Landslide 2

a) Orthophoto Landslide 2

The orthophoto of landslide 2 illustrated that 90% of the landslide 2 area are covered by forestry. The area that are clear to be seen are the highway and a few of clear/bald area in the forestry. There are factory/residential building can be seen near the starting highways at the right side of orthophoto. The also TNB electrical substation can be seen near the end of highway at the left side of orthophoto . Figure 5.4 show the orthophoto of Landslide 2 area

Figure 5.4: Orthophoto Landslide 2 area

b) Digital Elevation Model

The DEM of Landslide 2 illustrated the elevation of the landform in Landslide 2 area. The highest elevation is 350 m while the lowest elevation is 140 m. The DEM resolution is 20.6 cm/pix. The DEM point density is 23.6534 points per sq. m. Figure 5.5 show the DEM of Landslide 2 area.

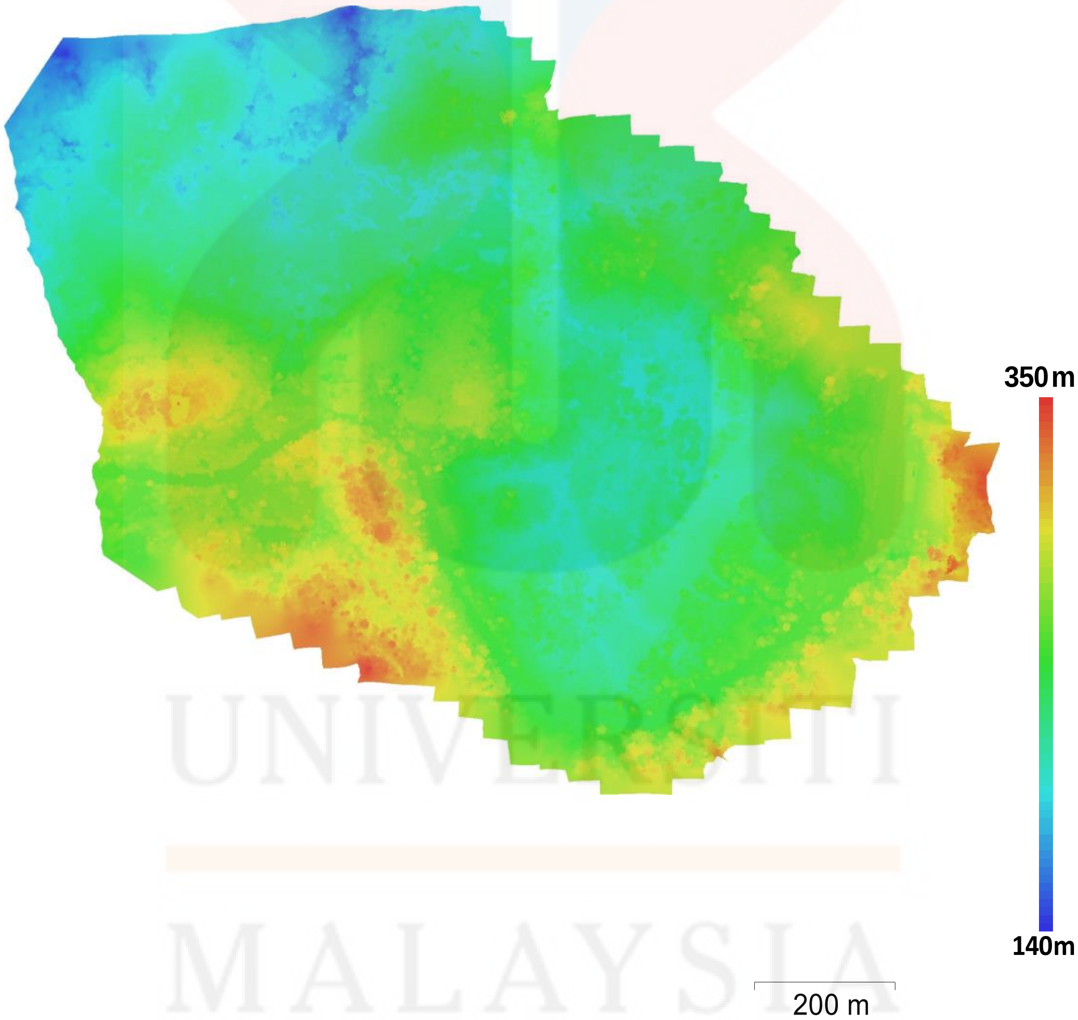

Figure 5.5: DEM of Landslide 2

5.3.3 Landslide 3

a) Orthophoto Landslide 3

The orthophoto of Landslide 3 illustrated that 95% of the landslide 3 area are covered by forestry area minus the highway and 1 clear/bald area can be seen near the highway at the middle of orthophoto. Figure 5.6 show the orthophoto of Landslide 3 area.

Figure 5.6: Orthophoto of Landslide 3

b) Digital Elevation Model Landslide 3

The DEM of Landslide 2 illustrated the elevation of the landform in Landslide 2 area. The highest elevation is 310 m while the lowest elevation is 110 m. The DEM resolution is 20.0 cm/pix. The DEM point density is 24.9704 points per sq. m. Figure 5.7 show the DEM of Landslide 3 area.

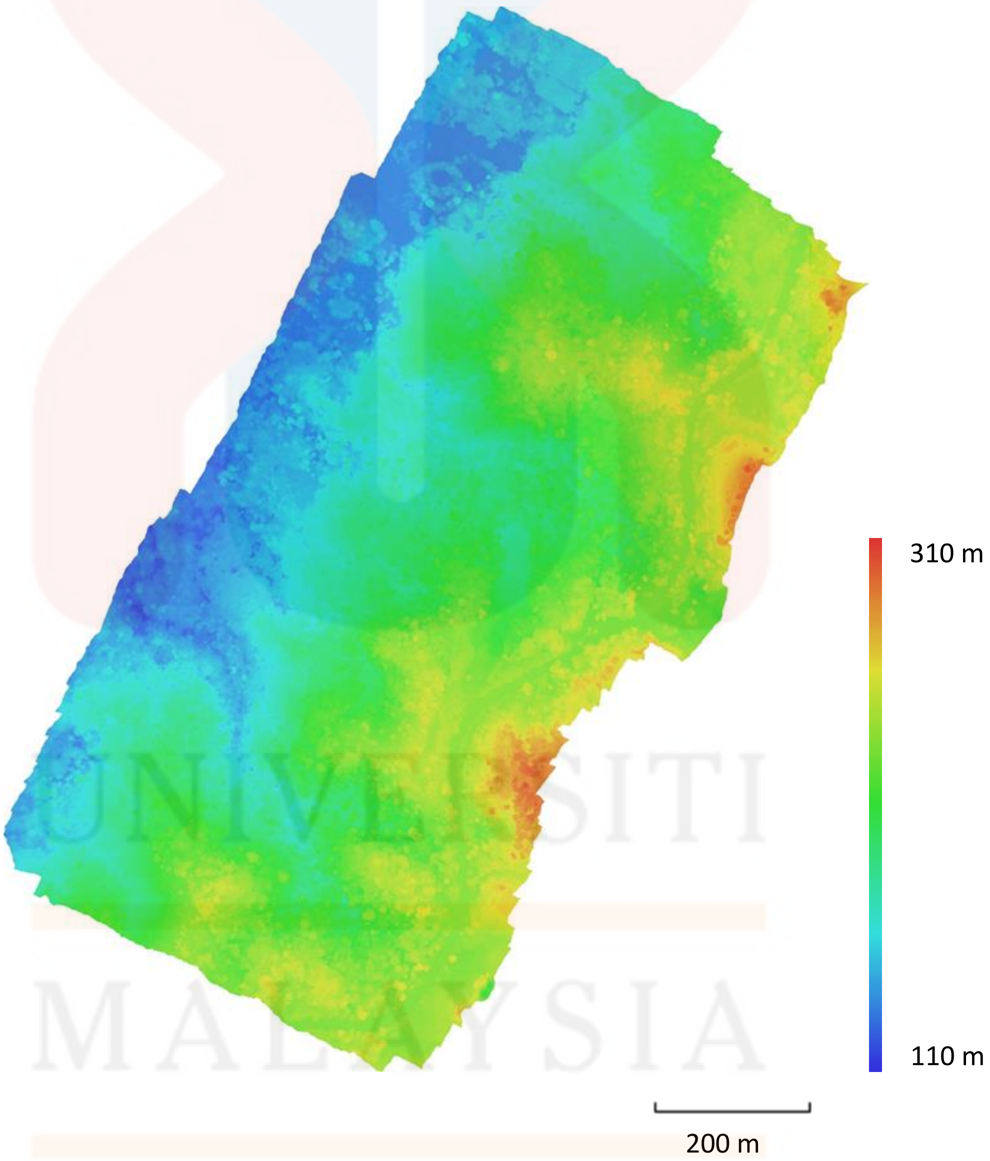

Figure 5.7: DEM of Landslide 3

5.4 3D Model

The 3D model are one of the digital photogrammetric products of UAV technology other than orthophotos and DEMs. The 3D model for Landslide 1 is the mathematical representation of any surface of an object in three dimensions. The 3D model was developed via specialized Agisoft Photoscan Pro software. The 3D model illustrated the actual shape of the landform/landscape of Landslide 1. Figure 5.8 shows the 3D model of Landslide 1.

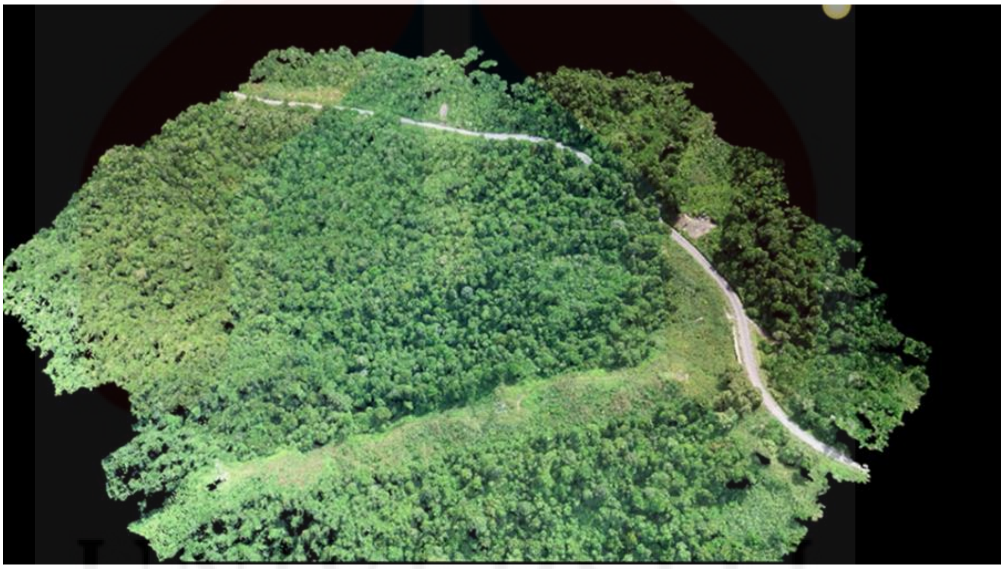

Figure 5.8: 3D model of Landslide 1

5.5 Root Mean Square Error (RSME) Analysis

The root mean square error (RMSE) is a measure of the difference between ground true points and the points from data processing including locations from satellite imagery and digitised data. The following Equation 5.1, 5.2 and 5.3 are the RMSE for X, Y and Z where X is longitude value, Y is latitude value and Z is elevation value.

$$RMSE_X = \sqrt{\frac{\Sigma(X - \dot{X})^2}{n - 1}} \quad \text{Equation 5.1}$$

$$RMSE_Y = \sqrt{\frac{\Sigma (Y - \dot{Y})^2}{n - 1}} \quad \text{Equation 5.2}$$

$$RMSE_Z = \sqrt{\frac{\Sigma(Z - \hat{Z})^2}{n - 1}} \quad \text{Equation 5.3}$$

X, Y and Z = Observed coordinates from field mapping

$\dot{X}$, $\dot{Y}$ and $\hat{Z}$ = Observed coordinates from satellite imagery data

n = Number of observation points

Table 5.3: RMSE Analysis for GCPs in the study area.

Quantitative	**RMSE (m)**		
Analysis	X (m)	Y (m)	Z (m)
8 GCP	±0.003	±0.003	±0.179
Mean	±0.062		

Table 5.3 show the RMSE analysis for GCPs in the study area. In horizontal accuracy, a sub-meter ±0.003 m were obtained for X and Y coordinates respectively. Meanwhile the RMSE for Z coordinates is ±0.179 m. Average RMSE ±0.062 m was obtained by averaging the planimetry and vertical RMSE for the orthophoto of the landslide areas. Based on the analysis, sub-meter accuracy is obtained.

According to ASPRS, the accepted RMSE reading in meters for 1:25 000 map is ±6.25 m. While the accepted RMSE reading for NMAS in meters for 1:25 000 map is ±20.8 m. Based on both level of accepted level of accuracy reading, the orthophotos, DEM and 3D model result are very accurate with average RMSE ±0.062 m.

5.6 Landslide Risk Area Map

There are 3 landslide risk area map produce in this research equalizing to the number of landslide area in the study area which are Landslide 1, Landslide 2 and landslide 3. The risk area map separate the landslide area into three group which are Low Risk, Medium Risk and High Risk. The parameters that was used to make the landslide risk area map is slope, aspect and elevation. Figure 5.9 shows the landslide inventory map of the study area.

Slope parameter cover the angle of slope in the landslide area. Generally, the steeper the slope, the higher the risk of landslide occurring. This apply for both natural and man-made slope. For this research, the slope was divided into 5 categories which are 0^o-10^o, 11^o-20^o, 21^o-30^o, 31^o-40^o, and >41^o.

Aspect parameter cover direction of slope. The aspect of each landslide area are derive from DEM orthophotos. In this research, Aspect are divided into 5 classes which are Flat, North, East, South and West. Based on the distribution of past landslide in the study area, the landslide that occur in the study area incline toward North direction (40%). Other direction where landslide had occurred was west (20%), Northwest (20%) and East (20%).

Elevation is a very important parameter. Based on the distribution of past landslide in the study area, 40% occur in elevation 380-400m, followed by 20% occur at elevation 420-440m, 20% occur at elevation 280-300m and the last 20% occurred at elevation 200-220m.

5.6.1 Landslide 1

Figure 5.10 shows the elevation map of landslide 1. Figure 5.11 shows the slope of Landslide 1, Figure 5.12 shows the aspect of Landslide 1. Figure 5.13 shows the landslide hazard map of Landslide 1. Based on landslide risk area map, the area along Jeli-Gerik Highway is in the moderate high hazard.

5.6.2 Landslide 2

Figure 5.14 show the elevation of Landslide 2. Figure 5.15 shows the slope of Landslide 2. Figure 5.16 shows the aspect of Landslide 2. Figure 5.17 shows the risk area map of Landslide 2 area. Based on the landslide risk area map, the area around Jeli-Gerik Highway is in moderate to high risk area. The lower side at the middle of Jeli-Gerik Highway is in low hazard range.

5.6.3 Landslide 3

Figure 5.18 shows the elevation of Landslide 3. Figure 5.19 shows the slope of Landslide 3. Figure 5.20 shows the aspect of Landslide 3. Figure 5.21 shows the landslide risk area map of the Landslide 3. Based on the landslide risk area map, the area around Jeli-Gerik Highway is in moderate to high risk area. There are some are on the higher elevation site near Jeli-Gerik highway show very high hazard.

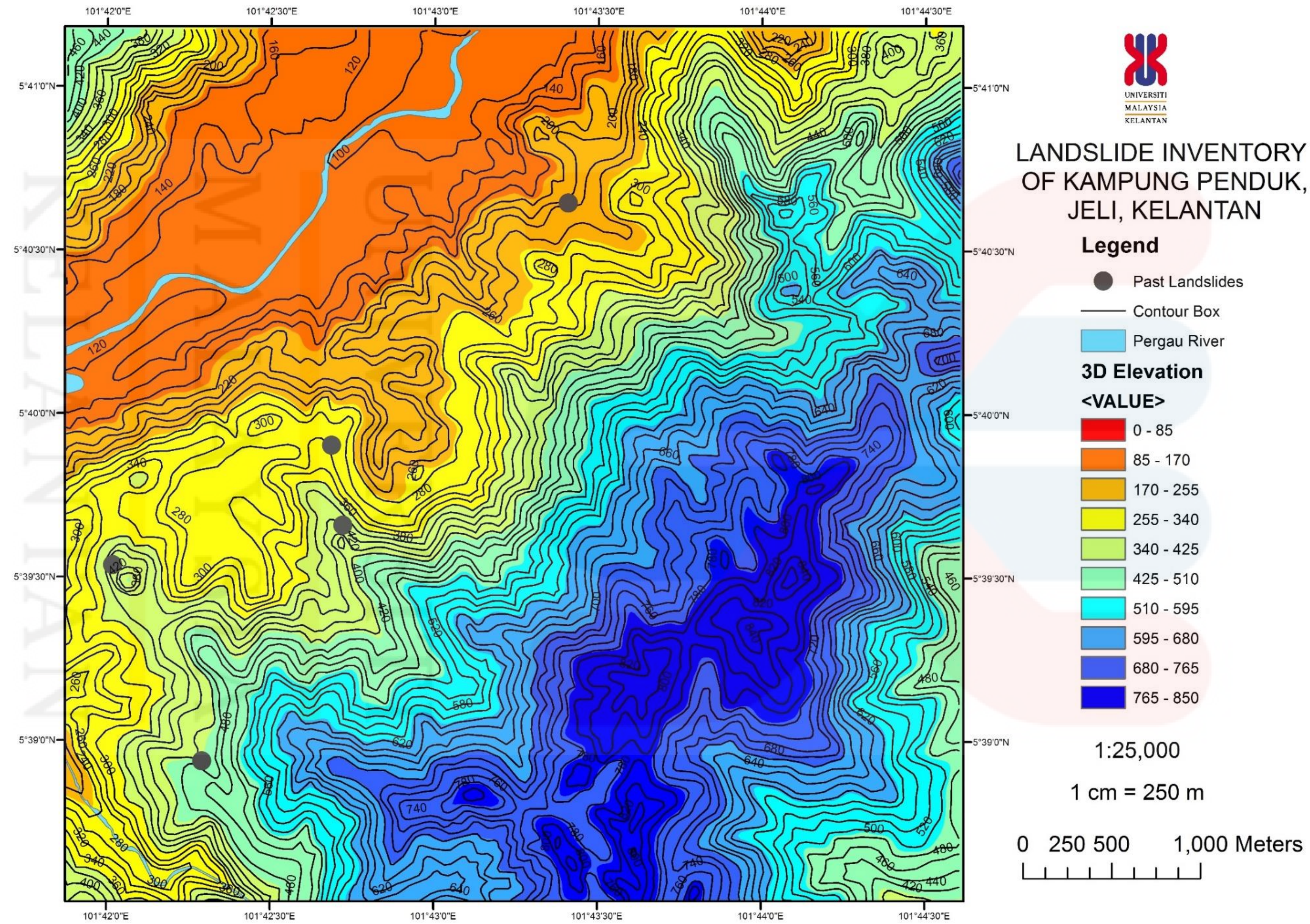

Figure 5.9: Landslide Inventory Map of the study area

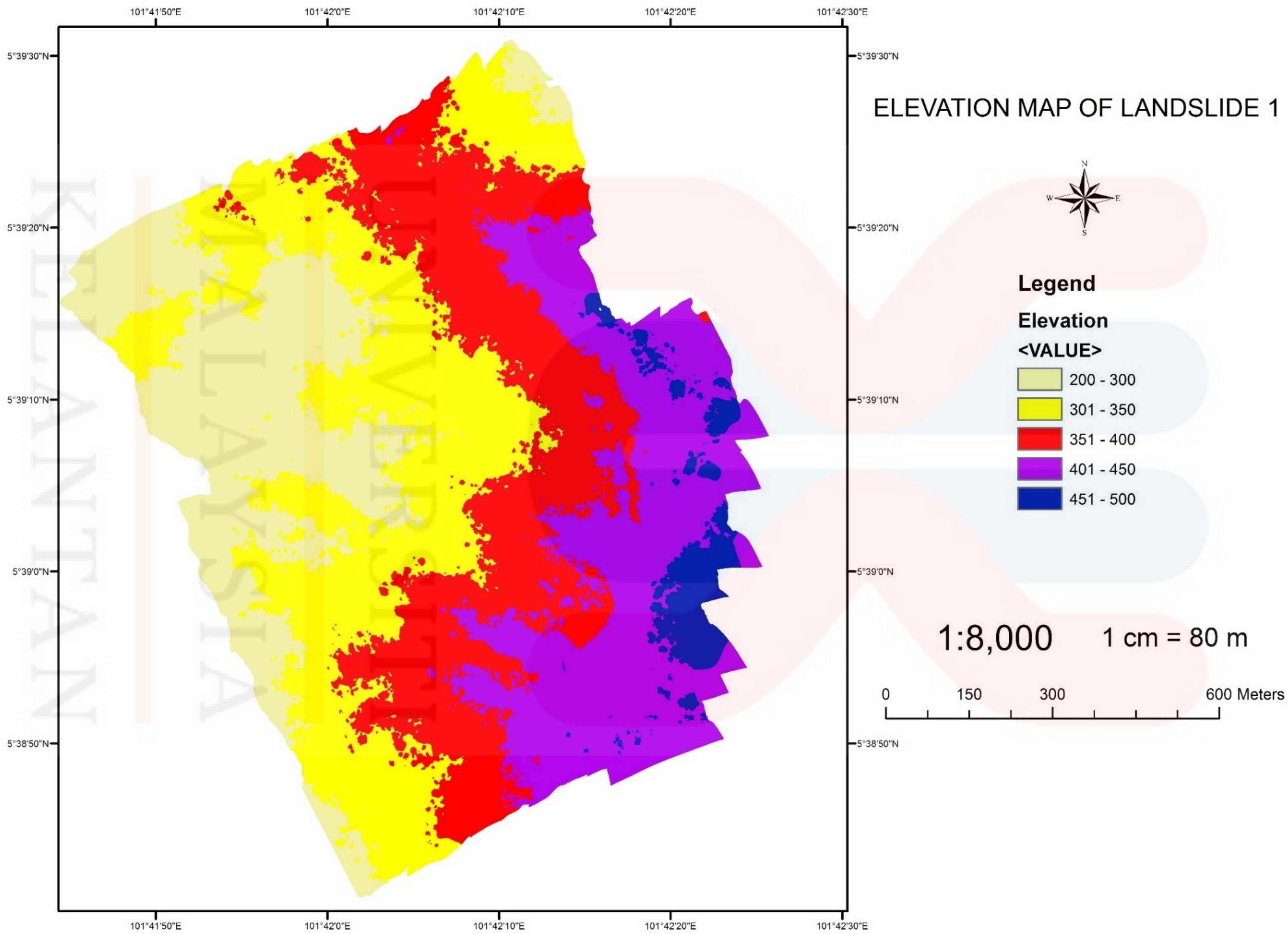

Figure 5.10: Elevation of Landslide 1

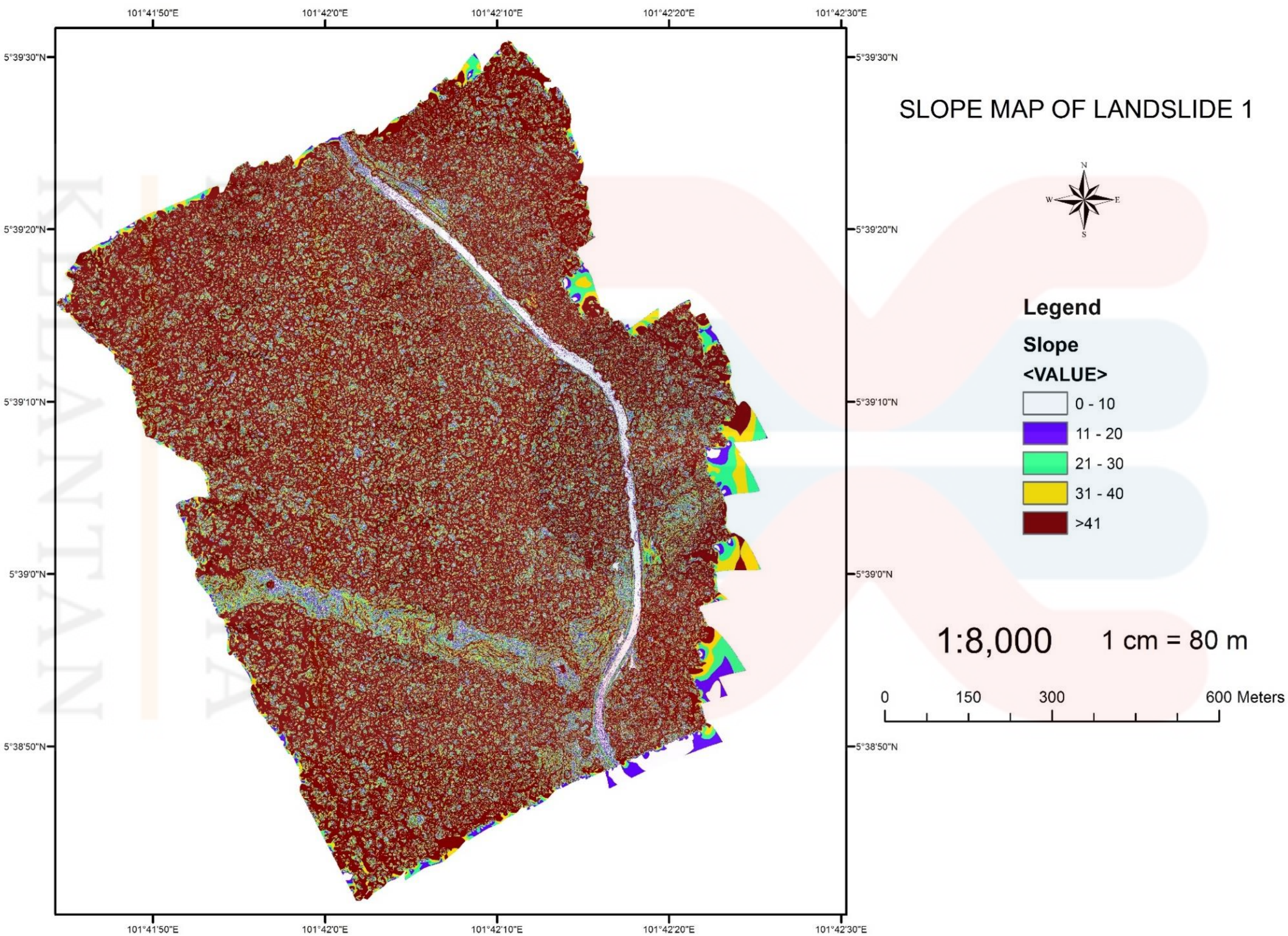

Figure 5.11: Slope of Landslide 1

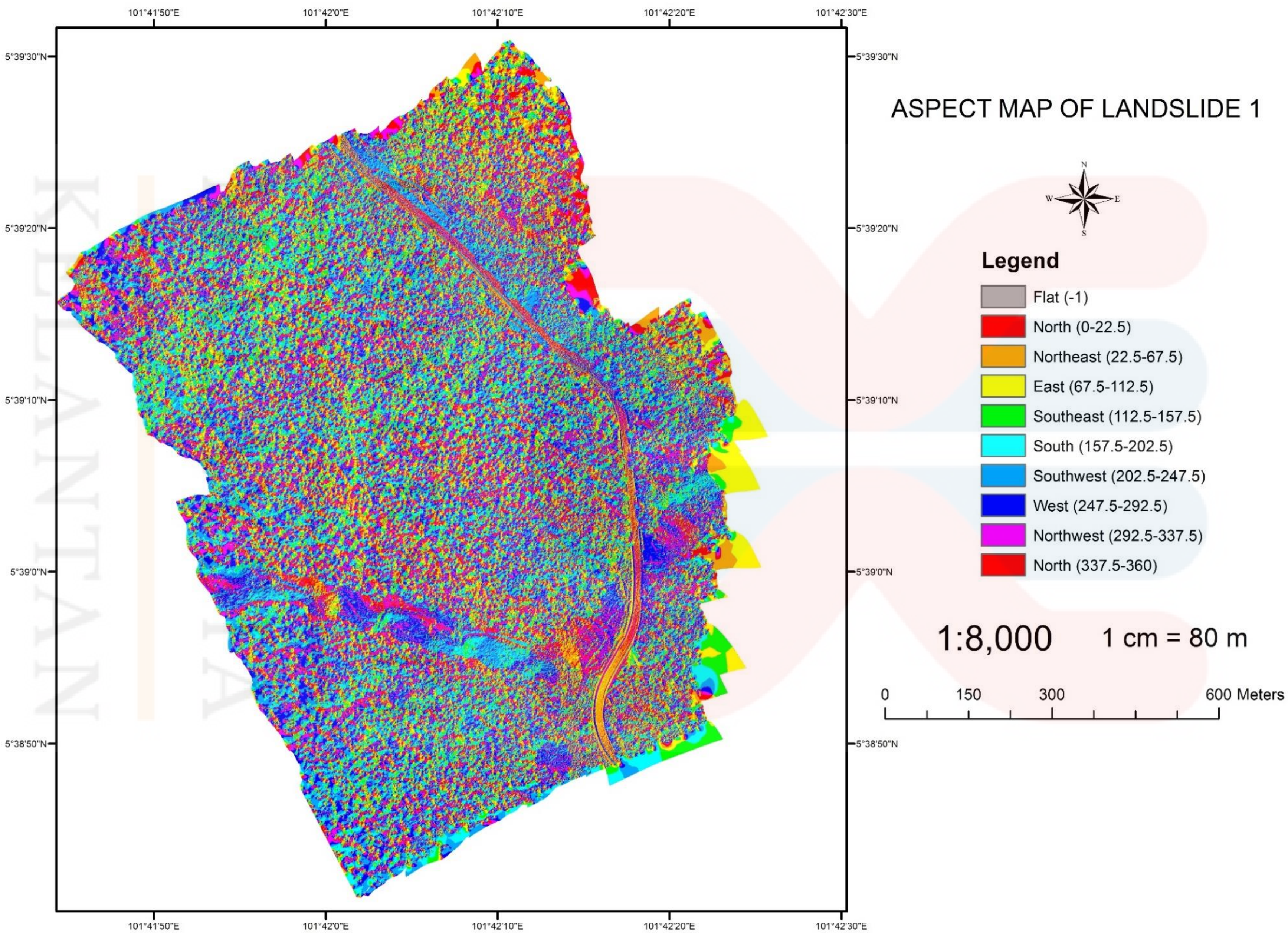

Figure 5.12: Aspect of Landslide 1

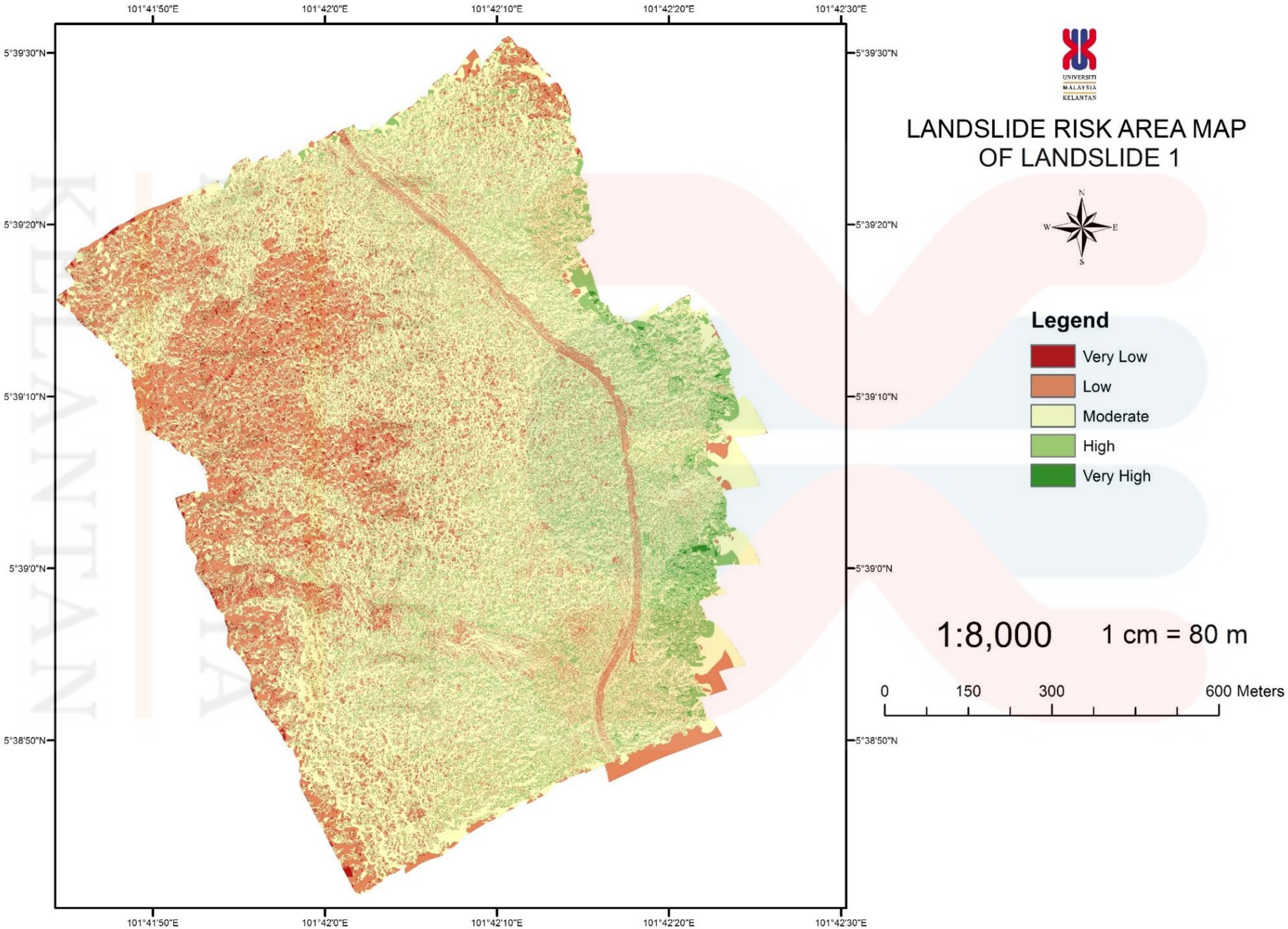

Figure 5.13: Landslide risk area map of Landslide 1

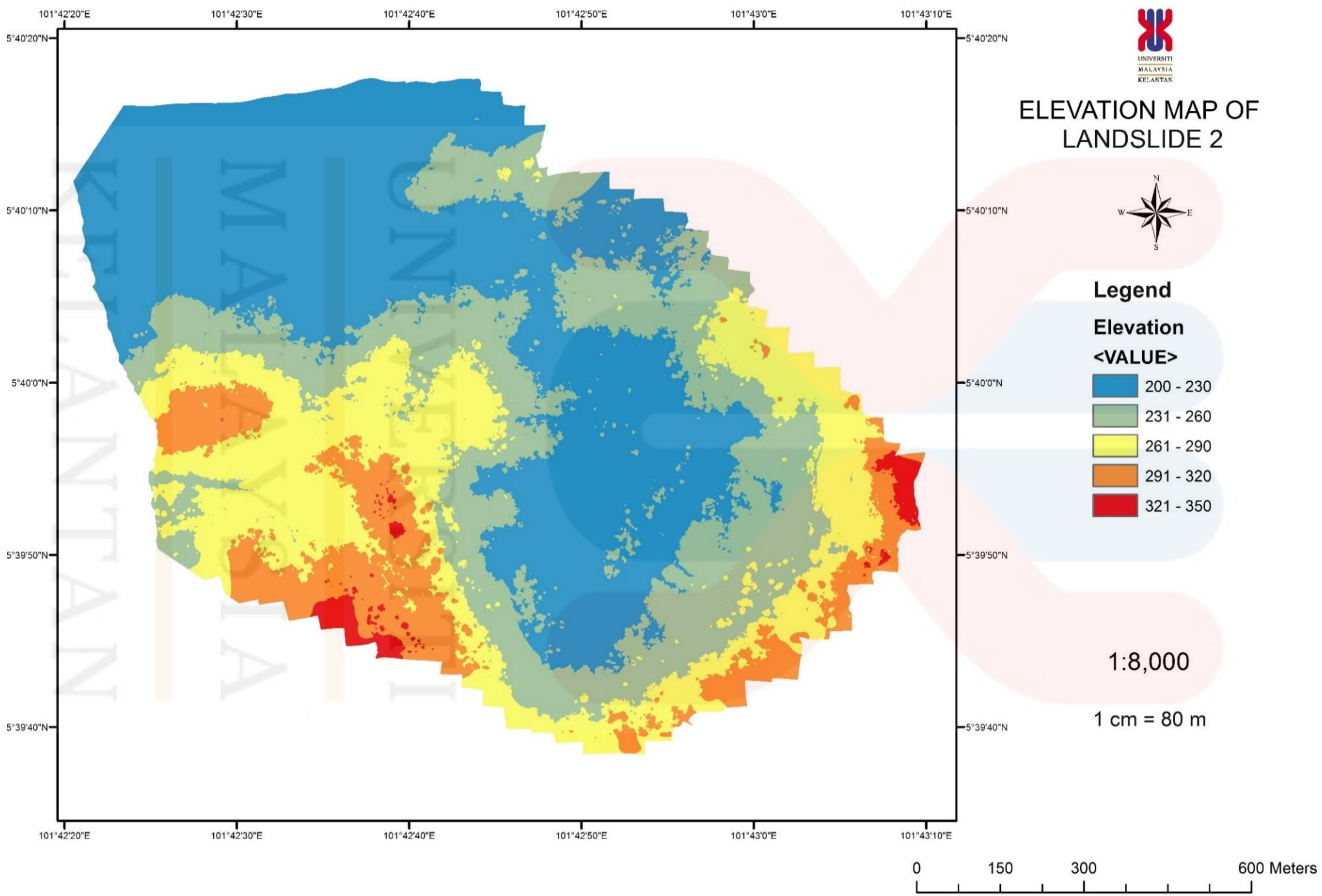

Figure 5.14: Elevation of Landslide 2

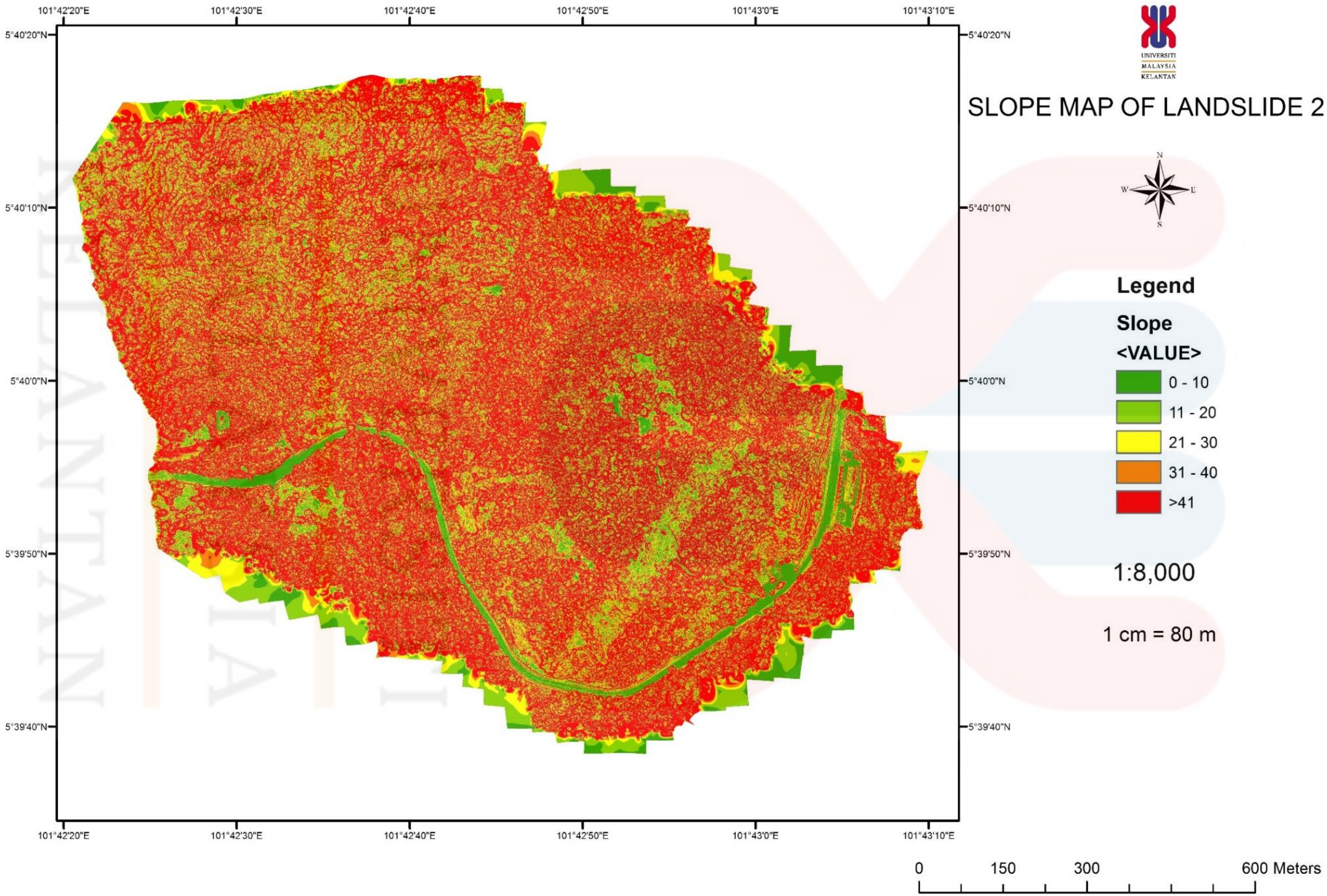

Figure 5.15: Slope map of Landslide 2

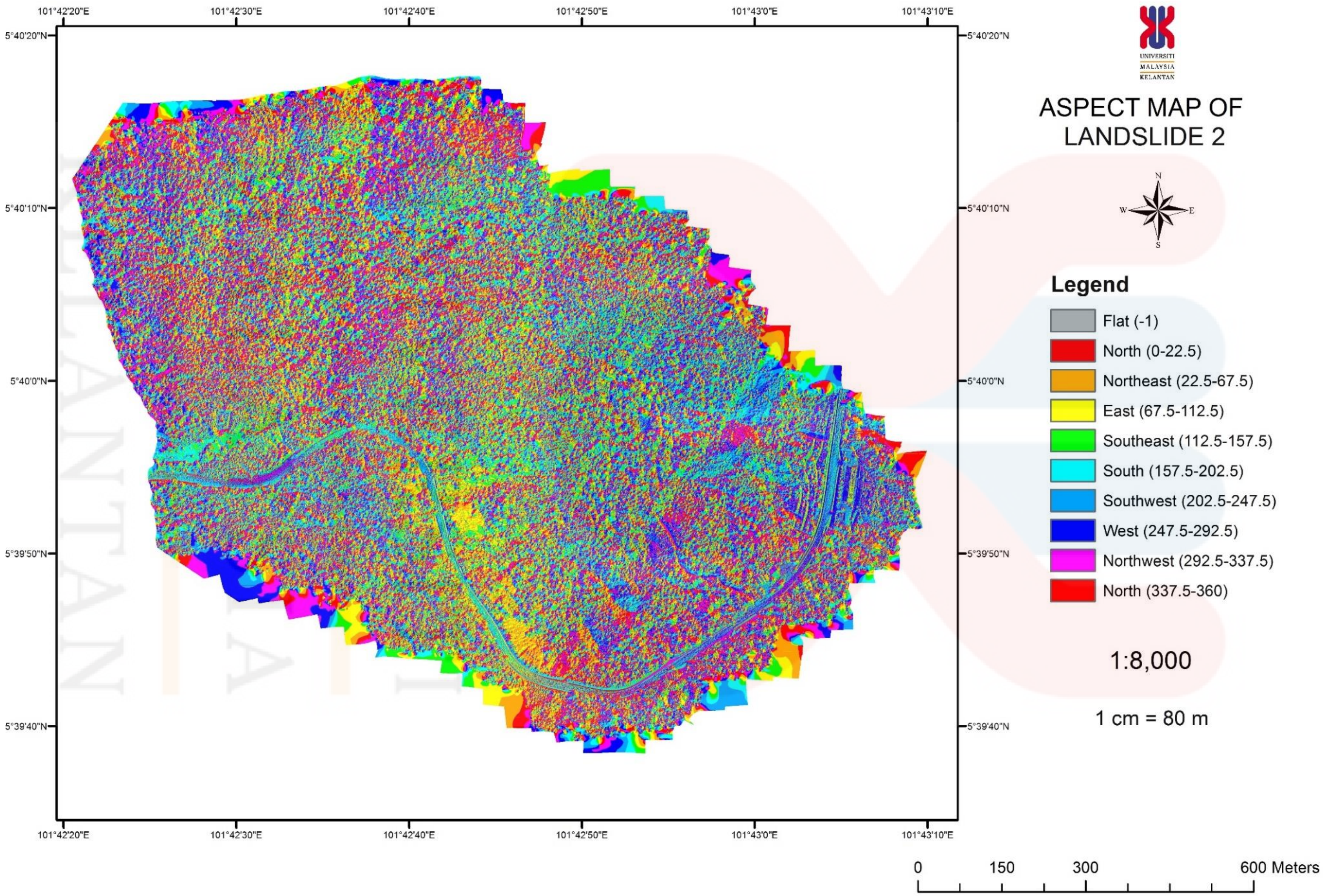

Figure 5.16: Aspect Map of Landslide 2

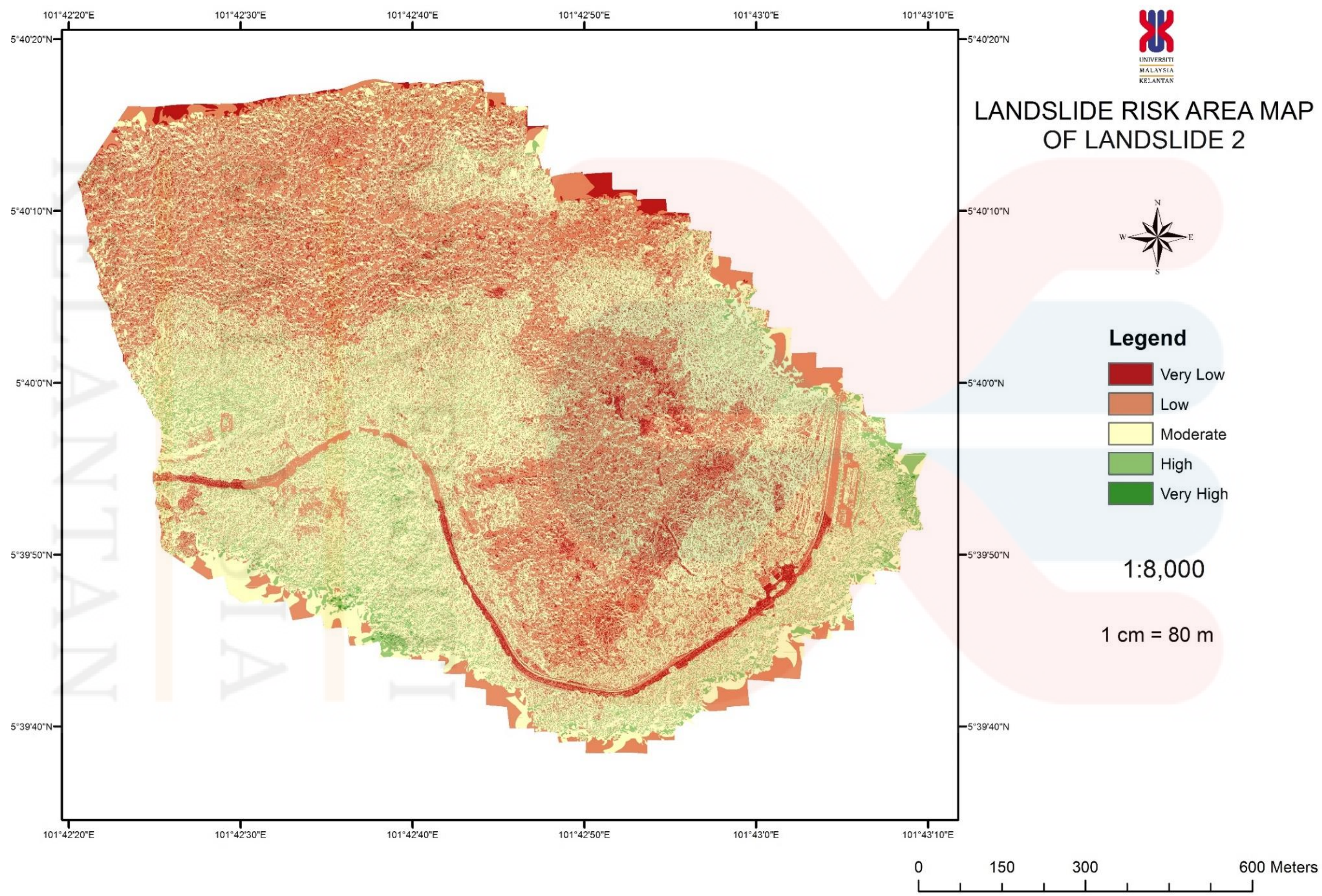

Figure 5.17: Landslide risk area map of Landslide 2

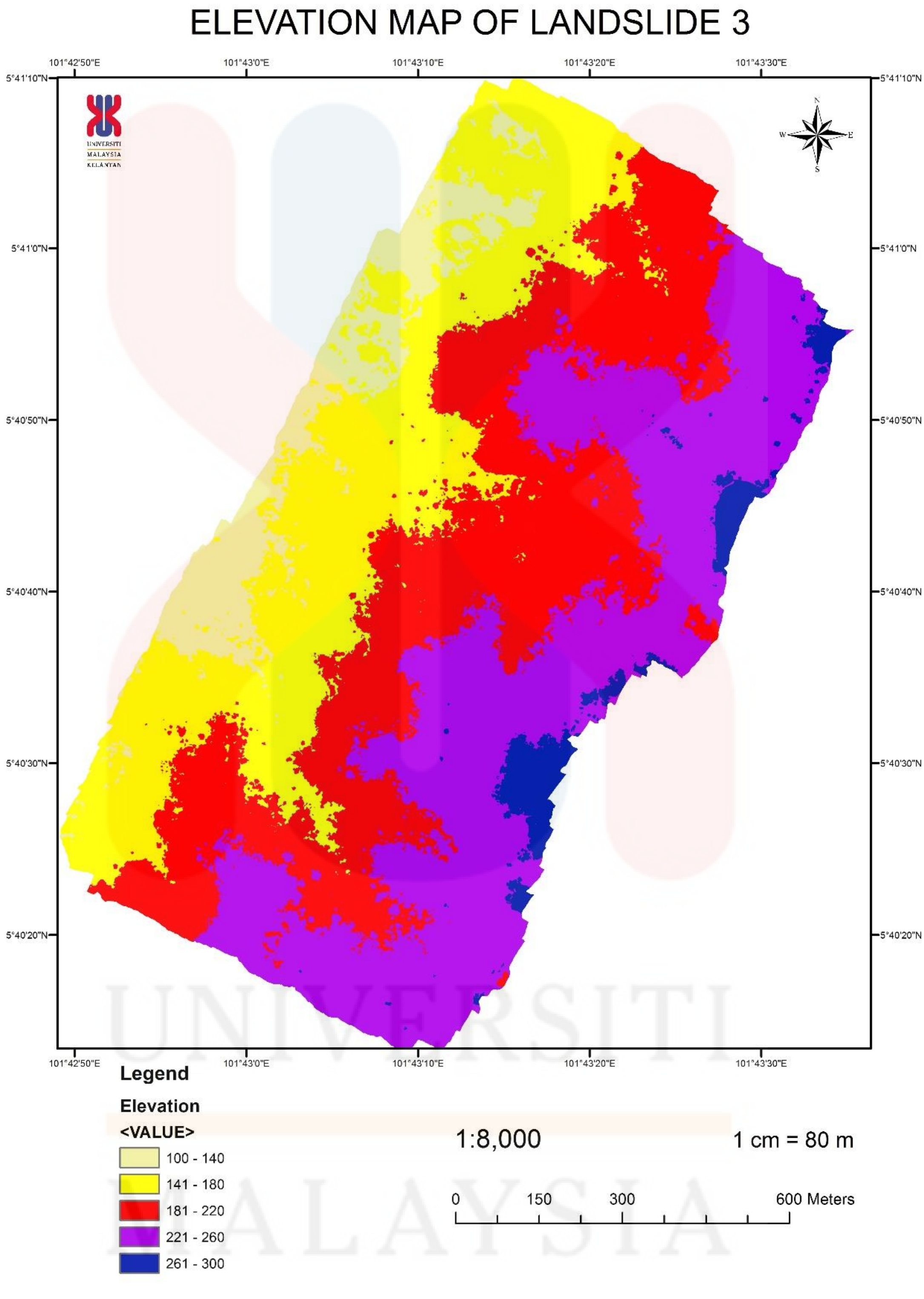

Figure 5.18: Elevation map of Landslide 3

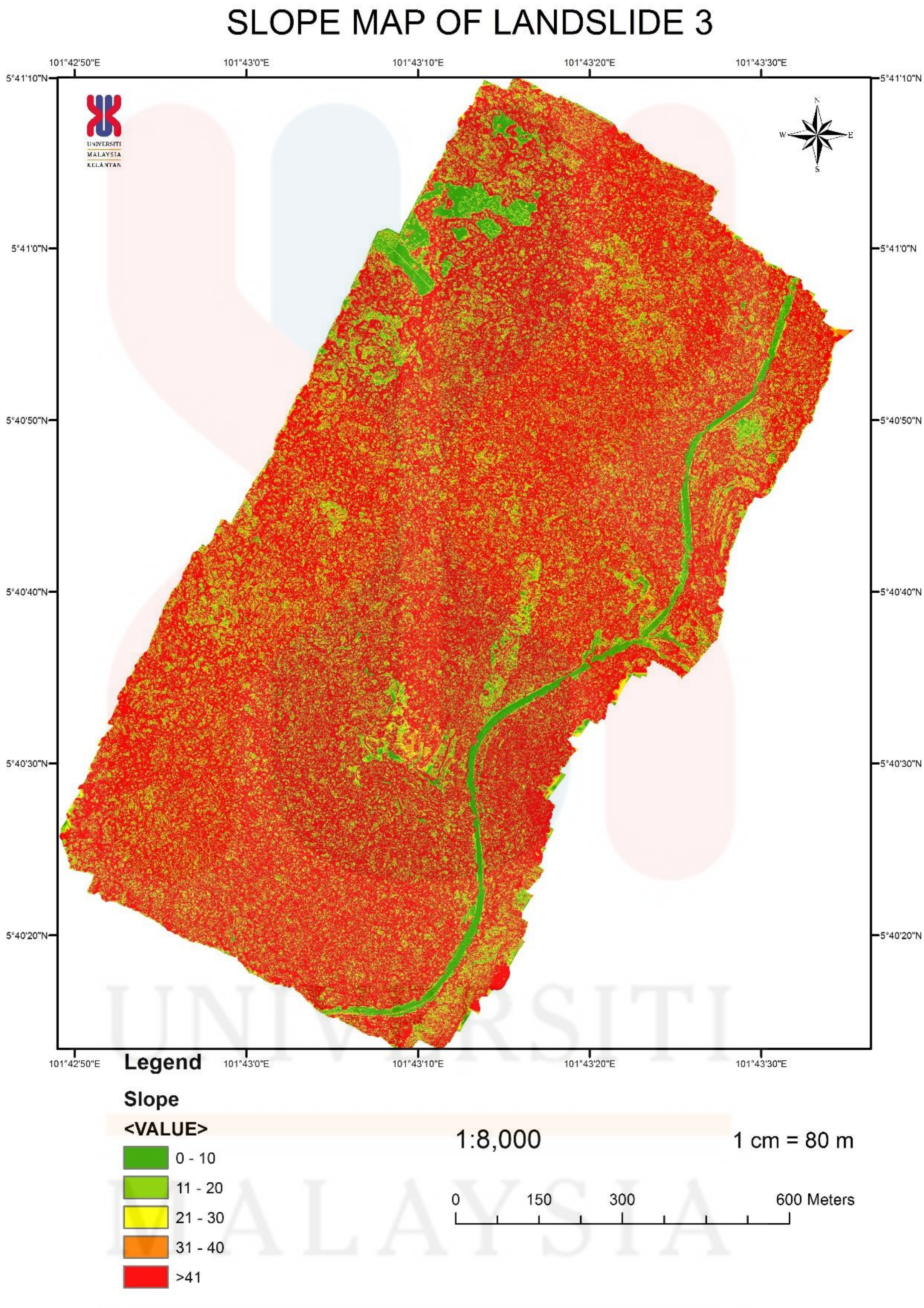

Figure 5.19: Slope map of Landslide 3

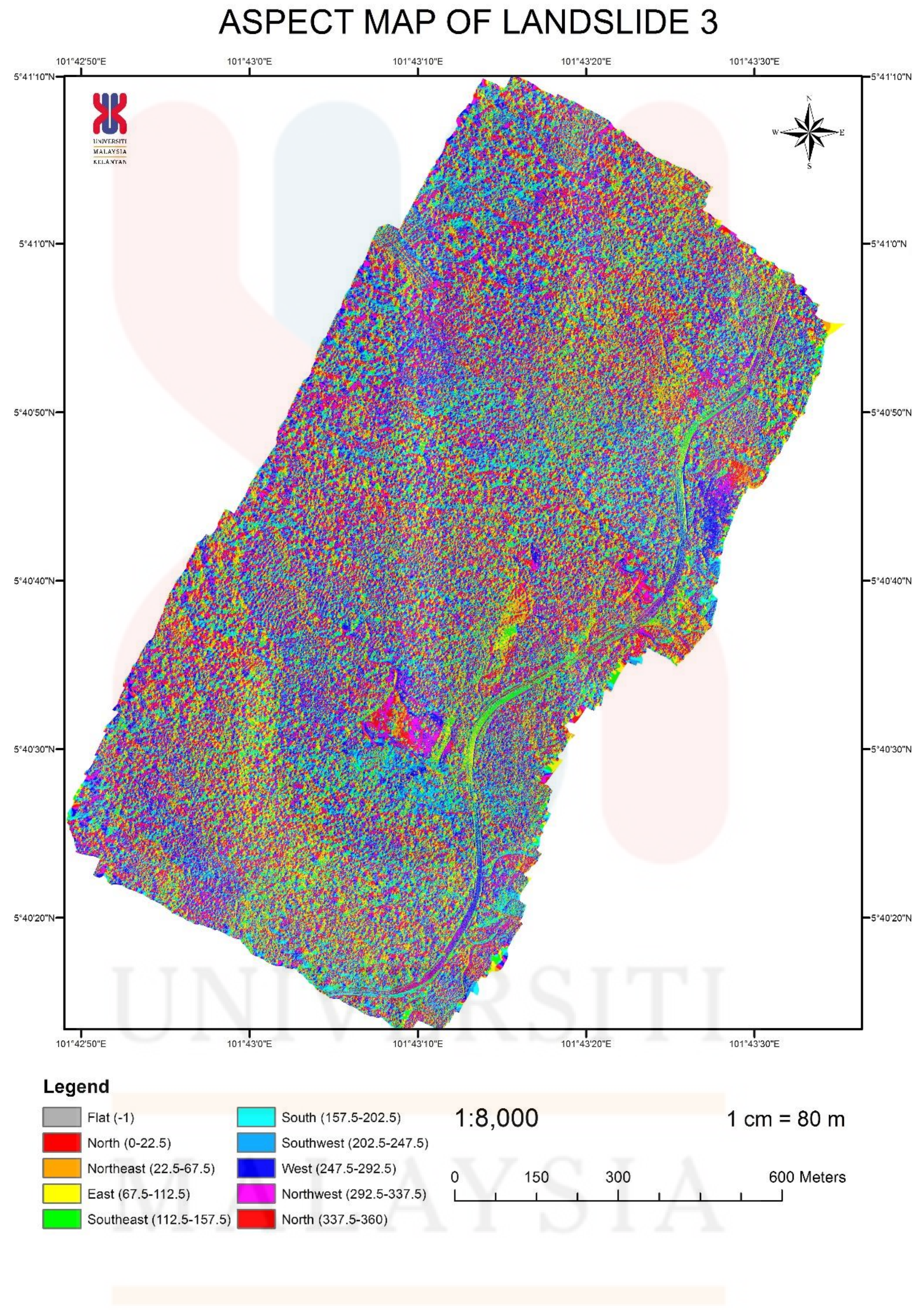

Figure 5.20: Aspect map of Landslide 3

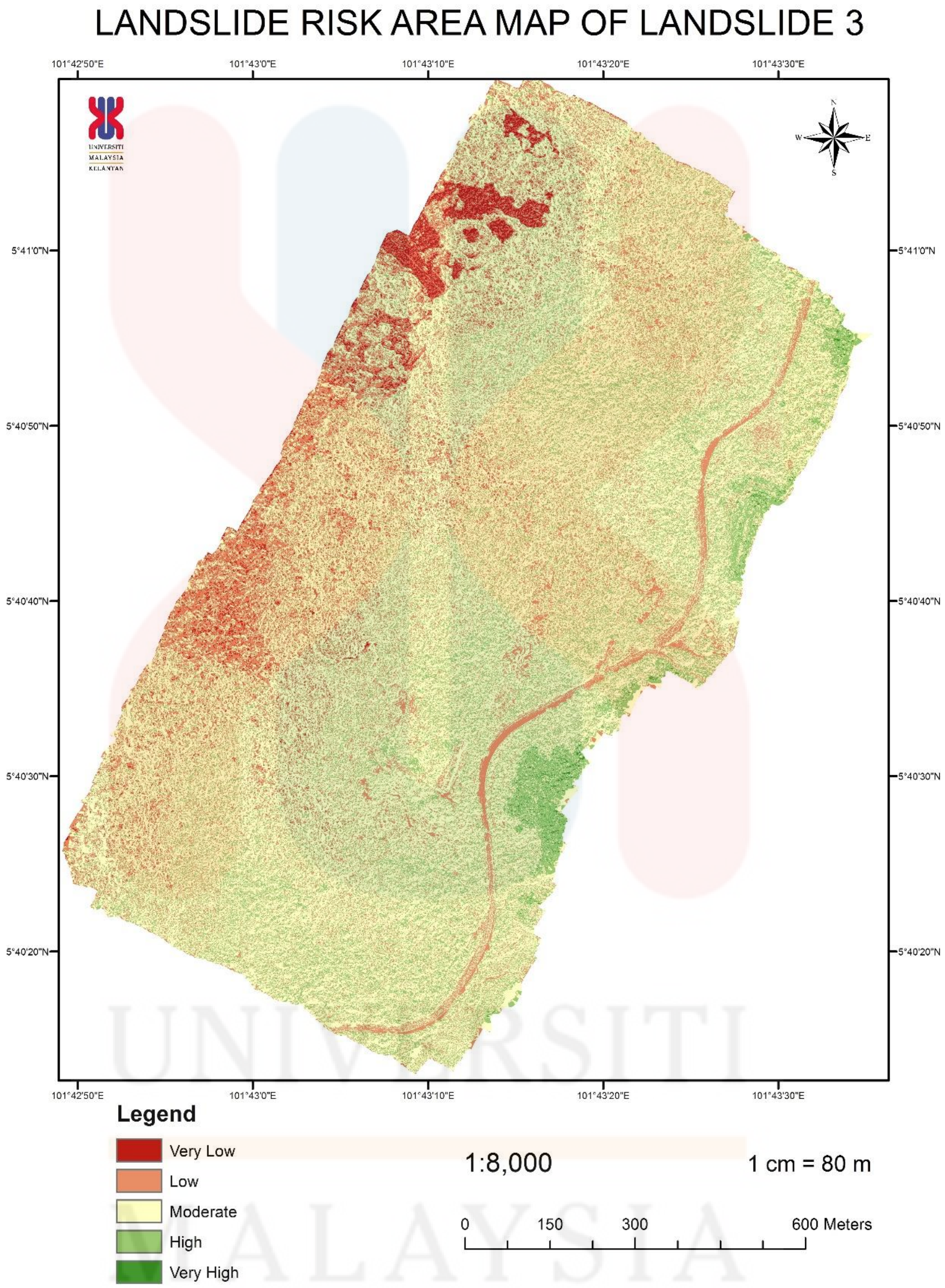

Figure 5.21: Landslide risk area map of Landslide 3

CHAPTER 6

CONCLUSION AND SUGGESTION

6.1 Conclusion

This chapter conclude all the results done from the general geology mapping, UAV mapping product and landslide hazard map using the UAV technology. From the general geology mapping, it enables to identify the lithology present in the study area. In the study area, granite, schist, slate, limestone and hornfels are found. Each of these rock unit exhibits in different conditions. The granite unit which distributed approximately 70% from the total extent in study area. The granite unit served as an acid intrusion in the study area is distributed on the right side of the study area. Small amount of dark grey limestone are found on the upper part of the Pergau River. Based on the data and information collected in the study area, an updated geological map of the study area are produce.

UAV system has potential use for large scale mapping and could be used by public work department in order to monitoring of landslide area with low cost, less manpower and faster. UAV produce high quality product such as orthophotos, DEMs and 3D image. The product are produced by Agisoft Photoscan Pro software. All the product have undergoes Root Mean Square Error (RMSE) analysis to calculate sub-meter accuracy. The average RMSE is $\pm$0.062 m which in acceptable level of accuracy reading by ASPRS and NMAS standard.

Three landslide hazard map was produced from integrated technique of UAV technology and GIS software. By using GIS software, the aspects, slope and elevation data was extracted from the DEMs of Landslide 1, 2, and 3. All the data extracted was overlay to produce landslide risk area map. All the landslide risk area map are categorise into 5 area which is very low, low, moderate, high and very high hazard area. By comparing all the landslide risk area map, Landslide 3 has the highest risk for occurrence of landslide. Thus, landslide hazard precaution are more needed in Landslide 3 area.

In conclusion, both geological and landslide risk area map are needed to plan a proper mitigation program if landslide occurred in the future. It also important future strategic planning in the study area to avoid huge loss in economy and give negative impact on humans, animals and environment.

6.2 Suggestion

This research can be used as a guideline for other researcher who want to conduct geohazards mapping research by using UAV technology in the study area. The core technique in conducting geohazards mapping by using UAV is quite similar but with a few different parameter needed to produce the hazard map. The map or the orthophotos produced from this system can be used as base map in Geographical Information System (GIS) but improvements are required to reduce data processing time for the efficient generation of orthophoto based on photogrammetric DEMs, in order to minimise georeferencing error.

Next, other researcher can focus on analysing the landslide area in the orthophotos to extract other data such as volume, magnitude, scale, and direction to calculate the area by landslide. The area affected by landslide can be calculated in ArcGIS software by subtracting the original data before landslide with the data after landslide.

REFERENCES

Chai, T., & Draxler, R. R. (2014). Root mean square error (RMSE) or mean absolute error (MAE)? – Arguments against avoiding RMSE in the literature. *Geoscientific Model Development*, 7(3), 1247-1250. Doi:10.5194/gmd-7-1247-2014

Crosilla, F., and Alberto, B. (2002). Use of generalised procrustes analysis for the photogrammetric block adjustment by independent models. ISPRS Journal of Photogrammetry and Remote Sensing. 56: 195-209.

Daanen, T. (2015). On the structure and tectonic evolution of the Taku Schists and their surrounding units, Kelantan, NE Malaysia. Retrieved from http://dspace.library.uu.nl/bitstream/handle/1874/316231/MScThesisTwanDaanen.pdf;sequence=2

Data Asas 2015/2016 (2016). Retrieved December 27, 2018, from http://www.kelantan.gov.my/index.php/ms/media/muat-turun/data-asas/284-data-asas-kelantan-darul-naim-2015-2016/file

DJI Phantom 4 Pro – Photography Drone – DJI. Retrieved from https://www.dji.com/phantom-4-pro

François, T., Ali, M. M., Matenco, L., Willingshofer, E., Ng, T., Taib, N., & Shuib, M. (2017). Late Cretaceous extension and exhumation of the Stong and Taku magmatic and metamorphic complexes, NE Peninsular Malaysia. *Journal of Asian Earth Sciences*, 143, 296-314. Doi:10.1016/j.jseaes.2017.04.009

Gasim, M.B., 1988. [Geological structure of Kapas Island, Terengganu]. Sains Malaysiana, 17: 3-15, (In Malay).

Gasim, M.B., I.B. Sahid, S.A. Rahim and E. Toriman, (2010). Characteristics of history, morphology and landform of the Dungun area, Terengganu, Malaysia with special reference to Bukit Bauk. Asian J. Earth Sci., 3: 213-221.

Google Earth. (2018). Retrieved from https://earth.google.com/

Innovative GNSS Receiver SOUTH Galaxy G6 Rugged/Versatile – 2 Pages. Retrieved from http://directindustry.com/pdf/south-surveying-mapping instrument-co-ltd/innovative-gnss-receiver-south-galaxy-g6-rugged versatile/160571-646310.html

Kelley, K., & Lai, K. (2011). Accuracy in Parameter Estimation for the Root Mean Square Error of Approximation: Sample Size Planning for Narrow Confidence Intervals. *Multivariate Behavioural research,* 46(1), 1-32. Doi:10.1080/00273171.2011.543027

Leoi, S. L., Chan, A., & Trisha. (2018, December 04). Malaysia among countries especially prone to landslide. Retrieved from https://www.thestar.com.my/news/nation/2018/12/04/msia-ranks-highly-for-landslides-country-experienced-185-occurrences-annually-in-past-10-years/

Malaysia and Thai working group, (2006). Geology Of The Batu Melintang-Sungai Kolok Transect Area Along The Malaysia-Thailand Border. Retrieved from http://www.dmr.go.th/download/Malaysia_Thai/Belum-Hala.pdf

Mantovani, F., Soeters, R., Van Westen, C.J. (1996). "Remote sensing techniques for land slide studies and hazard zonation in Europe". Geomorphology, 2016, Volume 15(3-4): 439 213-225.

Mekik, C., Yildirim, O., Bakici, S. (2011). The Turkish real time kinematic GPS network (TUSAGA-Aktif) infrastructure. Scientific Research and Essays. 6.19: 3986-3999.

Muhammad Barzani Gasim, Mohd Ekhwan Toriman and Hafizan Juahir, (2015). Phenomenon of Slope Failure Occurrences along Gerik-Jeli Highway, Malaysia. Journal of Applied Sciences, 15: 545-551. DOI: 10.3923/jas.2015.545.551 URL:https://scialert.net/abstract/?doi=jas.2015.545.551

Niethammer, U., Rothmund, S., Schwaderer, U., Zeman, J., Joswig, M. (2011). Opensource ımage processing tools for low cost UAV based landslide ınvestigations. In Proceedings of the International Archives of Photogrammetry, Remote Sensing and Spatial Information Sciences, ISPRS, 2011 September 14-16;Zurich.

Nagai, M., Chen, T., Ahmed, A., & Shibasaki, R. (2008). UAV borne mapping by multi sensor ıntegration. The International Archives of the Photogrammetry, Remote Sensing and Spatial Information Sciences, Vol. XXXVII, Part B1, 2008 July 3-11Beijing.

Rai, P. K., Mohan, K., & Kumra, V. K. (2014). Landslide Hazard And Its Mapping Using Remote Sensing And Gis. Retrieved from http://www.bhu.ac.in/research_pub/JournalScientificResearchVol.58PDF/1.LandslideHazard-Dr.PKRai.pdf

Rau, J.Y., Jhan, J.P., Lo, C.F., Lin, Y.S. (2011) "Landslide mapping using imagery acquired by a fixed –wing UAV". International Archives of Photogrammetry Remote Sensing and Nat. Hazards Earth Syst. Sci. Discuss., https://doi.org/10.5194/nhess-2018-13

Rohayu Che Omar, 1994. Petrochemistry of the Palaeozoic rocks along the East West Highway, Gerik-Jeli, Perak/Kelantan. National University of Malaysia MSc. Thesis, 381p. (in Malay).

Tjia, H.D., 1989. Tectonic History of the Bentong-Bengkalis Suture. Geologi Indonesia. 12(1): pp.89-111.

Turner, D., Lucieer, A., DeJong, S.M. (2015). Time series analysis of landslide dynamics using an Unmanned Aerial Vehicle (UAV). Remote Sensing. 7: 1736-1757.

Van Westen, C. J. & Lulie Getahun, F. (1999). Analyzing the evolution of the Tessina landslide using aerial photographs and digital elevation models. Geomorphology 2003, 54, 77–89.

Watson, G.A. (2006). Computing helmert transformations. Journal of Computational and Applied Mathematics, 197:2: 387-394.

Wei Hou, Xuejun Lu, Pengda Wu, An Xue, & Liuke Li, (2017). An Integrated approach for Monitoring and Information Management of the Guanling Landslide (China). Retrieved from http://www.mdpi.com/2220-9964/6/3/79

Yaprak, S., Yildirim, O., Susam, T., Inyurt, S., & Oguz, I. (2018, January). The Role of Unmanned Aerial Vehicles (UAVs) in Monitoring Rapidly Occurring Landslides. Retrieved from https://www.nat-hazards-earth-syst-sci-discuss.net/nhess-2018-13/nhess-2018-13-AC6-supplement.pdf

APPENDICES

APPENDIX 1

LINEAMENT READING

NO	ANGLE (°)	NO	ANGLE(°)
1	37	16	56
2	284	17	82
3	42	18	39
4	6	19	86
5	63	20	66
6	285	21	87
7	80	22	59
8	55	23	87
9	18	24	354
10	45	25	292
11	355	26	45
12	347	27	358
13	297	28	303
14	21	29	70
15	330		

APPENDIX 2

JOINT READING

No.	Angle (^{o})	Length (m)	No.	Angle (^{o})	Length (m)
1	50	2	19	78	1
2	20	1	20	70	5
3	36	1	21	5	2
4	34	5	22	40	3
5	38	2	23	340	2
6	117	2	24	140	4
7	82	3	25	320	1
8	20	2	26	200	4
9	48	3	27	230	1
10	46	1	28	220	3
11	92	2	29	150	3
12	58	2	30	90	1
13	32	2	31	130	3
14	92	2	32	120	2
15	84	2	33	290	1
16	20	1	34	60	3
17	84	2	35	70	1
18	20	1	36	50	3